UNIVERSITY OF SOUTHAMPTON

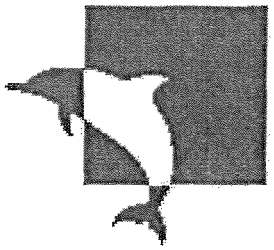

University of Southampton

Synthesis and Characterisation of Chromium and Vanadium Complexes

by

Charlotte Diane Beard

A Thesis Submitted for the Degree of Master of Philosophy

School of Chemistry

November 2006

UNIVERSITY OF SOUTHAMPTON

ABSTRACT

FACULTY OF ENGINEERING, SCIENCE AND MATHEMATICS
SCHOOL OF CHEMISTRY

Master of Philosophy

SYNTHESIS AND CHARACTERISATION OF CHROMIUM AND VANADIUM COMPLEXES

By Charlotte Diane Beard

A range of Cr(III), V(III) and V(V) complexes have been prepared and analysed *via* IR, UV-vis, X-Ray crystallography, multinuclear NMR spectroscopy (vanadium(V) species only) and microanalysis.

Vanadium(V) complexes with hard and soft ligands have been synthesised including the novel complexes $[VOCl_3(EtSCH_2CH_2SEt)]$ and $[VOCl_3(MeSCH_2CH_2SMe)]$ in anhydrous CH_2Cl_2. The complexes made during this work are the first extended series of complexes of vanadium(V) with neutral donor ligands.

A series of six-coordinate Cr(III) and V(III) species were synthesised involving crown ether, crown thioether and mixed ether/thioether crowns. The complexes $[MCl_3(crown)]$ (M = Cr or V; crown = 12-crown-4, 15-crown-5, 18-crown-6, $[12]aneS_4$, $[15]aneS_5$, $[9]aneS_2O$, $[15]aneS_2O_3$, $[18]aneS_3O_3$) were formed by reacting $[MCl_3(thf)_3]$ with rigorously dry crown in anhydrous CH_2Cl_2. Mono-aqua species were also synthesised in the presence of small amounts of water $[MCl_3(H_2O)(crown)]$ (M=Cr or V; crown=15-crown-5,18-crown-6). Crystal structures of $[CrCl_3(H_2O)(18\text{-crown-6})]$, $[VCl_3(H_2O)(15\text{-crown-5})]$ and $[CrCl_3([15]aneS_5)]$ have been analysed by X-ray crystallography. The affinity for 15-crown-5 and 18-crown-6 to pick up H_2O is rationalised due to the strain within the adjacent five-membered chelate rings in the anhydrous κ^3-coordinated species. A wider survey showed S-M-S angles in five-membered chelate rings are typically around 82°, where as O-M-O have a substantially more acute angle at around 75°. The crown ether complexes relieve this strain by switching to κ^2-coordination with the addition of the H_2O ligand. The use of the mixed thia/oxa crowns to probe the M-O vs. M-S binding, showed an overall preference for Cr(III) and V(III) to bind to thioether rather than the ether donor atoms, which is in contrast to the expected behaviour stated by HSAB theory.

Contents

Chapter 3

List of Figures

List of Tables

Acknowledgements

I would like to thank my supervisors Prof. Gill Reid and Prof. Bill Levason for their support and supervision during the course of this work. I am grateful for the help with crystallography from Martin Davis, Mike Brown and Annie Middleton.

I would also like to thank Dr. Mike Webster for his help with crystallography and histograms within this thesis. Thanks also go to Loretta Carr for help synthesising $[VCl_3([9]aneS_2O_3)]$ and $[CrCl_3([9]aneS_2O_3)]$ and Louise Norman for the crystal structure of $[CrCl_3(H_2O)(18\text{-crown-}6)]$.

I would like to thank the EPSRC for aiding in my funding during my MPhil research project. I would also like to thank the group past and present, with special thanks to Mike for his help during my first month in the lab. I would also like to thank my family and Richard for all the help and support they have provided throughout my thesis.

Abbreviations

Spectroscopy

NMR	Nuclear Magnetic Resonance
IR	Infra Red
UV-vis	Ultraviolet-visible

Solvents

Et_2O	diethyl ether ($(CH_3CH_2)_2O$)
n-hexane	hexane (C_6H_{14})

Ligands

Ph_4AsCl	tetraphenylarsonium chloride
$NaVO_3$	sodium metavanadate
bipy	2,2'-dipyridyl
phen	1,10-phenanthroline
py	pyridine
tmen	N,N,N',N'-Tetramethylethylenediamine
Et_3N	triethylamine
Ph_3PO	triphenylphosphine oxide
Me_3PO	trimethylphosphine oxide
Ph_3AsO	triphenylarsine oxide
$Ph_2P(O)CH_2P(O)Ph_2$	1,1-bisdiphenylphosphine oxidemethane
Me_2S	dimethyl sulfide
Ph_2S	diphenyl sulfide
$MeSCH_2CH_2SMe$	1,2-bis(methylthio)ethane
$EtSCH_2CH_2SEt$	1,2-bis(ethylthio)ethane
$PhSCH_2CH_2SPh$	1,2-bis(phenylthio)ethane
$MeSCH_2CH_2CH_2SMe$	1,3-bis(methylthio)propane
12-crown-4	1,4,7,10-tetraoxacyclododecane
15-crown-5	1,4,7,10,13-pentaoxacyclopentadecane
18-crown-6	1,4,7,10,13,16-hexaoxacyclooctadecane
[9]aneS_3	1,4,7-trithiacyclononane
[12]aneS_4	1,4,7,10-tetrathiacyclododecane
[15]aneS_5	1,4,7,10,13-pentathiacyclopentadecane
[9]aneS_2O	1,4-dithia-7-oxacyclononane
[15]aneS_2O_3	1,4-dithia-7,10,13-trioxacyclopentadecane
[18]aneS_3O_3	1,4,7-trithia-10,13,16-trioxacyclooctadecane

General

thf	tetrahydrofuran (C_4H_8O)
Et	ethyl
Me	methyl
Ph	phenyl (C_6H_5)
mes	mesityl (2,4,6-trimethylphenyl)
X	halide
L	monodentate ligand
L-L	bidentate ligand
M	metal
I	nuclear spin
o	ortho
μ-	bridging
ν	vibrational frequency
Å	Angström
δ	chemical shift
s	strong/singlet
m	medium/multiplet
w	weak
d	doublet
t	triplet
sh	shoulder
b	broad
vb	very broad
λ	wavelength
$\{^1H\}$	Proton decoupled NMR
$w_{½}$	width of resonance at half peak height
Hz	Hertz
ε_{mol}	extinction coefficient
J	coupling constant
ppm	parts per million
fac	facial coordination
mer	meridional coordination
cis	adjacent coordination
trans	opposing coordination
HSAB	Hard soft acid base

Chapter 1

Introduction Chapter

1.1 Introduction

The work within this Thesis is concerned with species containing either vanadium(III) or (V) or chromium(III) bound to a selection of hard and soft ligands. The hard ligands containing either N- or O-donor atoms, were used as a comparison to the soft S-donor ligands. The combination of these metals and ligands allow developments of the coordination chemistry of these transition metals and the boundaries of HSAB theory to be tested. Vanadium and chromium exist in a variety of oxidation states which are tabulated (Table 1.1 and Table 1.2).

Oxidation State	Coord. No.	Stereochemistry	Examples
-1(d^6)	6	octahedral	$[Li\{V(bipy)_3\}(C_4H_8O)_4]$ $[V(CO)_6]^-$
0 (d^5)	6	octahedral	$[V(bipy)_3]$, $[V(CO)_6]$, $[V\{Me_2P(CH_2)_2PMe_2\}_3]$
+1 (d^4)	6	octahedral	$[V(bipy]_3]^+$
+2 (d^3)	6	octahedral	$[V(H_2O)_6]^{2+}$, $[V(CN)_6]^{4-}$
	5	square pyramidal	$[(2,6\text{-}Ph_2C_6H_3O)_2V(py)_3]$
+3 (d^2)	6	octahedral	$[V(C_2O_4)_3]^{3-}$, $[VCl_3(thf)_3]$, $[VF_3]$, $[V(NH_3)_6]^{3+}$
	5	trigonal bipyramidal	$[VCl_3(NMe_3)_2]$, *trans*-$[VCl_3(SMe_2)_2]$
	4	tetrahedral	$[VCl_4]^-$
+4(d^1)	8	dodecahedral	$[VCl_4(diars^a)_2]$, $[V(S_2CMe)_4]$
	6	Octahedral	$K_2[VCl_6]$, $[VO_2]$, $[VCl_2(acac^b)_2]$,
	5	tetragonal pyramidal	$[VO(acac^b)_2]$, $[PCl_4^+VCl_5^-]$
	4	Tetrahedral	$[VCl_4]$, $[V(CH_2SiMe_3)_4]$, $[V(NEt_2)_4]$
+5(d^0)	7	pentagonal bipyramidal	$[VO(NO_3)_3(CH_3CN)]$, $[VO(Et_2NCS)_3]$
	6	Octahedral	$[VF_6]^-$, $[VF_5](s)$, $[V_2O_5]$ (very distorted), $[VO_2(ox^c)_2]^{3-}$, $[V_2S_5]$
	5	trigonal bipyramidal	$[VF_5](g)$, $[VNCl_2](quinuclidine)_2$
	4	Tetrahedral	$[VOCl_3]$

Table 1.1 The oxidation states of vanadium[1]

(a= *o*-phenylenebisdimethylarsine $[o\text{-}C_6H_4(AsMe_2)_2]$,b= acetylacetonate anion, c= oxalate anion $[C_2O_4]^{2-}$)

Oxidation State	Coord. No.	Stereochemistry	Examples
-4	4	tetrahedral	$Na_4[Cr(CO)_4]$
-2	5	trigonal bipyramidal	$Na_2[Cr(CO)_5]$
-1	6	octahedral	$Na_2[Cr_2(CO)_{10}]$
0 (d^6)	6	octahedral	$[Cr(CO)_6]$, $[Cr(CO)_5I]^-$, $[Cr(bipy)_3]$
+1 (d^5)	6	octahedral	$[Cr(bipy)_3]^+$, $[Cr(CNR)_6]^+$
+2 (d^4)	6	distorted octahedral	$[CrF_2]$, $[CrCl_2]$, [CrS]
	5	trigonal bipyramidal	$[Cr(Me_6tren^a)Br]^+$
	4	distorted tetragonal	$[CrCl_2(MeCN)_2]$, $[CrI_2(OPPh_3)_2]$
	4	square	$[Cr(acac^b)_2]$
	3	trigonal planar	$[Cr(NPr^c_2)_2]_2$
	3	T shape	$[Cr(OC^tBu_3)_2]$, [LiCl(thf)]
	2	bent	$[Cr[N(Ph)B(mes^d)_2]_2]$
+3 (d^3)	6	octahedral	$[Cr(NH_3)_6]^{3+}$,$[Cr(acac^b)_3]$, $K_3[Cr(CN)_6]$
	5	square planar	$[CrCl(tmtaa^e)]$
	5	trigonal bipyramidal	$[CrCl_3(NMe_3)_2]$
	4	distorted octahedral	$[PCl_4]^+[CrCl_4]^-$, $[Cr(CH_2SiMe_3)_4]^-$
	3	planar	$[Cr[N(SiMe_3)_2]_3]$
+4(d^2)	8	dodecahedral	$[CrH_4\{Me_2P(CH_2)_2PMe_2\}_2]$
	6	octahedral	$K_2[CrF_6]$, $[Cr(O_2)_2(en^f)]H_2O$, *trans*-$[Cr(NCHMe)_2\{Me_2P(CH_2)_2PMe_2\}_2]^{2+}$
	4	tetrahedral	$[Cr(OC_4H_9)_4]$, $[Ba_2CrO_4]$,
+5(d^1)	8	quasi-dodecahedral	$[K_3Cr(O_2)_4]$
	6	octahedral	$K_2[CrOCl_5]$
	5	square planar	$[CrOCl_4]^-$
	5	distorted trigonal bipyramidal	$[CrF_5]$ (g)
	4	tetrahedral	$[CrO_4]^{3-}$
+6 (d^0)	4	tetrahedral	$[CrO_4]^{2-}$, $[CrO_2Cl_2]$, $[CrO_3]$

Table 1.2 The oxidation states of chromium[1]

(a= tris(2-aminoethyl)amine $[N(CH_2CH_2NH_2)_3]$,b= acetylacetonate anion, c=propyl, d= mesityl, e= dibenzotetramethyltetraaza[14]annulene, f= ethylenediamine)

Chapter 2 focuses on the chemistry of Vanadium(V) which is diamagnetic. This allows more spectroscopic data to be obtained, to help determine the possible geometry of the complex synthesised. The use of vanadium(V) created problems as the complexes synthesised had significant sensitivity to moisture. For this reason vanadium(V) anions were also made, as they would be the more likely products of the hydrolysed $VOCl_3$ starting material.

The uses of vanadium(III) and chromium(III) with macrocyclic ligands allowed comparisons between the complexes synthesised. Anhydrous complexes were synthesised along with their aqua analogues and the analytical and structural data obtained show unexpected trends- this is further explained in Chapter 3.

1.2 HSAB theory[2]

R. G. Pearson introduced the theory of Hard/Soft Acid/Base theory, where substances were classified as hard acids, hard bases, soft acids and soft bases.[3] Originally substances were named by class; class a (hard) and class b (soft) this was introduced by Ahrland, Chatt and Davies.[4] HSAB theory was based on the principle of energy produced during the formation of a complex, which is measured as an equilibrium constant K_f. For hard acids it was observed that they bind to halides in the order seen in Fig 1.1 and the soft acids bind in an opposing manner.

HARD ACIDS $I^- < Br^- < Cl^- < F^-$

SOFT ACIDS $F^- < Cl^- < Br^- < I^-$

Fig 1.1 Binding abilities of halides to hard and soft acids

It has been observed that hard acid cations tend to form complexes with simple electrostatic interactions, whereas soft acid cations form complexes with covalent bonds. Hard acids, which are electron pair acceptors, have low-energy unfilled orbitals and therefore are unable to form covalent bonds readily with bases. Hard bases are electron pair donors which also have no high energy orbitals and are therefore not able to form covalent bonds either. The acids and bases are more often positively and negatively charged and thus form ionic bonds. Soft acids tend to have low-energy orbitals which are

unfilled allowing covalent bonds to form and soft bases have high energy filled orbitals also allowing the formation of covalent bonds to occur.

From this it was seen that hard acids tend to bind to hard bases and soft acids bind to soft bases. The classification of hard and soft acids is decided by the thermodynamic stability of the formed complexes and some of the classifications can be seen in Table 1.3.

	Hard	**Borderline**	**Soft**
Acids	H^+, Li^+, Na^+, K^+, Be^{2+}, Mg^{2+}, Ca^{2+}, Cr^{2+}, Ti^{4+}, Cr^{3+}, Al^{3+}, SO_3, BF_3	Ni^{2+}, Fe^{2+}, Cu^{2+},Co^{2+}, Pb^{2+}, Zn^{2+}, SO_2, BBr_3	Tl^+, Cu^+, Au^+, Ag^+, Pd^{2+}, Pt^{2+}, Cd^{2+}, Hg^+, Hg^{2+}, BH_3
Bases	F^-, HO^-, NO_{3-}, H_2O, O^{2-}, NO_3^-, PO_4^{3-}, SO_4^{2-}, ClO_4^-	Br^-, $\underline{N}O_2^-$, N_2, N_3^-, SO_3^{2-},C_6H_5N, $SC\underline{N}^-$	H^-, R^-, I^-, $\underline{S}CN^-$, R_3P, C_6H_6, R_2S, $\underline{C}O$, $\underline{C}N^-$

Table 1.3 Hard/soft acid/bases

Bonding interactions observed between hard acids and hard bases closely resemble ionic or dipole-dipole interactions. This is not the same for the softer acids and bases because they are more polarisable and so take on more covalent characteristics between the two groups. Other things such as rearrangement of the substituents, steric repulsion and competition for solvent can affect the equilibrium constant and thus effect the Gibbs energy, which is used to determine the stability of the complex formed. This phenomenon of HSAB theory is used to explain certain aspects of geochemistry, such as the Goldschmidt classification. It is seen that there are two main types of elements the lithophile and chalcophile elements. The lithophile elements are found within the earth's crust, these are types of silicate minerals, which can include lithium, magnesium, titanium, aluminium and chromium. They are all found as cations and are considered as hard acids. The chalcophile elements are found as sulfide minerals which include cadmium, lead, antimony and bismuth. They are formed as cations and are considered as soft acids. The lithophiles are associated with hard bases such as O^{2-} and chalcophiles with soft bases

such as S^{2-}. The zinc cations are classified as borderline and so can form either with hard or soft bases.

The hard metals are seen to have high positive charge, this means that the valence electrons are held more tightly, and so any metal-ligand bonding is seen to be ionic. Hard metals tend to favour hard donor atoms, which have high electronegativity, such as oxygen or nitrogen. The soft metals have low positive charge and therefore a low charge density, making them easily polarized. Any metal-ligand (soft donor atom) bond formation tends to have covalent characteristics.[5]

1.3 Vanadium

Vanadium is a Group five transition metal element.[6] It can adopt various oxidation states (Table 1.1) ranging from -1 up to +5, these oxidation states will vary depending on the ligand used.[7] Vanadium was discovered by Sefstöm in 1831,[8] it can be found within the earth's crust and the sea (conc. ~ 2ppm).[8] Vanadium is most commonly extracted from the mineral vanadinite. Trace amounts of vanadium can also be found in various foods and consequently within the body, where it is used in a variety of physiological roles. This is one reason why it is of interest to scientists. There is a need to know what role the element plays within our bodies.[9]

1.3.1 Vanadium(V) Chemistry

$VOCl_3$ is commercially available and is the starting material for the complexes obtained within Chapter 2 of this Thesis. It is a yellow liquid that is highly moisture sensitive and easily hydrolysed. The metal centre has C_{3v} symmetry and is sometimes seen to produce unwanted by products such as $[VOCl_4]^-$ and $[VO_2Cl_2]^-$, when in the presence of water.[10,11] Vanadium(V) has not been fully studied previously due to its instability, complexes were found to decompose in a matter of hours not allowing full analysis to be obtained. Further information on vanadium(V) complexes can be seen in Chapter 2 (2.1.1 Vanadium(V) chemistry).

1.3.2 Vanadium(IV) Chemistry

Oxovanadium(IV) has been used along with picolinate ligands in the hope it might behave as an insulin-mimetic, which would provide an oral alternative to the injection. [12] Vanadium(IV) has also been used with both hard and soft donor atoms, this has occurred by reducing the $VOCl_3$ starting material to $VOCl_2$ using mild conditions.[13] Complexes with ligands such as Et_3N, py, MeCN and PhCN have been obtained by this method.[13] Complexes such as $[VOCl_2(py)_2]$ [14], $[VOCl_2(tmen)]$ [15], $[VOCl_2(Ph_3PO)_2]$ [16] and $[VOCl_2(py)_3]$ [17] have also been synthesised providing analytical data on vanadium(IV) species.

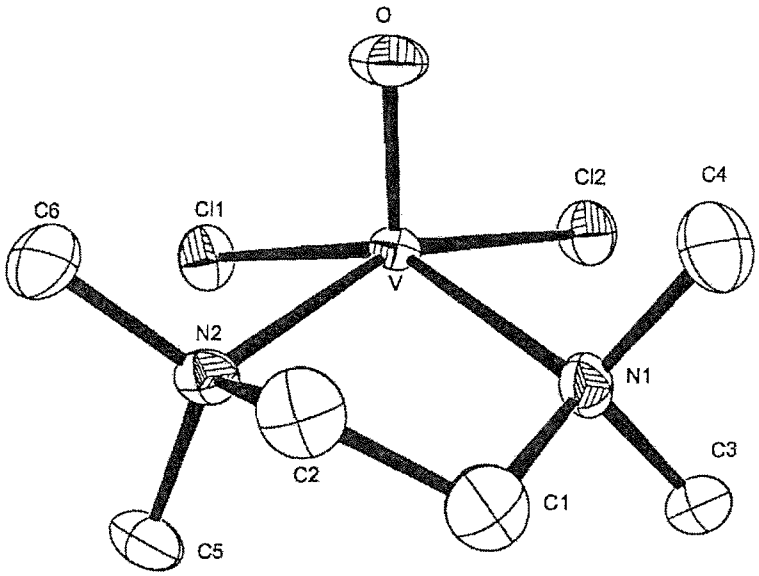

Fig 1.2 Structure of $[VOCl_2(tmen)]$[15]

By reacting $VOCl_3$ with tmen in mild conditions the vanadium(V) metal centre was reduced to vanadium(IV). The vanadium(IV) metal centre is observed to be five coordinate with a square pyramidal geometry see Fig 1.2. The oxygen occupies the axial position and the chlorines are present in the *trans* position to the tmen N-donor atoms. The vanadium was observed to be raised out of the plane, which had been formed by the nitrogen and chlorine atoms.

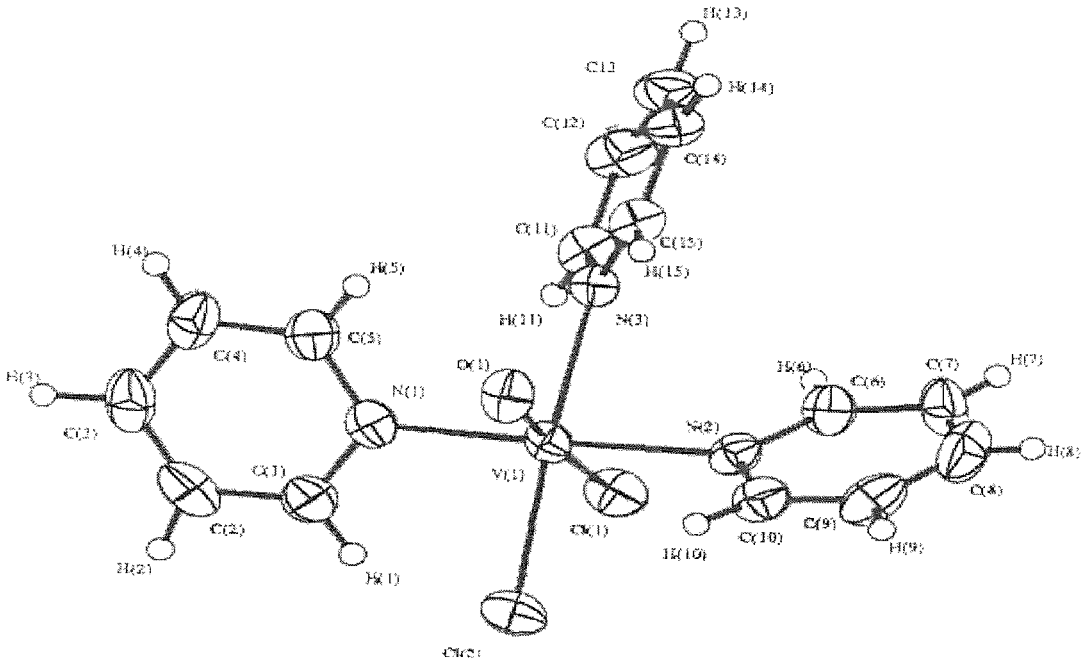

Fig 1.3 The crystal structure obtained for the complex $[VOCl_2(py)_3]$[17]

Motevalli *et al.* obtained the crystal structure of $[VOCl_2(py)_3]$, which is seen in Fig 1.3. The bond angles were consistent with the complex containing a distorted octahedral geometry around the vanadium metal centre.[17] The pyridines were observed to occupy meridional positions with chlorines that were *cis* to each other, one was observed to be *trans* to the vanadyl oxygen. Along with the ligands mentioned so far, vanadium(IV) metal centres have been used to form complexes with macrocycles such as the hard crown ethers 15-crown-5[18] and soft thioethers [9]aneS$_3$ $[VOCl_2([9]aneS_3)]$.[19] Vanadium(IV) complexes with mixed donor macrocycles such as [9]aneN$_2$S have also been synthesised, e.g. $[VOCl_2([9]aneN_2S)]$.[20]

1.3.3 Vanadium (III) Chemistry

$[VCl_3(thf)_3]$ is the most common choice of starting material, it is a dark red coloured solid, which when combined with a macrocycle such as 15-crown-5, can take on a pink colour. Vanadium(III) has been of interest to scientists especially with its potential ease of extracting sulfur from crude oil, due to the binding of sulfur to vanadium, this is covered further in Chapter 3 (3.1.1 Vanadium(III) Chemistry). $[VCl_3(thf)_3]$ has been used as one

of the main starting materials in reactions, including the reaction with macrocycles such as 18-crown-6[21] and [9]aneN$_3$.[22]

Macrocycles containing sulfur donor atoms have also been reacted with vanadium(III), supporting the idea that soft atoms can form strong bonds with hard metal centres.[23] Other complexes have been formed incorporating [10]aneS$_3$[24] or [18]aneS$_6$.[24] In all these instances it was observed that under careful experimental conditions, especially stringent avoidance of protic solvents, the vanadium(III) metal centre formed bonds readily with the thioethers even though this was not expected due to HSAB theory.

1.4 Chromium

Chromium was first discovered by Nicolas Louis Vauquelin in 1798, when he detected the element in the Pallas meteorite.[8] Chromium is a hard transition metal which is part of the Group 6 elements[6] and has been used previously due to its high kinetic inertness and its ability to stabilise the complexes that are synthesised. Chromium can exist in various oxidation states (Table 1.2), ranging from -4 to +6, the most common forms are +2 and +3.[25] Chromium is obtained from the mineral chromite or from chrome ochre.[26]

1.4.1 Chromium(III) Chemistry

Chromium(III) in the form [CrCl$_3$(thf)$_3$] has been shown to be a useful sython used with many ligands. Chromium complexes have been synthesised using a variety of hard and soft donor atoms such as 15-crown-5 and tetrahydrothiophene ligands.[27,28] Willey *et al.* successfully synthesised a [*mer*-CrCl$_3$(tetrahydrothiophene)$_3$] complex.[28] Harder O– donor macrocycles have been used with [CrCl$_3$(thf)$_3$], for example 15-crown-5, the crystal structure is seen in Fig 1.4.[27,29]

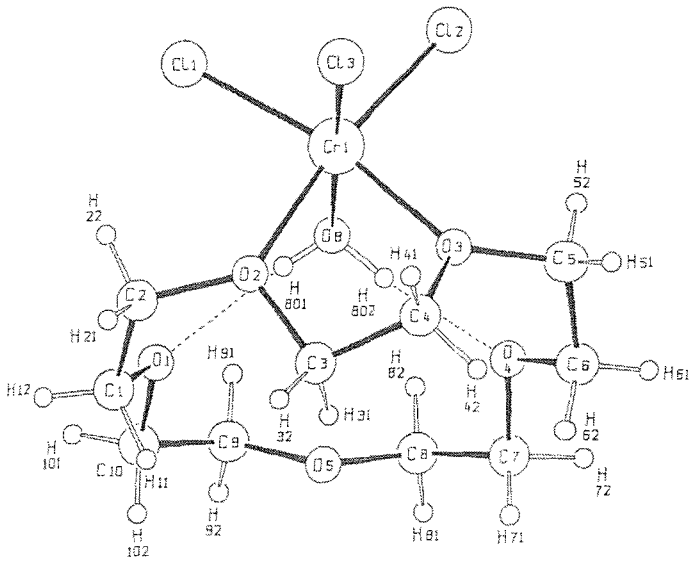

Fig 1.4 The structure of $[CrCl_3(H_2O)(15\text{-crown-}5)]$[27]

In Fig 1.4 the chromium metal centre is coordinated to two ether crown oxygen atoms and one water molecule, which is then hydrogen bonded to the macrocycle O-donor atom. This molecule shows the metal centre is coordinated to the macrocyclic ligand *via* primary and secondary coordination. Primary coordination involves a direct bond between the metal and the O-donor atom of the crown ether and a secondary coordination occurs when there are water molecules coordinated to the metal centre which are then attached to the crown ether O-atoms *via* hydrogen bonding. Other examples of this are discussed in Chapter 3 (section 3.1).

$[CrCl_3(thf)_3]$ has also been used to investigate the possibilities of binding with soft ligands such as thioether crowns, [9]aneS$_3$,[30] [10]aneS$_3$,[30] [18]aneS$_6$[30] and [14]aneS$_4$[31]giving both neutral and cationic species. In some incidences the $[CrCl_3(thf)_3]$ starting material has been observed to form complexes with some very soft ligands, such as [16]aneSe$_4$ giving $[CrCl_2([16]aneSe_4)]PF_6$.[32]

1.5 Ligands

During the course of this Thesis vanadium(V) complexes were synthesised with either monodentate, bidentate or macrocyclic ligands to give either a 5- or 6-coordination

geometry around the metal centre. The ligands possessed hard and soft donor properties, to test the boundaries of hard soft acid base theory (section 1.2). Complexes with softer ligands such as thio- and seleno- ethers tend to be dominated by the middle and late transition metals, with medium oxidation states. They have also been reacted with early transition elements such as Ti(IV)[33] and Mo(VI).[34]

1.5.1 Monodentate Ligands

Monodentate ligands are bound to metal centres *via* just one donor.[2] In this Thesis monodentate ligands such as py, Me_3PO, Ph_3AsO and Ph_3PO have been used to test their abilities to bind *via* a 1:1 or 1:2 ratio with the metal centre.

1.5.2 Bidentate Ligands

Bidentate ligands bind to a single metal centre simultaneously *via* two heteroatoms. Bidentates can either form chelate rings when coordinated to one metal or bridges between two metal centres. They have been used within this Thesis to gain spectral analysis on a full series of ligands. There is limited spectroscopic data available on the $[VOCl_3(bipy)]$ complexes in the literature so this made part of the N-donor atom ligand series.[35,36] One advantage of the use of bidentate ligands is the presence of the chelate ring mentioned previously, this creates what is known as the chelate effect (section 1.5.3 Chelate Effect). The chelate effect can help stabilise the more unusual combinations of softer S-donor atom ligands with hard metals, e.g within Chapter 2 the complex $[VOCl_3(MeSCH_2CH_2SMe)]$ was synthesised.

1.5.3 Chelate effect

When a bidentate ligand binds to a metal centre a ring is formed (Fig 1.5) this is known as a chelate ring.

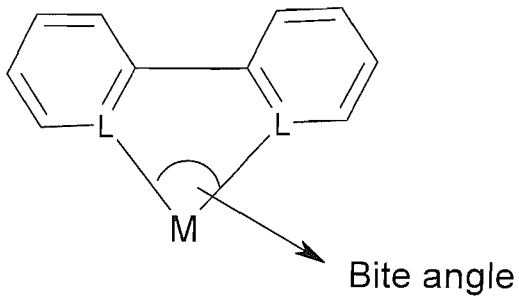

Fig 1.5 Bidentate ligand bound to a metal centre

Fig 1.5 shows illustration of a 5-membered ring. The chelate ring can aid in the stability of the complex which is formed, and this increase in stability, compared to a complex with monodentate ligands, i.e. $[M(L)_2]$, is known as the chelate effect. The phenomenon is observed to increase the stability of a complex when there is an increase in the number of chelate rings.[37] Within the chelate ring a L-M-L bond angle is created which is referred to as the bite angle. In most six coordinate species the theoretical bite angle is 90°, but certain ligands can alter this value creating a strain on the complex formed. When using ligands such as phen, there is more strain in the complex due to the more rigid back bone present (Figure 1.6).

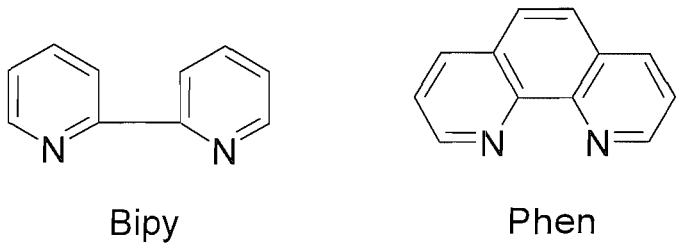

Fig 1.6 Bipy and phen complexes showing the difference in back bone

In a bidentate ligand with a rigid back-bone the ligand may be preorganised for chelation, meaning that the ligand has to bind with a certain bite angle. This can mean that the bite angle could be observed to be greater or lower than 90°, and this will affect the geometry around the metal centre and may affect the properties and reactivities of the complexes obtained.

1.6 Macrocycles[37]

Macrocycles are cyclic polydentate ligands which contain donor heteroatoms. A macrocycle is usually defined as containing at least nine atoms, but occasionally there can be as many as thirty three atoms. Macrocycles play key roles in natural processes as in the cytochrome P-450. Cytochrome P-450 is an enzyme which contains mono-oxygenases, these can catalyse many oxidation reactions and are capable of cleaving CH -bonds within aromatic systems. The cytochrome P-450 contains one haem group, this is the macrocyclic part of the complex which holds the Fe(III) ion in place.

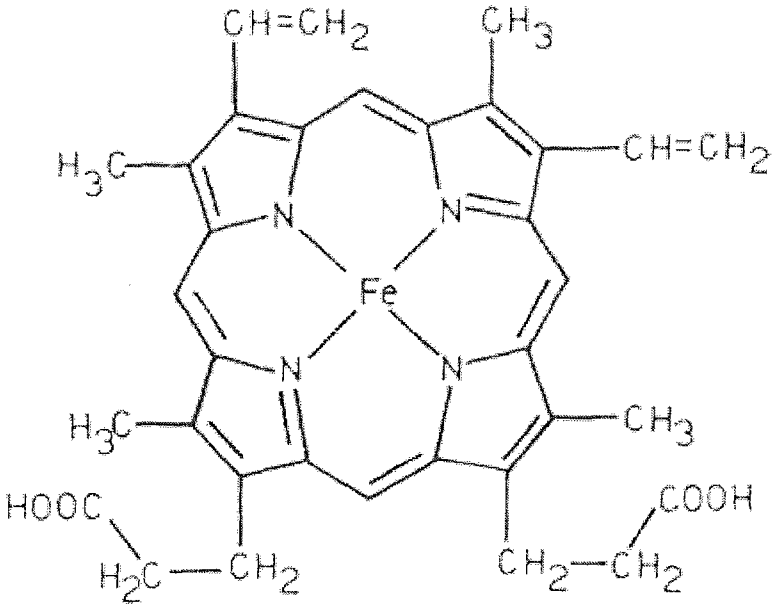

Fig 1.7 Haem group bound to the Fe(III) metal.

The Fe(III) present within cytochrome P-450 has one axial site which is occupied by cysteine sulfur. The catalytic cycle investigated by Groves *et al.* can be seen in (Fig 1.8).[38]

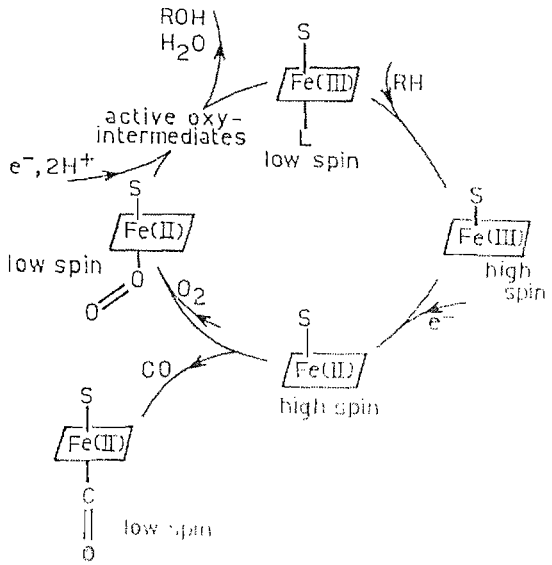

Fig 1.8 Catalytic cycle for the cytochrome P-450 (S = cysteine)

The iron is reduced from low-spin Fe(III) to high-spin Fe(II). With the addition of an O_2 molecule the high-spin Fe(II) converts to a low spin resting state. Then a process of hydroxylation occurs causing the activated dioxygen to react to the substrate and the O-O bond to cleave. The hydroxylation plays a large role in our kidneys; this process can create an increase in the substrates solubility in water, substrates such as foreign substances, which allow them to be, excreted from the body more efficiently.

Macrocycles also play an important role within photosynthesis and within our bodies for example as means to transport oxygen around the body in haemoglobin. The reason that macrocycles are useful within these roles is due to their enhanced kinetic inertness and thermodynamic stability of their metal complexes, this allows them to bind to metal ions securely, and hence there is much interest in this area of chemistry. Crown ethers are used within solvent extraction procedures as they allow the selective transfer of metal ions from water to organic phases based upon the match between the macrocycle cavity size (binding site) and the metal ion radius.

1.6.1 Macrocyclic Effect[37]

Work by Cabbiness and Margerum demonstrated the macrocyclic effect when using the Cu(II) complex of a reduced Curtis macrocycle compared to the open-chain analogue.[39]

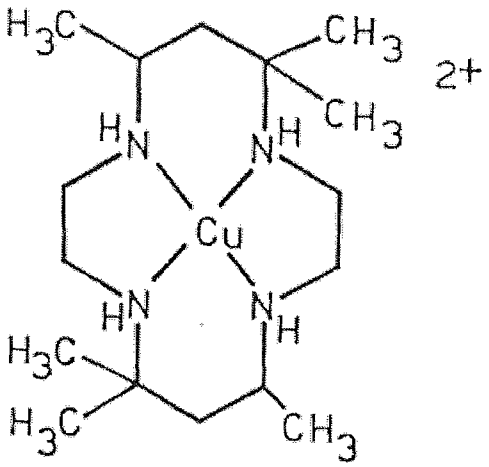

Fig 1.9 Reduced Curtis macrocycle.[39]

Thermodynamic aspects of macrocycles and metal ion interactions have been studied such as the behaviour of cyclic ligands compared to the open chain analogues. The required stability constant can be calculated by the equation:

$$M + L \rightleftharpoons ML$$

$$K = \frac{[ML]}{[M][L]}$$

If the stability constant values are measured along with enthalpy then entropy values can be calculated using the equation:

$$\Delta G = \Delta H - T\Delta S$$

G= Gibbs free energy
H= Enthalpy
T = Temperature
S = Entropy

Open-chain and macrocyclic N_4 donor systems were compared to see if ΔH values could determine if entropy or enthalpy was the most important aspect macrocyclic stability. The

experiments were performed in an aqueous media, under basic conditions. This allowed the metal ions which were either nickel(II) or copper(II) to be present as hydroxo species. The enthalpy change associated with the reaction was determined calorimetrically and showed that the entropy term contributes greatly to the macrocyclic effect.

Micheloni *et al.* observed that for Ni(II) species the enthalpy and entropy terms both contributed to the stability of the macrocyclic complex *via* template assistance, with the entropy term dominating the macrocyclic effect (Table 1.4).[40]

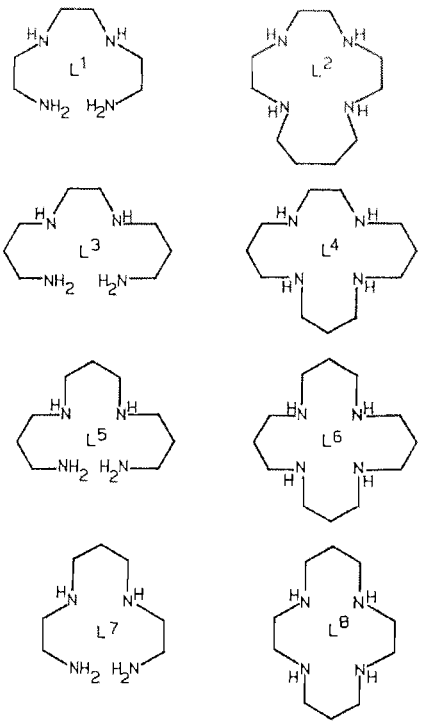

$$[NiL_{oc}]^{+2} + L_{mac}^{2+} \rightleftharpoons [NiL_{mac}]^{2+} + L_{oc}$$

(oc = open chain and mac = macrocyclic)

L_{oc}/L_{mac}	$-\Delta G/KJmol^{-1}$	$\Delta H/KJmol^{-1}$	$T\Delta S/KJmol^{-1}$
L^1/L^2	2.43	5.1	7.4
L^3/L^4	21.05	5.3	26.4
L^5/L^6	15.69	3.5	19.2
L^7/L^8	33.67	-20.5	13.2

Table 1.4 The illustration of the macrocyclic effect with a selection of tetraaza macrocycles and their open chain analogues using high-spin Ni(II) metal centre.[40]

These values were compared along a series of complexes and it was observed that the enthalpy and entropy terms contribute to the complex stability in different capacities along the series used. It is observed that when the entropy term is larger the macrocyclic effect is greater; if the enthalpy term is negative the macrocyclic effect is greater also. If the enthalpy value is positive it will decrease the value of ΔG and thus lower the macrocyclic effect. Therefore the higher value of the entropy value is usually the favourable factor to create the overall observed macrocyclic effect.

1.6.2 Macrocyclic Synthesis

There are a variety of methods used in the synthesis of macrocycles, such as high-dilution and template synthesis. High dilution often involves the relevant fragments required for the macrocycle being combined in a 1:1 condensation reaction. This process tends to favour the half condensed species reacting with itself in a cyclisation process rather than forming with another molecule in an intermolecular condensation reaction, which would result in polymerisation. Dilute solutions of reactants are added at the same rate but slowly to allow concentrations of the unreacted reagents to be extremely small at any given time during the synthesis. This allows high yields of macrocycles to be formed due to the cyclisation process being statistically more probable than oligomerisation or polymerisation (Fig 1.10).

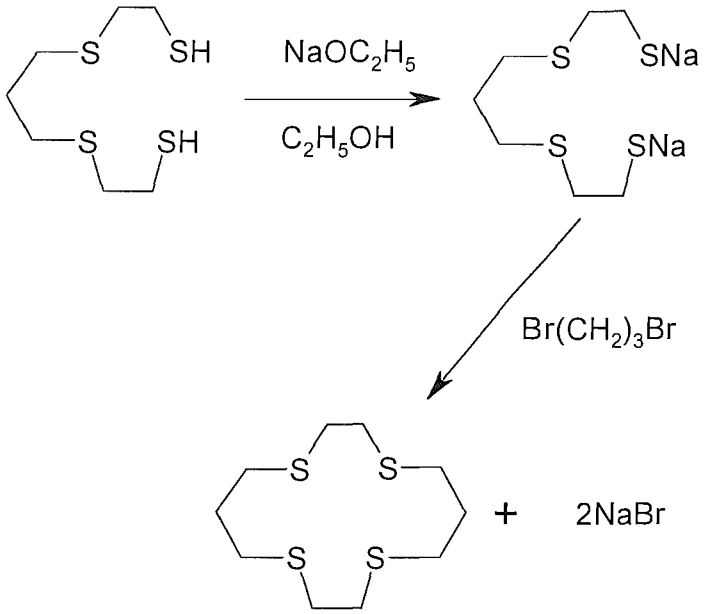

Fig 1.10 Synthesis of [14]aneS_4

Problems that arise from this technique are the production of undesirable products such as polymerised molecules, the need for large quantities of solvent and the lack of stereochemical control resulting in variable yields.

Metal-ion template synthesis was the first technique used to produce a macrocycle in 1928.[37] This was achieved by reacting phthalic anhydride and ammonia in an iron vessel. The expected phthalimide had not been achieved instead the phthalocyanine macrocycle was isolated. This had similar properties to the porphyrin systems which are found within nature. There is no single method that can be assigned to all the complexes though the procedure has occurred more widely for macrocyclic systems since 1960 when Curtis discovered a way to synthesis Ni(II) macrocyclic complexes using this method.[41] Now this method has been adapted for use to synthesise a selection of macrocycles such as [9]aneS_3 see Fig 1.11 for the synthetic route.

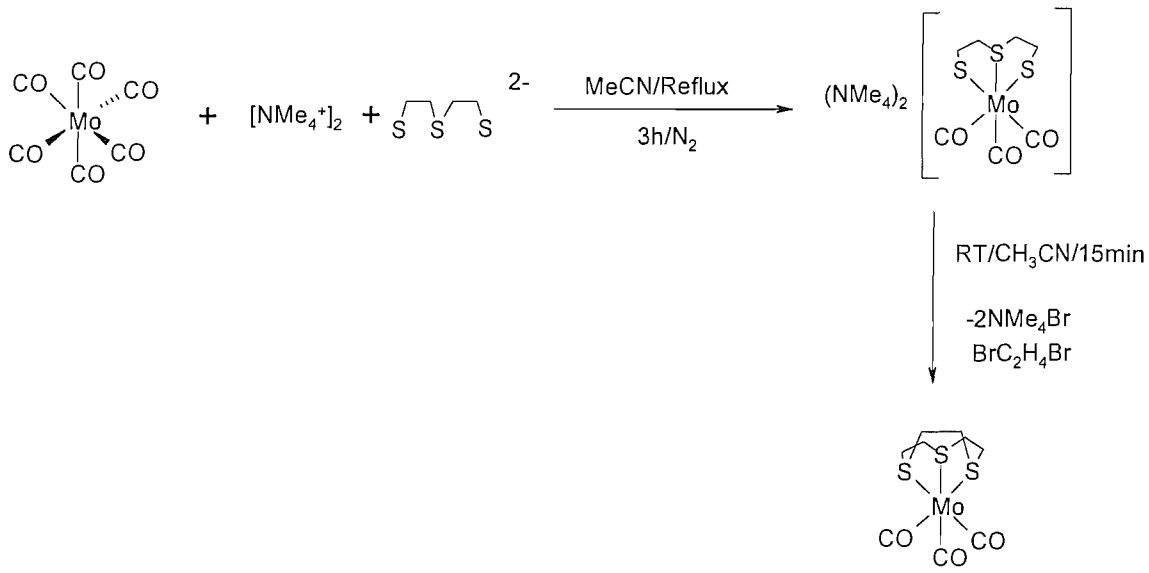

Fig 1.11 Template process for producing [9]aneS_3[42]

The template synthesis is aided by the addition of the metal ion helping to promote the cyclisation process which is required for the synthesis of the macrocycle. The role of the metal ion within this process has been previously investigated and there are two main effects that the metal ion has within the synthesis of the macrocycle, they are the kinetic template effect and the thermodynamic template effect. The thermodynamic template effect means that the coordinated macrocycle is favoured and therefore the equilibrium position within the synthesis is pushed in favour of the macrocycle formation and the kinetic template effect creates a favoured environment for the formation of the cyclic product.

1.6.3 Crown Ethers[43]

Crown ethers are usually obtained by metal-ion template synthesis e.g. 18-crown-6 uses K^+ ions to help promote cyclisation, this was made by Green in 1972.[44] The crown ethers were first synthesised in 1967 by C. J. Pedersen, he isolated the macrocycle 18-crown-6.[1] The synthesis of the crown ether macrocycles are now almost all based on this original procedure. Crown ethers are normally obtained by Group 1 metal ion template assisted cyclisation reactions e.g. Fig 1.12 or by ring expansion of epoxides in the presence of Group 1 metal ions.

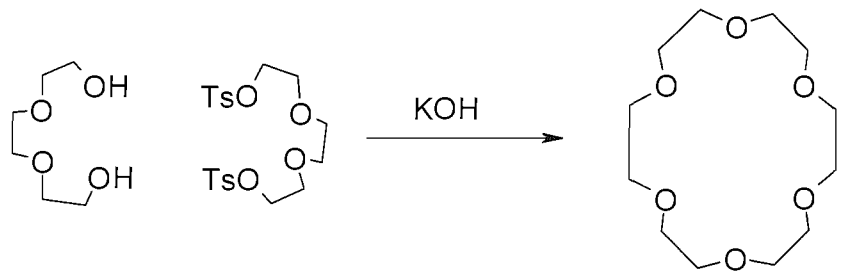

Fig 1.12 The synthesis of 18-crown-6.[45]

Li^+ ions have been used in the synthesis of 12-crown-4 and Na^+ ions for 15-crown-5, these two macrocycle formations were perfected by Cook *et al.* in 1974.[46] This interaction of the crown with the metal ion is weak, work by Pederson showed the ether oxygen interactions with the metal cations were essentially electrostatic.[47]

These ligands possess the hard oxygen donor atoms and are therefore expected to bind to hard metal centres according to HSAB theory. The majority of coordination studies with these ligands involve Group 1 and Group 2 metal ions, and the ability of the ligands to selectively bind to specific metal ions from mixtures, has led to significant interest and research activity within this area. The chemistry of crown ether macrocycles with early transition elements has been much less studied, however, complexes such as $[TiCl_3(H_2O)(18\text{-crown-6})]$ have been isolated and single crystal X-ray diffraction data obtained.[48] It was observed that the Ti(III) metal centre was bound *via* primary and secondary coordination to the O-donor atoms within the crown ether ligand. The crystal structure can be seen in Fig 1.13. A more detailed discussion of early transition metal crown ether complexes is presented in Chapter 3.

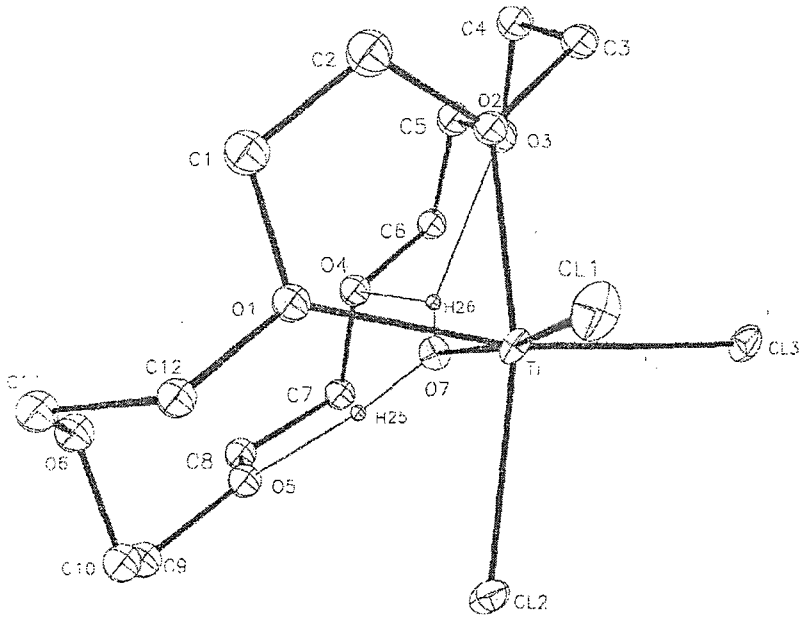

Fig 1.13 Crystal structure of $[TiCl_3(H_2O)(18\text{-crown-}6)]$[48]

1.6.4 Thioether Crowns

Most sulfur donor macrocycle systems are synthesised using high dilution techniques except [9]aneS_3 which can use either template-ion synthesis (Fig 1.11) or high dilution synthesis. Other S-donor atom macrocycles that maybe produced using template methods are dibenzo-[18]aneS_6 and dibenzo-[15]aneS_5.[49]

Thioether macrocyclic chemistry has been previously limited to mainly middle and late transition metals with low or medium oxidation states. There are a few exceptions such as $[VCl_3([9]aneS_3)]$,[24] $[VOCl_2([9]aneS_3)]$[24] and *cis*-$[CrCl_2([14]aneS_4)]PF_6$[50]. One observation is that the thioether macrocyclic ligands are capable of stabilising unusual oxidation and/or reduction of the products. Thioethers can also undergo a chemical transformation itself when bound to a metal centre. One example occurs within the complex $[Rh([9]aneS_3)_2]^{3+}$, which can undergo a α-carbon deprotonation which opens the ring to produce the vinyl thioether complex $[Rh([9]aneS_3)\{S(CH_2)_2S(CH_2)_2SCH{=}CH_2\}]^{2+}$. Coodination complexes of [12]aneS_4 usually adopt a folded conformation of the macrocycle on octahedral metals, which allows two *cis* coordination sites free for co-ligands this was observed in the complex $[Ru([12]aneS_4)(dmso)Cl]^+$ (Fig 1.14).[51]

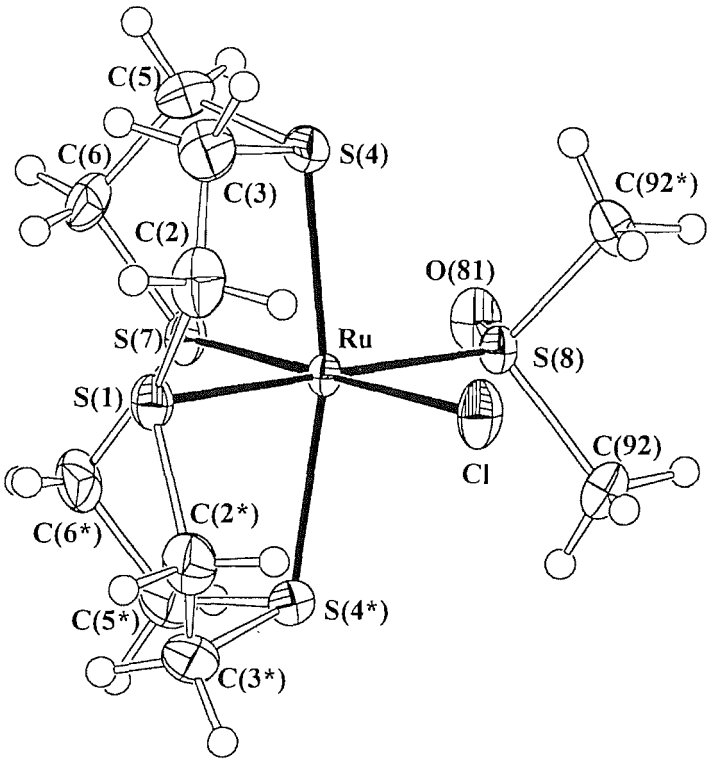

Fig 1.14 The structure of $[Ru([12]aneS_4)(dmso)Cl]^{+}$ [51]

The complex in Fig 1.14 shows the Ru is in a distorted octahedral geometry, with two sulfur atoms from the thioether macrocycle; one chlorine and one sulfur from the dmso are all present on the equatorial plane. The two remaining sulphur atoms within the thioether macrocycle then occupy the axial positions. [51]

The use of the macrocyclic ligand helps stabilise complexes which would otherwise not form with the open chain analogues. These ligands have been used in past complexes, with hard metals such as chromium, e.g. $[CrBr_2([14]aneS_4)][PF_6]$. [52]

1.6.5 Mixed donor macrocycles[43]

Mixed donor macrocyclic systems made and used within this Thesis were prepared from literature methods involving the high dilution method (Chapter 3). Mixed donor macrocycles are useful when investigating hard and soft donor ligands with transition metals as they bring together the two types of donor ligand in close proximity. This allows new types of selectivity to occur with metal ion bonding such as Pt(IV) with mixed

macrocycles containing hard N-donor atoms and soft S-donor atoms in the complex $[PtBr_3([9]aneSN_2)]^+$. [53] Chapter 3 describes $[9]aneS_2O$, $[15]aneS_2O_3$ and $[18]aneS_3O_3$, which were made using literature routes, which were similar to high dilution syntheses.[54] The reaction scheme for $[15]aneS_2O_3$ and $[18]aneS_3O_3$ can be seen in Fig 1.15.

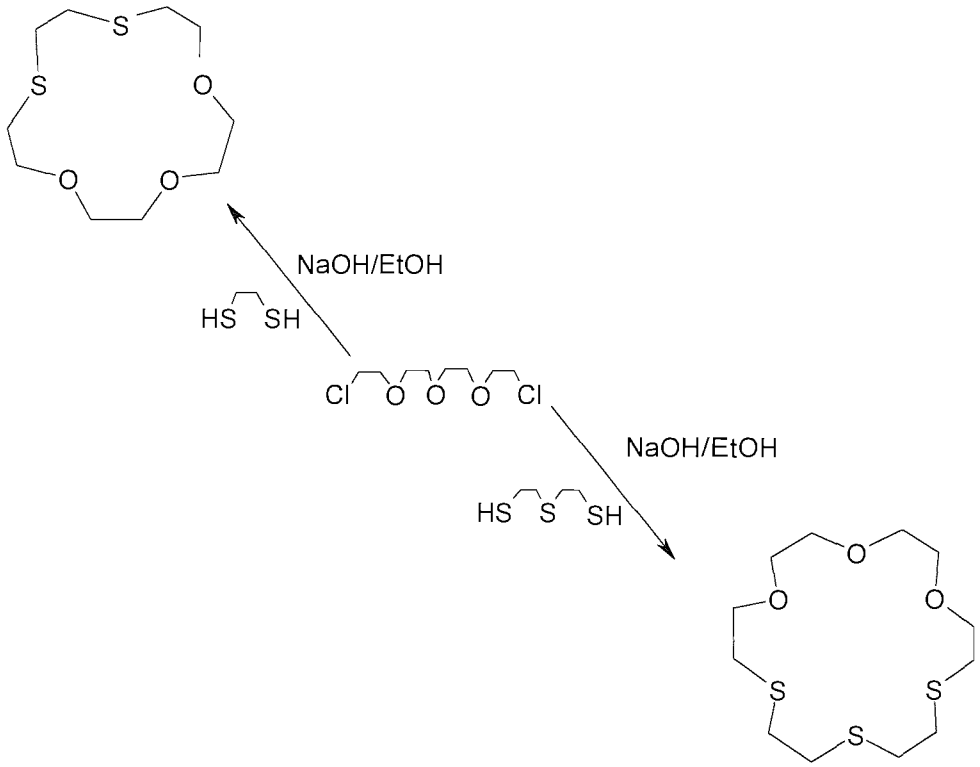

Fig 1.15 Reaction scheme for the preparation of $[18]aneS_3O_3$ and $[15]aneS_2O_3$

The soft sulfur and hard oxygen donors can be brought together in the same macrocycle, giving the metal centre the choice of donor, but in the same vicinity. These types of macrocycles have been used previously with other soft metals such as Ru(II) in the complex $[RuCl(PPh_3)([15]aneS_2O_3)_2]^+$,[55] Pt(II) in complex $[PtCl_2([15]aneS_2O_3)]^+$[55] and Pd(II) in complex $[PdCl([18]aneS_3O_3)]^+$.[56]

1.7 Metal Thioether Bonding[57]

Sulfur is part of the Group 16 elements. The thioether ligands only carry two R subsituents and thus steric effects are observed to be less important than within the phosphine ligands. Thioether ligands such as R_2S have two lone pairs on the sulfur atom.

One lone pair is observed to form σ- bonds to a metal acceptor, while the second lone pair can form a second σ- bond with an additional metal acceptor creating a bridging group, or it can act as a π-donor, to electron poor metals. The sulfur atom may behave as a π-acceptor, by accepting electrons into the lowest empty *d*-orbital or into the S-C σ^* orbital, the latter is considered the more feasible process due to the energy compatibilities. In certain instances such as the presence of an electron rich metal the second lone pair would be a source of π-repulsion. Even though the π-acceptance has been thought to have been of little relevance to the bonding of acyclic thioether ligands it is now thought to be of importance in the binding of thioether crowns in certain systems.[58]

Schumann *et al.* observed that the Fe-E bond (in low valent iron systems) increased in stability and inertness during the progression down the Group 16 elements (Te>>Se>S>O). The increased strength of the binding of telluroethers was attributed to an enhanced σ-donation.[59] This was further supported by NMR and IR analysis which had shown an increase of electron density around the metal centre, down the group (Te>>Se>S>O). This was observed with metals such as Mn(I), Re(I), Cr(0), Mo(0) and W(0). Connolly *et al.* showed that the complexes *fac*-$[MX(CO)_3(E\text{-}E)]$ (M = Mn or Re; X = Cl, Br or I; E-E = dithio, diseleno- or ditelluro- ether) were consistent with E→Mn σ donation increasing down Group 16.[60] This observation is thought to be due to a decrease in electronegativity from S to Se to Te. Low valent metals allow good overlap of the d-orbital with the σ-orbital of the ligand, but when there is a higher oxidation state in the metal, the orbital is contracted meaning a reduction in this overlap. It is therefore thought that this is the explanation as to why the Te donor atom is not seen to bind to Pt(IV), whereas the thioethers and selenoethers are capable of binding e.g. in $[PtX_2([n]aneS_4)]^{2+}$ and $[PtX_2([16]aneSe_4)]^{2+}$ (where X = Cl or Br; n = 12, 14, 16).[61]

$MeECH_2EMe$ will tend not to chelate with a metal centre *via* the two E groups but instead will act as a bridging ligand between two metal centres, this is due to the strain that is present with 4-membered chelate rings. There are exceptions to this observation such as $[SnCl_4(MeECH_2EMe)]$ (where E= S and Se) which have been obtained.[62] Thioethers have been seen to coordinate harder metals from the early d-block elements, such as Ti(IV) and

Zr(IV) to form the complexes $[TiCl_4(MeS(CH_2)_2SMe)]$ and $[ZrCl_4(MeS(CH_2)_2SMe)]$, this occurs under strictly anhydrous conditions.[52]

1.8 Pyramidal inversion[57]

Pyramidal inversion is defined as an interchange between two configurations that are energetically equivalent *via* a planar transition.[63] This process is observed in complexes containing thioether, selenoether or telluroether ligands. Sulfur can bind *via* two lone pairs present on the atom, where one lone pair coordinates to the metal *via* σ-donation. When monodentate ligands are used such as SR_2 and the R groups are different then the coordination through one lone pair leads to chirality at the S position. The chirality can change *via* pyramidal inversion and this process may be observed *via* variable temperature NMR spectroscopy. For bidentate ligands four isomers are present in the solution, a pair of *meso* and a pair of *DL* enantiomers. These sterioisomers, also known as invertomers, can interconvert, *via* pyramidal inversion and is often observed to occur on the NMR timescale. The diastereoisomers produced by this process may be observed individually if the system is cooled, this cooling reduces the free energy below the activation energy needed for the inversion to take place. For a species such as $[VOCl_3(MeS(CH_2)_2SMe)]$ there are four possible invertomers that can be formed, Figure 1.16.

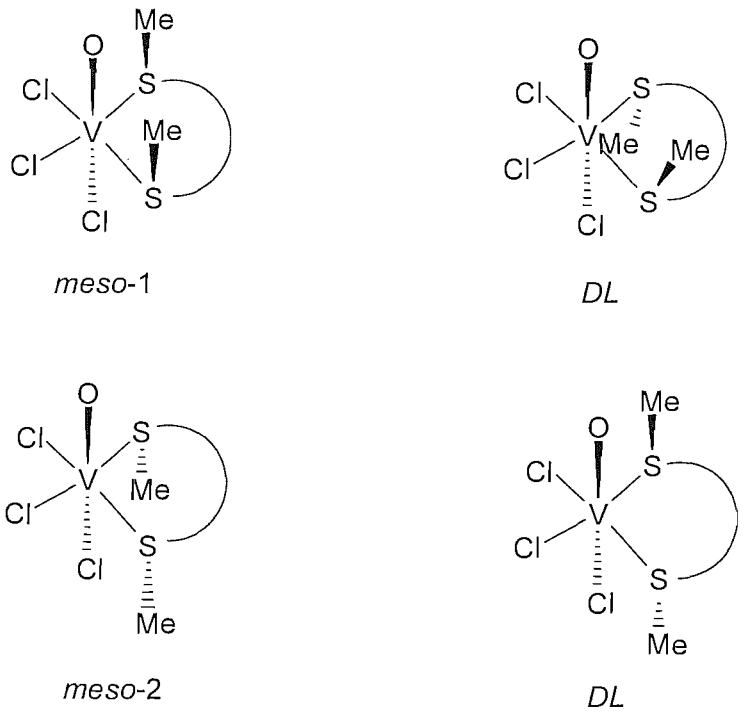

Fig 1.16 Four possible invertomers for *fac*-$[VOCl_3(MeS(CH_2)_2SMe)]$

Many factors can influence the energy barriers to pyramidal inversion, including the type of donor present S<Se<Te, the type of metal present and the oxidation state of the metal.[57] Also the *trans* ligand can influence the energy barrier required for the inversion, as well the substitution present on the E atom. The size of the chelate ring is also a factor. The process of pyramidal inversion is subtle, no bond cleavage is seen and no other reagent is needed for this action to occur. Work by Abel *et al.* on platinum(II) complexes such as $[PtCl_2(MeSCH_2CH_2SMe)]$ showed this phenomenon within their ^1H NMR studies.[63] Investigations into pyramidal inversion *via* NMR spectroscopy has allowed the *DL* and *meso* invertomers to be distinguished, but the two *DL* enantiomers are indistinguishable. The *meso* forms can also be indistinguishable if the axial ligands above and below the plane are the same.

1.9 Physical Measurements

The complexes synthesised during this Thesis were analysed *via* a range of methods. Microanalysis was performed by the University of Strathclyde for each complex. IR spectra and UV-vis spectra were obtained for each complex once they were isolated. The

vanadium(V) complexes were also analysed *via* NMR spectroscopy. In some instances single crystal X-ray diffraction data were obtained for some complexes where suitable single crystal could be obtained.

1.9.1 Nuclear Magnetic Resonance Spectroscopy

For the vanadium(V) complexes NMR spectroscopy was a key analysis performed as this allowed easy determination of the complex formed, showing whether the complex had hydrolysed to a vanadium(V) anion and if no peaks were present within the spectra this could be due to the metal centre being reduced to vanadium(IV) or vanadium(III), as both these species are paramagentic. Vanadium(III) and chromium(III) are both paramagnetic and hence NMR spectroscopy could not be performed.

1.9.1.1 *^{51}V NMR Spectroscopy*

^{51}Vanadium is quadrupolar with I = 7/2 and is 99.8% abundant. The typical chemical shift range is +800 to -1000 ppm. Vanadium(V) also has a small electric nuclear quadruple moment which allows the resonance signals to be relatively well defined.[64] NMR spectra were referenced to external neat $VOCl_3$.

1.9.1.2 *$^{31}P\{^1H\}$ NMR Spectroscopy*

^{31}P has a spin I = 1/2 and has a 100% abundance, as well as a receptivity related to the proton of 6.6 x 10^{-2}. This makes the nucleus very useful to study in compounds with a phosphorus atom. NMR spectra were referenced to external 85% phosphoric acid. The phosphorus resonances are able to couple to neighbouring protons which can be very useful when determining the geometry of complexes formed.[65]

1.9.2 Infra-Red Spectroscopy

For moisture sensitive species Nujol mulls are routinely prepared for IR spectroscopy and these have been used on previous complexes containing vanadium(III), vanadium(V) and chromium(III) metal centres. The spectra were obtained using CsI plates to allow spectra to be obtained in the region 4000-200 cm^{-1}. This allowed the metal-halide stretches to be observed in the far IR region and possible structural deductions to be made. It has been

observed that the V-Cl stretches and the Cr-Cl stretches lie within the region ~ 300-400 cm^{-1}.[16,28] The V=O stretch in the $VOCl_3$ complexes are typically seen ~1000 cm^{-1}.[66] The M-S bands are more difficult to assign as they tend to be weak and also fall around ~300-400 cm^{-1}. The species were analysed to identify the point group and then the reduction formula was used for each complex:[67]

$$n_i = \frac{1}{h}\Sigma g_i \chi_i \chi_r$$

χ_r= reducible representation
χ_i= irreducible representation
n = coefficient
h = number of operations
g = number of symmetry operations

$[VO_2Cl_2]^-$ contains a tetrahedral geometry around the vanadium metal centre which corresponds to C_{2v} and $[VOCl_4]^-$ contains a square pyramidal geometry around the vanadium metal centre, this corresponded to C_{4v}. The vanadium(V) complexes were all observed to possess an octahedral geometry and approximate in most cases to C_s, this is discussed further in Chapter 2. When the various point groups were used along with the reduction formula the IR active bands correspond to the V-Cl stretches and V=O stretches could be assigned.

Point group	V=O	V-Cl	Complex
C_{2v}	A_1, B_1	A_1, B_1	$[VO_2Cl_2]^-$
C_{4v}	A_1	A_1, E	$[VOCl_4]^-$

Table 1.5 The expected active bands for complexes made within Chapter 2.

The vanadium(III) and chromium(III) complexes possess octahedral geometries around the metal centre and equated to a point group of C_s in the cases of $[MCl_3(H_2O)(\kappa^2\text{-crown})]$ (where M = V or Cr; crown = 18-crown-6 and 15-crown-5). When the complex such as $[MCl_3(\kappa^3\text{-crown})]$ (where M = V or Cr; crown = 18-crown-6 and 15-crown-5), the metal

centre was seen to possess the similar octahedral geometry as the other complexes but due to the κ^3-coordination the point group approximates to C_{3v}. When the various point groups were used along with the reduction formula the following active bands were assigned to the M-Cl stretches (Table 1.6).

Point group	Y(M-Cl)
C_s	A', A', A''
C_{3v}	A_1, E

Table 1.6 The expected active bands for complexes made within Chapter 3.
M= V or Cr

1.9.3 UV-visible Spectra[68]

Analysis *via* solid and solution UV-visible spectroscopy was obtained on all complexes made within this Thesis. Solution UV-vis spectroscopy was not always a suitable method of analysis especially with complexes that were poorly soluble. The solution UV-visible spectra obtained relied on the use of Beer Lambert Law to calculate the extinction coefficient of the absorbance bands (Fig 1.17).

$$A=\log_{10}(I_0/I)=\varepsilon cl$$

ε= extinction coefficient
A= absorbance
c= molar concentration
l= path length

Fig 1.17 Beer Lambert Law[69]

1.9.3.1 Chromium(III)

Chromium(III) is a d^3 metal which has the free ion ground term ^4F, when in a complex possessing an octahedral environment the ground term is $^4A_{2g}$. This ground state creates three possible spin allowed transitions:

$$^4A_{2g} \rightarrow {}^4T_{2g}$$

$$^4A_{2g} \rightarrow {}^4T_{1g}(F)$$

$$^4A_{2g} \rightarrow {}^4T_{1g}(P)$$

From these transitions the following energy level diagram can be obtained, showing the expected energy levels for complexes with octahedral environments and C_{3v} symmetry (Fig 1.18).

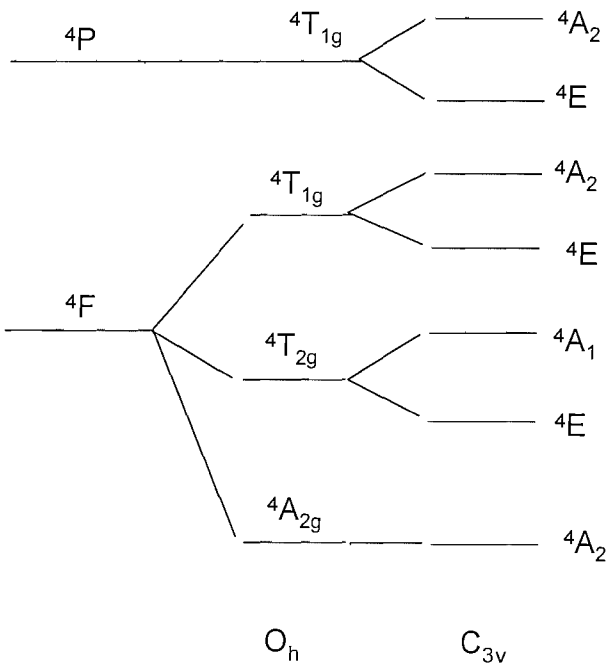

Fig 1.18 Diagram of the energy levels present for ^4F and ^4P metals[68]

Hence in a C_{3v} species the transistions are expected to split compared to a genuinely O_h species. However since splittings were not observed (some asymmetry of the bands was seen), the spectra were analysed on the basis of O_h species.

1.9.3.2 Vanadium(III)

Vanadium(III) is a d^2 metal which has the free ion ground term ^3F, when in a complex possessing an octahedral environment the ground term is $^3T_{1g}(F)$. This ground state creates three possible spin allowed transitions:

$^3T_{1g}(F) \rightarrow {}^3T_{2g}$

$^3T_{1g}(F) \rightarrow {}^3A_{2g}$

$^3T_{1g}(F) \rightarrow {}^3T_{1g}(P)$

The UV-vis spectra tends to show two bands which are consistent with $^3T_{1g} \rightarrow {}^3T_{2g}$ and $^3T_{1g} \rightarrow {}^3T_{1g}(P)$ transitions.

1.9.3.3 Vanadium(V)

Vanadium(V) has no d electrons, therefore d-d transitions can not occur, the bands present in the UV-vis spectra are therefore usually characteristic of charge transfer bands. Due to no d electrons being present transitions observed are ligand to metal charge transfer. A simplified diagram of this process is seen in Fig 1.19, with υ_1 being the lowest energy LMCT transition.

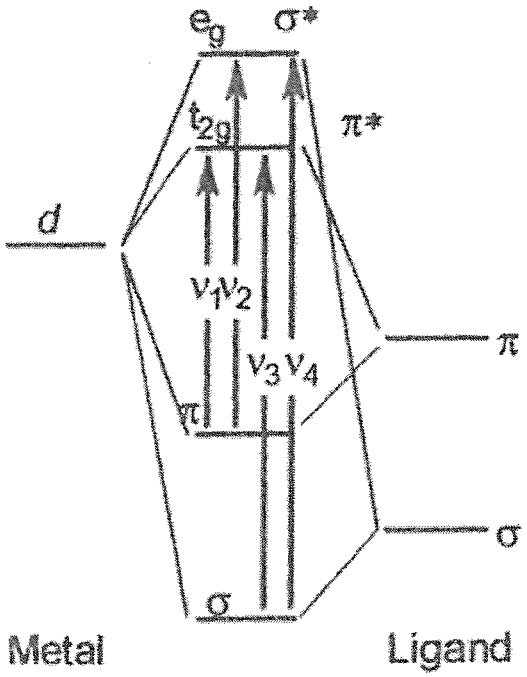

Fig 1.19 Ligand to metal charge transfer[69]

1.10 Aims of the project

The aim of this study is to probe the chemistry of hard metals with soft ligands. Vanadium(V) was used to investigate the binding of the hard d^0 metal to a series of N- and O- donor ligands, as well as testing the ability to bind to the softer S-donor ligands.

Macrocyclic ether, thioether and mixed S/O ligands were reacted with Cr(III) and V(III) species. The thioether macrocycles were used to test the boundaries of Hard Soft Acid Base theory, using the thioethers as macrocycles rather than open chain ligands to aid in the stability of the complexes formed. Mixed thia/oxa macrocycles were used to probe the HSAB theory further by allowing investigation of M-S vs M-O coordination competitively the metal ions to selectively choose its binding position.

1.11 References

[1] F. A. Cotton, G. Wilkinson, C. A. Murillo, M. Bochmann, *"Advanced Inorganic Chemistry"*, 6th edition, Wiley-Interscience publication, New York, **(1999)**.

[2] D. F. Shriver, P. W. Atkins, *"Inorganic Chemistry"*, 3rd edition, Oxford University Press, Oxford, **(1994)**.

[3] R. G. Pearson, *Coord. Chem. Rev.*, 100, **(1990)**, 403.

[4] S. Ahrland, J. Chatt, N. R. Davies, A. A. Williams, *J. Chem. Soc.*, **(1958)**, 264.

[5] C. E Housecraft, E. C. Constable, *"Chemistry: An Integrated Approach"*, 1st edition, Longman Ltd., London, **(1988)**.

[6] D. G. Cooper, *"The Periodic Table"*, 4th edition, Buttersworths London, **(1968)**, 55.

[7] D. C. Crans, J. J. Smee, *"Comprehensive Coordination Chemistry II"*, (J. A. McCleverty, T. J. Meyer, A. G. Wedd), 4, Elsevier, Oxford, **(2004)**, 175.

[8] J. Emsley, *"Nature's Building Blocks an A-Z Guide to The Elements"*, Oxford University Press, Oxford, **(2003)**.

[9] H. Sakurai, Y. Fujisawa, S. Fujimoto, H. Yasui and T. Takino, *J. Trace Elements in Experimental Medicine,* 12, **(1999)**, 393

[10] K. Ruhlandt-Senge, A. D. Bacher, G. Koellner, B. Siewert and U. Mueller, *Z. Naturforsch., Teil* B, 47 , **(1992)**, 814.

[11] D. A. Fletcher, R. F. McMeeking, D. Parkin, *J. Chem. Inf. Comput. Sci.*, 36, **(1996)**, 746; I. J. Bruno, J. C. Cole, P. R. Edgington, M. Kessler, C. F. Macrae, P. McCabe, J. Pearson, R. Taylor, *Acta Crystallogr., Sect. B,* 58, **(2002)**, 389; B. R. Elvidge, S. Arndt, P. M. Zeimentz, T. P. Spaniol, J. Okuda, *Inorg. Chem.*, 44, **(2005)**, 6777.

[12] A. C. Gonzalez-Baró, E. E. Castellano, O. E. Piro, B. S. Parajón- Costa, *Polyhedron*, 24, **(2005)**, 49.

[13] D.L. Kepert, *"The Early Transition Metals"*, Academic Press, London, **(1972)**.

[14] Y. Zhang, R. H. Holm, *Inorg. Chem.*, 29, **(1990)**, 911.

[15] P. B. Hitchcock, T. H. Lee, G. J. Leigh, *Inorg. Chim. Acta,* 349, **(2003)**, 159.

[16] J. Cave, P. R. Dixon and K. R. Seddon, *Inorg. Chim. Acta,* 30, **(1978)**, L349.

[17] M. Motevalli, D. Shah, S. A. A. Shah, A. C. Sullivan, *Polyhedron,* 15, **(1996)**, 2387.

[18] N. Azuma, T. Ozawa, K. Ishizu, *Polyhedron,* 13, **(1994)**, 1715.

[19] G. R. Willey, M. T. Lakin, N. W. Alcock, *J. Chem. Soc., Chem. Comm.*, **(1991)**, 1414.

[20] U. Heinzel, A. Henke, R. Mattes, *J. Chem. Soc. Dalton Trans.,* **(1997)**, 501.

[21] U. Kynast, S. G. Bott, A. L. Atwood, *J. Coord. Chem.,* 17, **(1988)**, 53.

[22] M. Köppen, G. Fresen, K. Wieghardt, R. M. Llusar, B. Nuber, J. Weiss, *Inorg. Chem.,* 27, **(1988)**, 721.

[23] M. C. Durrant, S. C. Davies, D. L. Hughes, C. LeFloc'h, R. L. Richards, J. R. Saunders, N. R. Champness, S. J. Pope, G. Reid, *Inorg. Chim. Acta,* 251, **(1996)**, 13.

[24] S. C. Davies, M. C. Durrant, D. L. Hughes, C. LeFloc'h, S. J. A. Pope, G. Reid, R. L. Richards, J. R. Sanders, *J. Chem. Soc. Dalton Trans.,* **(1998)**, 2191.

[25] I. Dellien, F. M. Hall, L. G. Helper, *Chem. Rev.,* 76, **(1976)**, 283.

[26] J. McCleverty, *"Chemistry of the First-row Transition Metals"*, (J. Evans), Oxford University Press, Oxford, **(1999)**.

[27] T. Ernst, K. Dehnicke, H. Goesmann and D. Fenske, *Z. Naturforsch, Teil* B, 45, **(1990)**, 967.

[28] J. Hughes, G. R. Willey, *Inorg. Chim. Acta.,* 11, **(1974),** L25

[29] P.C. Junk, A. L. Atwood, *J. Organo. Chem., 565, (1998), 179;* U. Heinzel, A. Henke, R. Mattes, *J. Chem. Soc. Dalton Trans,* **(1997)**, 501.

[30] G. J. Grant, K. E. Rogers, W. N. Setzer, D.G.VanDerveer, *Inorg. Chim. Acta,* 234, **(1995)**, 35.

[31] N. R. Champness, S. R. Jacob, G. Reid, C. S. Frampton, *Inorg. Chem.,* 34, **(1995)**, 396

[32] W. Levason, G. Reid, S. M. Smith, *Polyhedron,* 16, **(1997)**, 4253.

[33] W. Levason, B. Patel, G. Reid, V. Tolhurst, M. Webster, *J. Chem. Soc. Dalton Trans,* **(2001),** 3001.

[34] M. D. Brown, M. B. Hursthouse, W. Levason, R. Ratnani, G. Reid, *J. Chem. Soc. Dalton Trans,* **(2004),** 2487.

[35] H. Funk, W. Weiss, M. Zeising, *Z. Anorg. Allg. Chem.* , 295, **(1958)**, 327

[36] S. J. Miles, J. D. Wilkins, *J. Inorg. Nucl. Chem.,* 37, **(1975)**, 2271.

[37] L. F. Lindoy, *"The Chemistry of Macrocyclic Ligand Complexes"*, Cambridge University Press, Cambridge, **(1990)**,

[38] J. T. Groves, W. J. Kruper, R. C. Haushalter, *J. Am. Chem. Soc.*, 102, **(1980)**, 6375.

[39] D. K. Cabbiness, D. W. Margerum, *J. Am. Chem. Soc.*, 92, **(1970)**, 2151.

[40] M. Micheloni, P. Paoletti, A. Sabatini, *J. Chem. Soc, Dalton Trans.,* **(1983),** 1189.

[41] N. F. Curtis, *J. Chem. Soc.*, **(1960)**, 4409.

[42] D. Sellmann, L. Zapf, *J. Organmet. Chem.*, 289, **(1985)**, 57.

[43] E. C. Constable, *"Coordination Chemistry of Macrocyclic Compounds,* (Evans), Oxford University Press, Oxford, **(1999)**.

[44] R. N. Greene, *Tetrahedron. Let.*, **(1972)**, 1793.

[45] J. Yamawaki, T. Ando, *Chem. Lett.*, 5, **(1980)**, 533.

[46] F. L. Cook, T. C. Caruso, M. P. Byrne, C. W. Bowers, D. H. Speck, C. L. Liotta, *Tetrahedron Let.*, **(1974)**, 4029.

[47] C. J. Pedersen, *J. Am. Chem. Soc.*, 89, **(1967)**, 7017; C. J. Pedersen, *J. Org. Chem*, 36, **(1971)**, 254.

[48] S. G. Bott, U. Kynast, J. L. Atwood, *J. Inclusion Phenomena,* 4, **(1986)**, 241.

[49] D. Sellman, P. Frank, F. Knoch, *J. Organo. Chem.* 339, **(1988)**, 345.

[50] S. J. A. Pope, N. R. Champness, G. Reid, *J. Chem. Soc., Dalton Trans.*, **(1997)**, 1639.

[51] T. M. Santos, B. J. Goodfellow, J. Madureira, J. Pedrosade Jesus, V. Felix, M. G. B. Drew, *New J. Chem.*,23, **(1999)**, 1015.

[52] W. Levason, G. Reid, *J. Chem. Res,* **(2002)**, 467.

[53] U. Heinzel, R. Mattes, *Polyhedron,* 10, **(1991)**, 19.

[54]J. S. Bradshaw, J. Y. Hui, B. L. Haymore, J. J. Christensen, R. M. Izatt, *J. Heterocyclic Chem.*, 10 **(1973)**, 1; J. S. Bradshaw, J. Y. Hui, Y. Chan, B. L. Haymore, R. M. Izarr, J. J. Christensen, *J. Heterocyclic Chem.*, 11, **(1974)**, 45.

[55] A. J. Blake, G. Reid, M. Schröder, *J. Chem. Soc. Dalton Trans,* **(1990)**, 3849.

[56] A. J. Blake, R. O. Gould, C. Radek, M. Schröder, *J. Chem. Soc. Dalton Trans,* **(1995)**, 4045.

[57] W. Levason, G. Reid, *"Comprehensive Coordination Chemistry II"*, (J. A. McCleverty, T. J. Meyer, A. B. P. Lever), I , Elsevier, Oxford, **(2004)**, 391.

[58] G. E. D. Mullen, T. F. Fassler, M. J. Went, K. Howland, B. Stein, P. J. Blower, *J. Chem. Soc. Dalton Trans.* **(1999)**, 3759.

[59] H. Schumann, A. M. Arif, A. L. Rheingold, C. Janiak, R. Hoffmann, N. Kuhn, *Inorg. Chem.*, 30, **(1991)**, 1618.

[60] J. Connolly, A. R. J. Genge, W. Levason, S. D. Orchard, S. J. A. Pope, G. Reid, *J. Chem. Soc. Dalton Trans.*, **(1999)**, 2343.

[61] W. Levason, J. J. Quirk, G. Reid, C. S. Frampton, *Inorg. Chem.,* 33, **(1994)**, 6120; A. J. Blake, M. J. Bywater, R. D. Crofts, A. M. Gibson, G. Reid, M. Schröder, *J. Chem. Soc., Dalton Trans.,* 14, **(1996)**, 2979.

[62] A. R. J. Genge, W. Levason, G. Reid, *J. Chem. Soc.,Dalton Trans.,* **(1997)**, 4479.

[63] E. W. Abel, M. Booth, K. G. Orrell, *J. Chem. Soc., Dalton Trans.,* **(1980),** 1582.

[64] C. Weidemann, D. Rehder, *Inorg. Chim. Acta*, 120 **(1986)**, 15.

[65] J. G. Verkade, L. D. Quin, *"Phosphorus-31 NMR Spectroscopy in Stereochemical Analysis Organic compounds and metal complexes"*, (A. P. Marchand), VCH publishers, **(1987)**.

[66] W. Levason, B. Patel, G. Reid, *Inorg. Chim. Acta,* 357, **(2004)**, 2115.

[67] J. S. Ogden, *"Introduction to Molecular Symmetry"*, Oxford University Press, Oxford, **(2001).**

[68] A. B. P. Lever, *"Inorganic Electronic Spectroscopy"*, 2nd Edition, Elsevier Science Publishers, Netherlands, **(1986)**.

[69] A. K. Brisdon, *"Inorganic Spectroscopic Methods"*, Oxford University Press, Oxford, **(2003)**.

Chapter 2

Vanadium(V) Chemistry

2.1 Introduction

2.1.1 Vanadium (V) Chemistry

Oxovanadiumtrichloride ($VOCl_3$) is synthesised *via* a reaction of Cl_2 and V_2O_5 using a carbon reductant at 300°C. The yellow liquid smokes when exposed to the air due to its sensitivity to water. $VOCl_3$ is a tetrahedral complex with C_{3v} symmetry; with a vanadium(V) d^0 metal centre.[1] The research involving this complex has been influenced by the fact that vanadium(V) compounds have strong oxidizing properties and are used in organic synthesis.[2,3] The chemistry of high valent vanadium species is of relevance to understanding the role that vanadium plays in biological systems, for example the vanadate-dependent haloperoxidases which mainly occur in marine organisms. [4] Maciejewska *et al* investigated the ability of vanadium(V) to act as a catalyst during the oxidation of L-glutamic acid and L-glutamine, the crystal structure of one of these catalysts can be seen in fig. 2.1.[5] Vanadium(V) chemistry has been dominated by the use of species including V_2O_5, iso- and hetero- polyvanadates and alkoxides.[5]

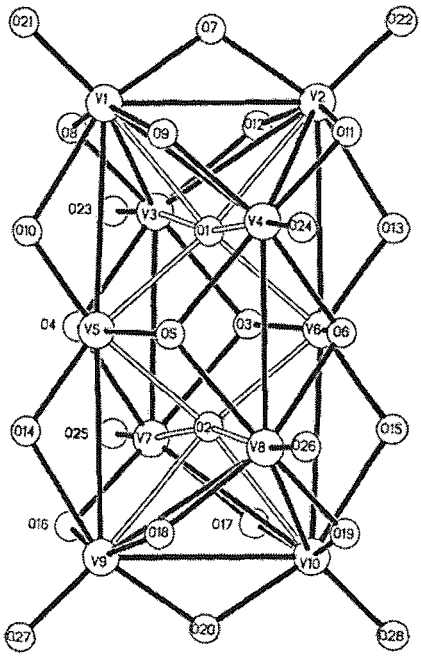

Fig 2.1 The decavanadate polyanion, which acts as a catalyst. [5]

Vanadium(V) compounds have been used in industrial processes for example in the production of sulfuric acid where vanadium easily oxidises SO_2 to SO_3.[6] However this is

of environmental concern due to the presence of sulfur in fuels, which when burnt can produce sulfur dioxide. Stanciulescu and Ikura have used catalysts containing vanadium to oxidise sulfur in order to extract the compound from fuels.[7] Hagen *et al* used $[VOCl_2(OCMe_2(\{2\}\text{-Py}))]$ to form polymerized compounds *via* nonchelating vanadium(V) oxo and imido complexes. These complexes are used within catalysis.[8] $VOCl_3$ has also been used in bioinorganic chemistry to synthesise catalysts.[9]

There have been claims that the compound VCl_5 has been prepared, but data has not supported this, the only fully analysed binary halide is VF_5.[10] Three oxide trihalides of the form VOX_3 (X=F, Cl and Br) have been synthesied.[1] Studies involving $VOCl_3$ with a selection of neutral ligands have been explored *via* ^{51}V NMR spectroscopy.[11,12,13] Vanadium is I = 7/2 and is 99.8% abundant with a chemical shift range of $\approx$ 800 to -1000ppm. Vanadium(V) also has a small electric nuclear quadruple moment which allows the resonance signals to be well defined.[11] Wiedemann *et al.* prepared a selection of complexes using $VOCl_3$ and a selection of neutral nitrogen and oxygen donor ligands such as bipy, pyridine, Et_2O and Ph_2CO.[11] These complexes were analysed *via* ^{51}V NMR but no other spectral analysis was gained. There has been some structural evidence of reaction of $VOCl_3$ with nitriles such as $[VOCl_3(PhCN)_2]$, which was found to have an octahedral metal centre with Cl/O disorder. Other complexes obtained are of the form $[VOCl_3(RCN)]$ (R=Me, Ph and $PhCH_2$).[14,15,16]

Complexes such as carbene $[VOCl_3\{(mes)NCH_2N(mes)C\}]$[17] have been seen to have a square pyramidal geometry around the metal centre, this can be seen in fig 2.2.[17]

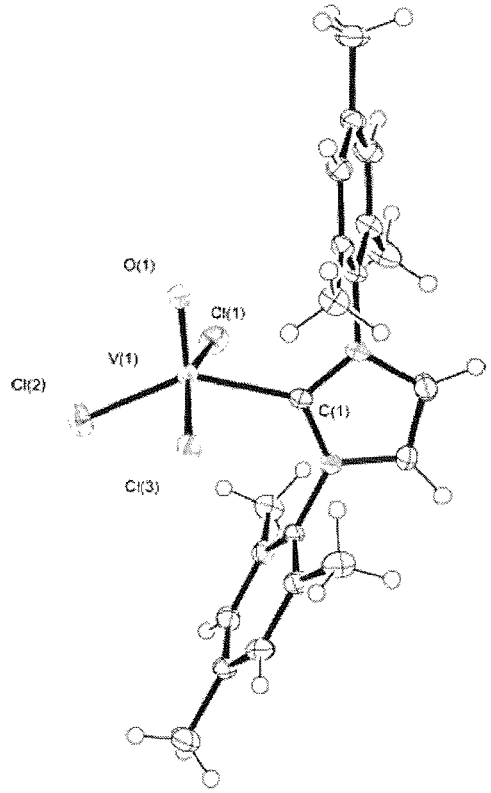

Fig 2.2 Crystal structure of $[VOCl_3\{(mes)NCH_2N(mes)C\}]$[17]

$[VOCl_3$(adamantan-2,2'-homoadamantan-3-one)$]$[18] is also seen to be consistent with a square pyramidal vanadium metal centre. There have also been six coordinate vanadium complexes formed such as $[VOCl_3\{$(2-nitrophenyl)pyridine-2-carboxamide$\}]$.[19] This is consistent with the metal centre being bound to *mer* chlorines and amide oxygens being *trans* to the V=O.[20] There have been numerous attempts to isolate such compounds however[21] the spectroscopic data has been limited and is occasionally inconsistent. The problems seen with vanadium(V) neutral ligand species are due to the $VOCl_3$ being extremely moisture sensitive. Many of the complexes formed also readily decomposed as they were very moisture sensitive. The vanadium is also seen to be reduced to V(IV) or V(III) with great ease by trace amounts of water.

Baker *et al.* reacted $VOCl_3$ with thioether ($(CH_3)_2S$) and arsine oxide (Ph_3AsO) ligands but found that the complexes result in partial reduction of the metal centre to

vanadium(IV).[22] Schlenk line techniques are widely available and have been developed over the past 50 years. These techniques help to reduce the risk of hydrolysis of $VOCl_3$ complexes.

Due to hard/soft acid base theory it is expected that the hard vanadium(V) centre is not likely to bind to soft ligands, such as selenoethers and thioethers. Work on vanadium(V) compounds has usually involved the use of ligands with mostly oxygen or nitrogen donors. Vanadium(V) has been found to have a great affinity for oxygen donors.[23] Hagen *et al* used vanadium(V) with oxygen ligands to obtain complexes such as [$VOCl_2$(OCMe$_2$([2]-Py))], which is used as a catalyst in ethene polymerisation.[24] Miles *et al* found that by reacting $VOCl_3$ with 2,2'-bipyridyl a fairly stable complex could be obtained, and that the ligand would also bind in a bidentate manner to the metal centre. However there was limited spectroscopic data available on the complex.[25] This finding was also supported by work published by Funk *et al*[26], using $VOCl_3$ and pyridine, as well as 2,2'-bipyridyl but again there was limited spectroscopic data avalaible.[26]

Weidemann *et al* reacted uracil with $VOCl_3$, exploring the binding of mixed donor ligands to a vanadium centre.[11] Oxygen and nitrogen donor ligands are the ligands of choice due to their stabilising properties on high oxidation state metals.[8] Complexes made using $VOCl_3$ tend to form charge-transfer interactions. Such work was published by Dijkgraaf,[27] who found a charge-transfer interaction between the chlorine on the vanadium and the aromaticity of the ligand- in this case hydrocarbons.[27] Other work has been published discussing the possibility of metal-oxygen π bonding giving stronger interactions.

When $VOCl_3$ was reacted with 1,2-dimethoxyethane (dme) there was the possibility of two possible isomers, *fac* or *mer* structures. They found the *fac* structure shown, in Fig. 2.3 to be the preferred species.[25]

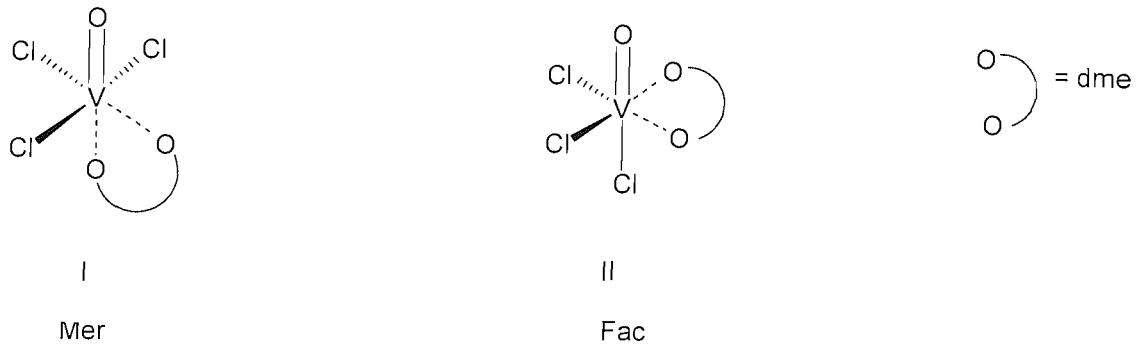

Fig. 2.3 Fac and Mer structures of $VOCl_3(dme)$.[25]

Complexes containing VOF_3, such as $VOF_3(L)$, (where L is bipy and phen) have been prepared by Chakravorti *et al.*[28] The V=O stretches appear in a characteristic region in the IR spectra (ca. 960cm^{-1}).[28] Hibbert[29] synthesised complexes using VOF_3 with phen and bipy, and the resulting complexes were analysed by NMR techniques; peaks in ^{51}V NMR spectra at -738(d) and -739(dt) ppm respectively were found. At room temperature the complexes were found to be fluxional.[29] The coordination properties of neutral ligands containing oxygen, sulfur, nitrogen and phosphorus have also been explored using $VOBr_3$ as a starting material and there is no evidence for vanadium(V) complexes of $VOBr_3$.[30]

$VOCl_3$ was a useful starting material due to it being diamagnetic allowing NMR data to be obtained. If more than one NMR resonance peak is present it will correspond to more than one species.[11] Vanadium(V) has no d electrons which allows electrons to be transferred to these empty orbitals *via* charge transfer interactions. Probing of these charge transfer transitions can be carried out with UV-vis analysis.[11, 22]

2.1.2 Vanadium(V) Anion Chemistry

Vanadium(V) anions are often the result of hydrolysis of vanadium(V) neutral complexes, and are usually red or brown in colour. Their structures are determined by various analytical techniques such as IR, UV-vis and in some instances X-Ray crystallography. Gomez *et al* used $[VO_2X_2]^-$(where X=F, Cl, Br and I) to simulate the expected bond lengths and analytical behaviour of these types of complexes.[30a] Other groups have

successfully made and analysed such anions as $[VO_2Cl_2]^-$ [31] and $[VOCl_4]^-$. [32,33] These anions were made using literature methods to act as a comparison to the vanadium(V) neutral complexes. Fenske *et al.* obtained crystallographic data on the $[VO_2Cl_2]^-$ anion. [34]

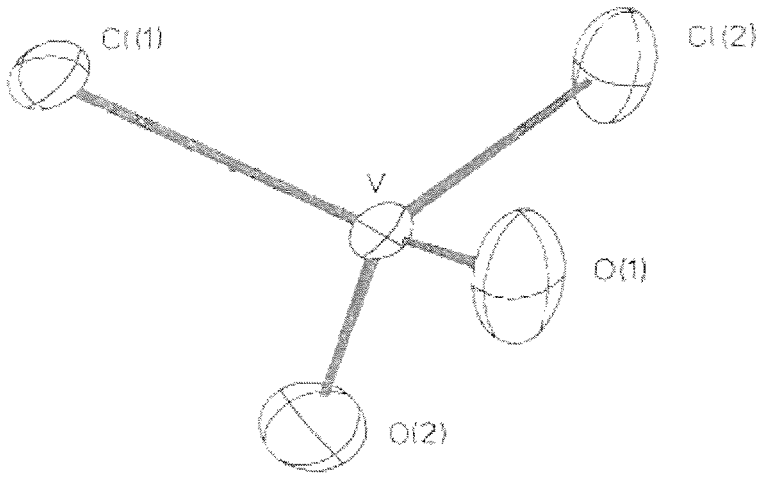

Fig 2.4 Crystal structure of $[VO_2Cl_2]^-$ [34]

The crystal structure of the complex $[VO_2Cl_2]^-$, in fig. 2.4, shows a four coordinate metal centre with C_{2v} symmetry.

2.1.3 Other Hard Metal/Soft Ligand Chemistry

Other work involving hard metal and soft ligand combinations has been carried out using Ti(IV),[35] Cr(III)[36] and Mo(VI)[37,38], with a variety of different ligands. Brown *et al* used the hard metal Mo(VI) with soft ligands such as $MeS(CH_2)_2SMe$ as well as $MeSe(CH_2)_2SeMe$ to obtain yellow solids.[38] One other such success was the formation of titanium(IV) with phosphine and arsine ligands. Hart *et al* used the hard metal Ti(IV) with soft ligands such as *o*-$C_6H_4(AsMe_2)_2$ to produce a crystal structure of the eight-coordinate $[TiBr_4\{o\text{-}C_6H_4(AsMe_2)_2\}_2]$.[39] There has also been much investigation on chromium(III) and vanadium(III) (see Chapter 3), but little work has been undertaken with vanadium(V).

2.1.4 Aims For This Chapter

In this chapter a series of complexes of the form $[VOCl_3L]$ (where L is py, Ph_3PO and Ph_3AsO), $[VOCl_3(L)_2]$ (where L is py and Me_3PO), $[VOCl_3(L\text{-}L)]$ (where L-L is bipy,

phen, tmen, $Ph_2P(O)CH_2P(O)Ph_2$, 15-crown-5, $MeSCH_2CH_2SMe$ and $EtSCH_2CH_2SEt$) and $[Cl_3OV(\mu\text{-L-L})VOCl_3]$ (where L-L = 18-crown-6 and $Ph_2P(O)CH_2P(O)Ph_2$), have been synthesised to explore the chemistry of the hard vanadium(V) with a range of hard (N- and O-) and soft (S-) donor ligands. The experiments require rigorously dry conditions in order to minimise the risk of vanadium(V) reducing to vanadium(IV) or being hydrolysed for example to $[VOCl_4]^-$ and/or $[VO_2Cl_2]^-$ species.

2.2 Results and Discussion

2.2.1 Vanadium(V) anions

The $[VO_2Cl_2]^-$ and $[VOCl_4]^-$ anions form readily when the $[VOCl_3]$ starting material and complexes thereof are hydrolysed. Hence, to enable ready identification of these decomposition products we have synthesised $[Ph_4As][VO_2Cl_2]$ and $[Ph_4As][VOCl_4]$ and characterised them by IR, ^{51}V NMR and UV visible spectroscopy (Tables 2.1, 2.2 and 2.3). These salts were synthesised using literature methods.[31,32,33] Thus, the former was obtained by addition of an aqueous solution of Ph_4AsCl to $NaVO_3$ in 25% HCl, giving the $[Ph_4As][VO_2Cl_2]$ as a yellow solid. The latter was obtained by two methods – either treatment of $VOCl_3$ with one mol. equiv. of Ph_4AsCl in concentrated HCl saturated with HCl gas at low temperature, or by addition of Ph_4AsCl to $VOCl_3$ in anhydrous MeCN solution, producing the red/brown solid $[Ph_4As][VOCl_4]$. The IR spectrum of $[Ph_4As][VO_2Cl_2]$ shows two V=O stretches at 967, 957 cm^{-1} and a V-Cl stretching vibration at 431 cm^{-1}. These compare with the data quoted in the literature, ν(V-Cl) = 435 cm^{-1} and ν(V=O) = 971 and 960 cm^{-1}, consistent with the C_{2v} $[VO_2Cl_2]^-$ anion which has also been confirmed crystallographically (fig. 2.4).[34] The $[VOCl_4]^-$ anion has C_{4v} symmetry, and the IR spectrum from the sample obtained in this work shows a V=O stretch at 1025 cm^{-1} and three V-Cl stretches at 437, 393 and 372 cm^{-1}. These data are not consistent with the literature,[31] which quotes the V=O stretch at 970(A_1) and 960(s) cm^{-1} and V-Cl stretches at 399(A_1) and 377(E) cm^{-1}. Based upon the results from our work on both $[VO_2Cl_2]^-$ and $[VOCl_4]^-$ it seems likely that the literature sample was in fact a mixture of $[VO_2Cl_2]^-$ and $[VOCl_4]^-$.

Complex	V-O stretch/cm^{-1}	V-Cl stretch/cm^{-1}
$[Ph_4As][VO_2Cl_2]$	967, 957	431
$[Ph_4As][VOCl_4]$	1025	437, 393, 372

Table 2.1. Selected IR spectroscopic data for salts of the vanadium(V) anions.

^{51}V NMR spectra of $[Ph_4As][VO_2Cl_2]$ and $[Ph_4As][VOCl_4]$ were obtained in CH_2Cl_2 solution. Rigorously anhydrous conditions were applied in order to prevent

decomposition or further hydrolysis to vanadium(V) species and to provide comparisons with the new vanadium(V) adducts reported in this chapter. The ^{51}V NMR data are consistent with literature values obtained by J. Hanich *et al*[40], giving δ = +48 ppm for $[Ph_4As][VOCl_4]$ and a peak at -362 ppm for $[Ph_4As][VO_2Cl_2]$ (Table 2.2).

Complex	^{51}V (δ)/ppm	$W_{1/2}$/Hz
$[Ph_4As][VO_2Cl_2]$	-362	158
$[Ph_4As][VOCl_4]$	48	300

Table 2.2. ^{51}V NMR spectroscopic data for the salts of the vanadium(V) anions.

The UV-vis spectra are also consistent with the literature (Table 2.3).

Complex	Solution/cm^{-1}($E/mol^{-1}dm^3cm^{-1}$)
$[Ph_4As][VOCl_4]^a$	15240, 18120(sh), 19840, 25000, 30490
$[Ph_4As][VOCl_4]^b$	15500(170), 19800(sh), 21500(1980), 31500(sh)

Table 2.3. UV/vis spectroscopic data for the salts of the vanadium(V) anions.

a = complex made in this work

b = complex made by Drake *et al.*[33]

2.2.2 Vanadium(V) Complexes with N- Donor Ligands

Nitrogen donor ligands are relatively hard donors and hence are expected to form complexes with vanadium(V) easily. The N-heterocyclic ligands bipy, phen and py, and the amine tmen were used and the IR spectroscopy data are presented in Table 2.7, the ^{51}V NMR spectroscopic data in Table 2.8 and the UV-vis spectroscopic data in Table 2.9. The reaction schemes for the procedures can be seen in Figure 2.5.

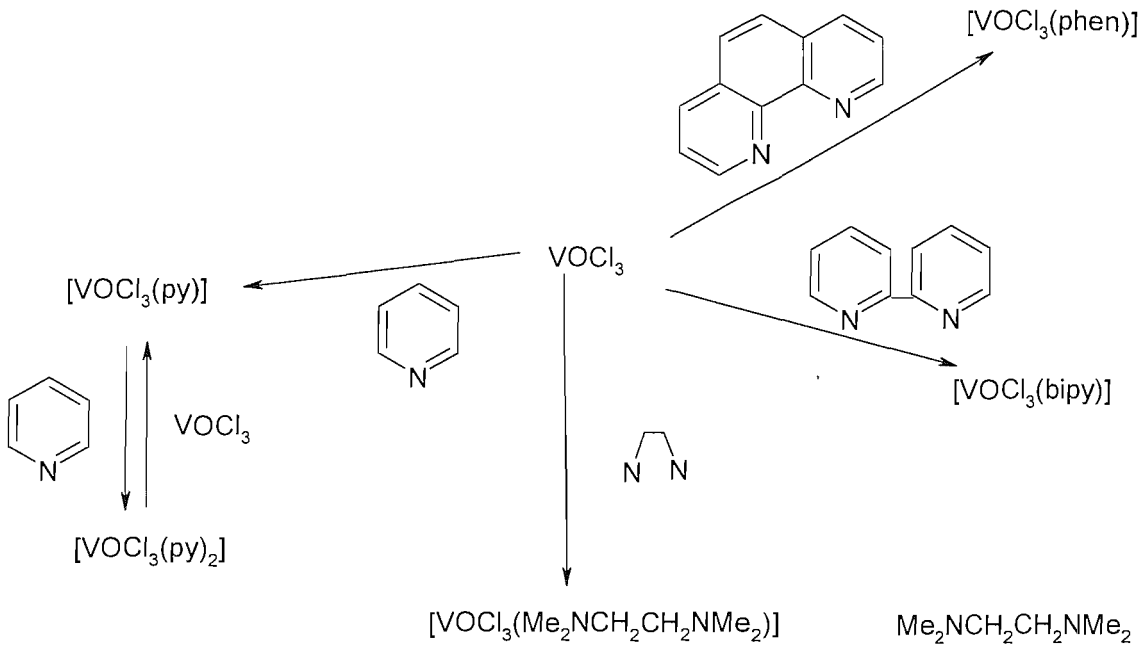

Fig 2.5 Schemes for V(V) complexes with N-Donor Ligands

$[VOCl_3(bipy)]$ was prepared from $VOCl_3$ and 1 mol. equiv. of bipy in dry CH_2Cl_2. The complex was obtained as a red/black solid in high yield. The purity of the bipy complex was established by microanalysis. IR spectroscopy shows a V=O stretch at 978 cm^{-1} and the V-Cl stretches at 381, 358 and 348 cm^{-1}. These data are consistent with a six coordinate V(V) complex with approximate C_s symmetry. In $VOCl_3$ complexes ν(V=O) ranges from ca. 950 to 1040 cm^{-1}, and comparing data only on structurally characterised compounds the value falls from the four coordinate $VOCl_3$ (1035 cm^{-1}) to five coordinate $[VOCl_3(RCN)]$, $[VOCl_4]^-$, $[VOCl_3\{(mes)NCH_2CH_2N(mes)C\}]$ (1025 – 1016 cm^{-1}), to six coordinate $[VOCl_3(RCN)_2]$ (below ca. 1000 cm^{-1}).[16,17,33,41,42] Miles *et al.* have reported the preparation of $[VOCl_3(bipy)]$ and quote the V=O stretch at 980 cm^{-1}.[25] The ^1H NMR spectrum of $[VOCl_3(bipy)]$ shows the bipy protons are shifted significantly to high frequency upon coordination. Also, the observation of a complex pattern suggests the presence of an unsymmetrical isomer, with the oxo ligand *trans* to one N-donor atom. Vanadium-51 NMR spectroscopy shows one resonance at -103 ppm, to low frequency of $VOCl_3$ itself (0 ppm) and consistent with the bipy ligand being coordinated to the metal centre. The diffuse reflectance spectrum showed bands at 17200, 19120, 21370, 32260

cm^{-1}. The solid state and solutions spectra are similar and the band present at 21000 cm^{-1} in the solution UV-vis spectrum is consistent with $\pi(Cl) \rightarrow V$ charge transfer.

Several attempts were made to grow crystals of the deep *red/black* $[VOCl_3(bipy)]$ suitable for a crystal structure analysis. Dissolving the (deep red) $[VOCl_3(bipy)]$ in dry CH_2Cl_2, layering with hexane and standing in a glove box for several days reproducibly formed a few small *orange* crystals identified as $[\{VOCl_2(bipy)\}_2(\mu\text{-}O)]$. Two sets of data were obtained, both of which showed the same rather poor crystal quality, thought to be due to partial twinning. The structure turned out to be the hydrolysed vanadium(V) complex. The crystallographic data are tabulated (Table 2.4).

	[{$VOCl_2$(bipy)}$_2$(μ-O)]
Formula	$C_{21}H_{19}Cl_7N_4O_3V_2$
Molecular Weight	752.67
Crystal Structure	Triclinic
Space Group	P-1 (no. 2)
a/Å	13.522(4)
b/Å	13.833(3)
c/Å	16.784(5)
α/°	105.216(12)
β/°	103.871(12)
γ/°	90.483(16)
U/Å^3	2932.4(14)
Z	4
μ(M_o-K_α)/mm^{-1}	1.354
Unique Reflections	10279
No. of parameters	678
R1[I_o>2σ(I_o)]	0.1052
R1[all data]	0.2330
wR2[I_o>2σ(I_o)]	0.2234
wR2[all data]	0.2733

Table 2.4. Crystallographic parameters for [{$VOCl_2$(bipy)}$_2$(μ-O)]

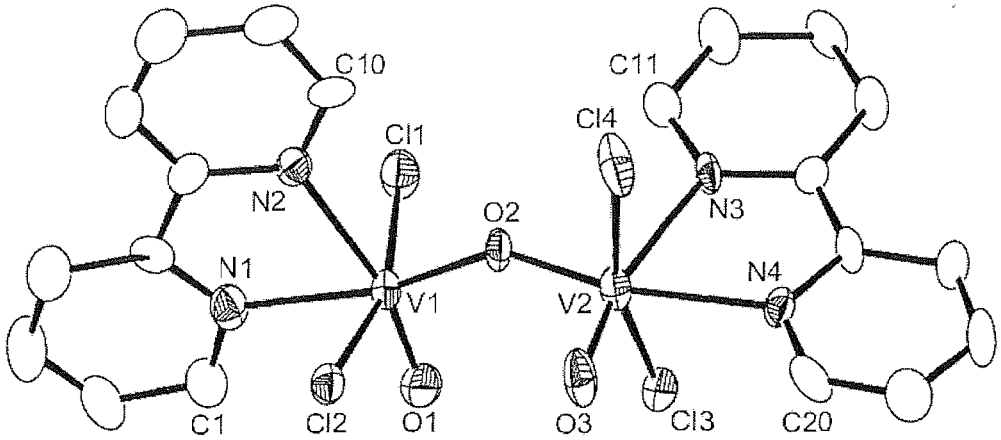

Fig 2.6. View of the structure of $[\{VOCl_2(bipy)\}_2(\mu\text{-}O)]$. For clarity the H atoms have been omitted and the ellipsoids are at shown at the 50% probability level.

	Bond Length/Å (esd's)
V(1)-Cl(1)	2.308(4)
V(1)-Cl(2)	2.330(3)
V(1)-O(1)	1.578(8)
V(1)-N(1)	2.164(10)
V(1)-N(2)	2.258(10)
V(1)-O(2)	1.783(7)
V(2)-Cl(3)	2.309(4)
V(2)-Cl(4)	2.290(4)
V(2)-O(3)	1.595(8)
V(2)-N(3)	2.228(9)
V(2)-N(4)	2.167(9)
V(2)-O(2)	1.785(8)

Table 2.5 Selected bond lengths for $[\{VOCl_2(bipy)\}_2(\mu\text{-}O)]$.

	Bond Angles/° (esd's)
Cl(1)-V(1)-Cl(2)	163.6(2)
N(1)-V(1)-N(2)	72.1(4)
N(1)-V(1)-O(2)	163.0(4)
N(2)-V(1)-O(1)	164.3(4)
V(1)-O(2)-V(2)	145.8(5)
Cl(3)-V(2)-Cl(4)	163.2(2)
N(3)-V(2)-N(4)	72.7(4)
N(4)-V(2)-O(2)	164.1(3)
N(3)-V(2)-O(3)	164.8(4)

Table 2.6 Selected bond angles for $[\{VOCl_2(bipy)\}_2(\mu\text{-}O)]$.

The structure of $[\{VOCl_2(bipy)\}_2(\mu\text{-}O)]$ shows (Figure 2.6, Tables 2.5 and 2.6) the vanadium atoms both in a slightly distorted octahedral geometry, each coordinated to two mutually *trans* chlorine atoms (V-Cl = 2.308(4), 2.330(3),{V(1)}; 2.309(4), 2.290(4){V(2)} Å), a bridging oxo ligand (V-O = 1.783(7), 1.785(8) Å) and a bidentate bipy ligand (V-N = 2.258(10), 2.167(9) Å). On the basis of the V-O distances the bridging oxygen is believed to be an O^{2-} ligand rather than an OH^- ligand - compare the V-O(H) distance in $[VOCl_3(OH)]^-$ of 2.033(4) Å.[43,44] It is likely that this has been caused by hydrolysis of the product during the crystallisation process.

$[VOCl_3(phen)]$ was prepared by an analogous route to $[VOCl_3(bipy)]$ to produce a red/brown solid in a good yield. The IR spectrum shows a band at 973 cm^{-1} and three bands between 380-340 cm^{-1}, which correspond to a V=O stretch and to three V-Cl stretches respectively. As with $[VOCl_3(bipy)]$, these data, together with the ^1H NMR spectroscopic data which shows a complex multiplet, indicates that $[VOCl_3(phen)]$ incorporates a six coordinate vanadium(V) centre with the oxo ligand *trans* to a phen N-donor atom, giving C_s symmetry. The ^{51}V NMR spectrum shows a peak at -108 ppm, very similar to the ^{51}V NMR shift for $[VOCl_3(bipy)]$. The diffuse reflectance UV-vis spectrum shows bands at 18000, 22220, 32895 cm^{-1}, similar to the $[VOCl_3(bipy)]$.

The $VOCl_3$-pyridine system turned out to be more complicated than those with bipy and phen systems described above. Initial attempts to isolate reproducible materials from the reaction of $VOCl_3$ with pyridine in either a 1:1 or 1:2 ratio in anhydrous CH_2Cl_2 were unsuccessful. However, reaction of $VOCl_3$ and py in a 2:1 molar ratio in CH_2Cl_2 solution gives the 1:1 complex $[VOCl_3(py)]$ as a dark brown solid. In contrast to this a 1:4 $VOCl_3$:py ratio produces a red solid which analyses as the 1:2 complex $[VOCl_3(py)_2]$. Both complexes were analysed using microanalysis, IR, UV-vis, ^1H and ^{51}V NMR spectroscopy. The IR spectrum of $[VOCl_3(py)_2]$ shows one band at 978 cm^{-1} and three bands between 390-340 cm^{-1}, consistent with a V=O stretch and three V-Cl stretches on a six-coordinate V(V) centre and the same isomer as for $[VOCl_3(bipy)]$ and $[VOCl_3(phen)]$. In contrast, $[VOCl_3(py)]$ shows one V=O band at 1020 cm^{-1}, i.e. at higher frequency than that in the $[VOCl_3(py)_2]$ complex. Three V-Cl stretches were also seen between 400-340 cm^{-1} which is slightly shifted from the values for the six coordinate neutral species of the form $[VOCl_3(L)]$ (where L = bipy, phen and 2 x py). This is consistent with a five coordinate vanadium(V) species. The solution NMR spectroscopic data from either $[VOCl_3(py)]$ or $[VOCl_3(py)_2]$ are similar, consistent with equilibrium mixtures in solution. The ^{51}V NMR spectra show only single resonances for solutions of either complex, which vary with concentration and temperature. However, at -90°C CH_2Cl_2 solutions of $[VOCl_3(py)_2]$ containing excess pyridine show a relatively sharp resonance at -58 ppm, which broadens and drifts to higher frequency on warming. This is thought to be due to the presence of the six coordinate $[VOCl_3(py)_2]$ adduct. A CH_2Cl_2 solution of the 1:1 $[VOCl_3(py)]$ at -90°C shows two resonances at -6 and -38 ppm. These are attributed to $VOCl_3$ and the $[VOCl_3(py)]$ respectively. These resonances broaden and coalesce at -40°C.

The six coordinate $[VOCl_3(tmen)]$ was prepared from $VOCl_3$ and tmen via a similar synthetic route used for $[VOCl_3(bipy)]$, but with cooling,. The product was isolated in good yield as a dark brown very poorly soluble solid. Initially we found that at room temperature the reaction was very exothermic, producing mixtures. For this reason the solutions were cooled in an ice bath prior to mixing. The IR spectrum of $[VOCl_3(tmen)]$ is also consistent with a six coordinate vanadium(V) complex. No ^{51}V NMR spectrum could

be obtained due to the poor solubility. The diffuse reflectance spectrum shows bands consistent with the other six coordinate neutral complexes discussed above.

Attempts to obtain $[VOCl_3(Et_3N)_2]$ produced vast quantities of heat similar to previous attempts with tmen, this caused decomposition of the product. The solutions were first cooled in an ice bath before being combined, but unlike tmen the final complex $[VOCl_3(Et_3N)]$ was still found to be analytically impure and this was not pursued.

Small quantities of solid $[VOCl_3(py)]$, $[VOCl_3(bipy)]$ and $[VOCl_3(phen)]$ complexes were opened in air to assess their stability. $[VOCl_3(py)]$ decomposes significantly within 30 minutes, changing from a brown solid to a green waxy solid. $[VOCl_3(bipy)]$ decomposes more slowly and $[VOCl_3(phen)]$ was the most stable complex, decomposing over ca. 24 hours. This may reflect the ligand structure, with the bidentate coordination of the rigid bipy and phen leading to increased stability (see Chapter 1).

Complex	**ν(V=O)/cm^{-1a}**	**ν(V-Cl)/cm^{-1a}**
Six coordinate		
$[VOCl_3(bipy)]$	978	381, 358, 348
$[VOCl_3(phen)]$	973	386, 347, 319
$[VOCl_3(py)_2]$	978	393, 372, 347
$[VOCl_3(tmen)]$	990	382, 340, 301
Five coordinate		
$[VOCl_3(py)]$	1020	419, 383, 344

Table 2.7 Selected IR spectroscopic data for the Vanadium(V) Complexes with N- Donor Ligands.

a = Recorded as a Nujol mull.

Complex	^{51}V (δ)/ppm	$w_{1/2}$/Hz
$[VOCl_3(bipy)]$	-103	370
$[VOCl_3(phen)]$	-108	560
$[VOCl_3(py)_2]$	-58	300
$[VOCl_3(py)]$	-36	800
$[VOCl_3(tmen)]$	Insoluble	-

Table 2.8. ^{51}V NMR spectroscopic data (CH_2Cl_2) for Vanadium(V) Complexes with N- Donor Ligands.

Complex	E_{max}/cm^{-1}	Solution/cm^{-1} (ε/$mol^{-1}dm^3cm^{-1}$)
$[VOCl_3(2,2'-bipy)]$	17200,19120, 21370, 32260	21550, 22730
$[VOCl_3(1,10-phen)]$	18000, 22220, 32895	18200, 21500(1680), 22730(1720)
$[VOCl_3(py)_2]$	20240, 27940	19800, 21740, 28730
$[VOCl_3(py)]$	16024, 20900, 33000	21500, 29110
$[VOCl_3(tmen)]$	15430, 20490, 33330, 43480	Insoluble

Table 2.9. UV-vis spectroscopic data for the Vanadium(V) Complexes with N- Donor Ligands.

2.2.3 Vanadium(V) Complexes with O- Donor Ligands

In order to probe the range of hard ligands which may form complexes with $VOCl_3$ we have examined a series of O-donor ligands including crowns ethers (15-crown-5 and 18-crown-6) and phosphin-oxide and arsine oxides (Ph_3PO, Me_3PO, Ph_3AsO and $Ph_2P(O)CH_2P(O)Ph_2$). The complexes were characterised by microanalyses, IR, UV-vis, ^1H, $^{31}P\{^1H\}$ and ^{51}V NMR spectropscopy as appropriate. The IR spectroscopic data are given in Table 2.10, the ^{51}V NMR spectroscopic data in Table 2.11, the $^{31}P\{^1H\}$ NMR in Table 2.12 and the UV-vis spectroscopic data in Table 2.13. The proposed schemes for reaction can be seen in Figure 2.7.

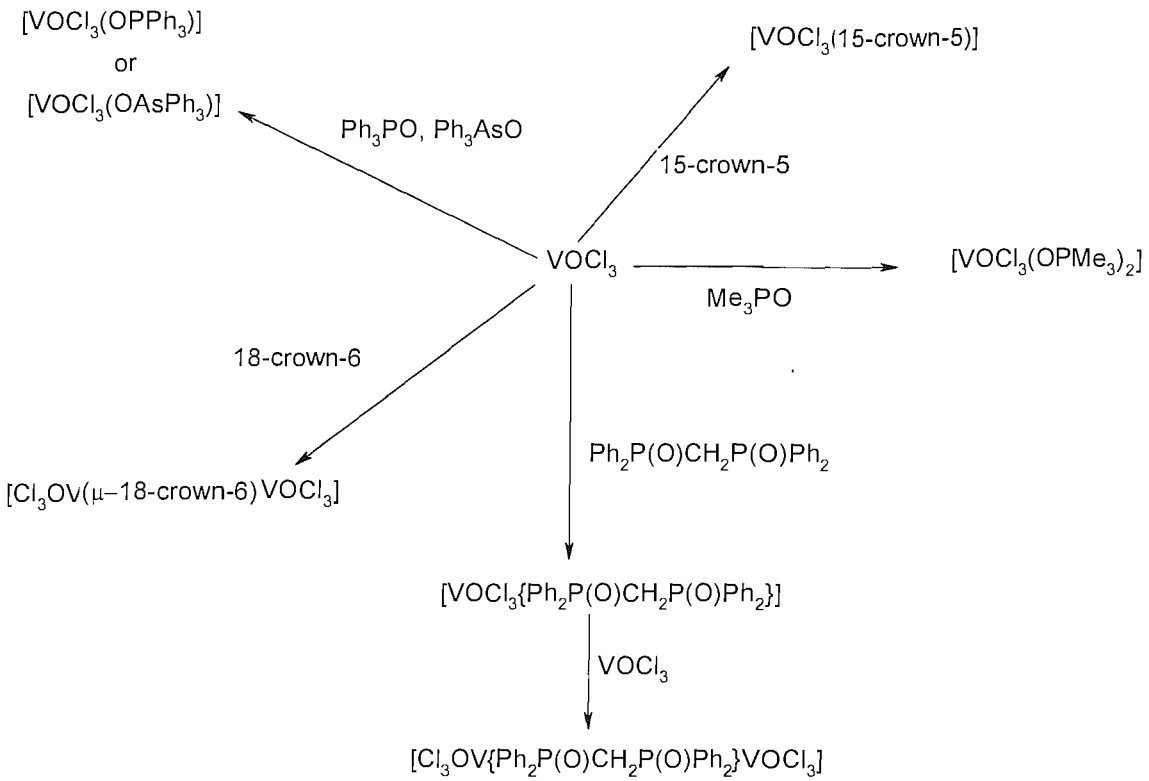

Fig 2.7 Schemes for V(V) complexes with O-Donor Ligands

$[VOCl_3(15\text{-crown-5})]$ was prepared by the reaction of excess $VOCl_3$ with rigorously dried 15-crown-5 in anhydrous CH_2Cl_2. The complex was obtained as a red/brown solid in good yield. IR spectroscopy shows a V=O stretch at 983 cm^{-1} and the V-Cl stretches at 428, 395, 351 cm^{-1}, corresponding to a six coordinate complex with approximate C_s symmetry. The ^1H NMR spectrum shows a singlet for the CH_2 groups over the temperature range +25 to -95°C, indicating a dynamic system probably due to reversible ligand dissociation and/or "ring-whizzing". Vanadium-51 NMR spectroscopy shows one peak at -21 ppm, which drifts to low frequency on cooling, with the effects reversing on warming. In the presence of excess $VOCl_3$ we do not see separate resonances, but instead an averaged shift. This is also consistent with reversible ligand dissociation from the six coordinate $[VOCl_3(\kappa^2\text{-}15\text{-crown-}5)]$. Similar to the behaviour observed on the analogous $[TiCl_4(\kappa^2\text{-crown})]$.[17] The diffuse reflectance spectrum showed bands at 16000, 20620 cm^{-1}, the latter is consistent with a $\pi(Cl) \rightarrow V$ charge transfer.

The dinuclear $[(VOCl_3)_2(18\text{-crown-6})]$ was prepared by an analogous route to $[VOCl_3(15\text{-crown-5})]$ and isolated as a red/brown solid. The IR spectrum is also consistent with six coordination at vanadium. The UV-vis and NMR spectroscopic behaviour is similar to $[VOCl_3(15\text{-crown-5})]$ with the ^{51}V NMR spectra showing a resonance at -6 ppm.

Repeated attempts to obtain a complex with 12-crown-4 using similar procedures were not successful, giving sticky black materials which contained significant amounts of $[VO_2Cl_2]^-$ by ^{51}V NMR spectroscopy. Hydrolysis of the isolated V(V) crown complexes with traces of water in CH_2Cl_2 solution produces $[VO_2Cl_2]^-$ ($\delta^{51}V$ = -363 ppm). Also, adding 18-crown-6 to a solution of $[Ph_4As][VO_2Cl_2]$ showed no change in the ^{51}V NMR shift, indicating that there is no significant interaction between these components in solution.

The six coordinate $[VOCl_3(Me_3PO)_2]$ was prepared from $VOCl_3$ and a 2 molar equivalents of Me_3PO in anhydrous CH_2Cl_2, giving the product as a brown solid in good yield. This compound shows a V=O stretch at 952 cm^{-1} and three V-Cl stretches between 380-340 cm^{-1} in the IR spectrum. The ^{51}V NMR spectra showed a peak at -92 ppm which is similar to the ^{51}V NMR shift for the $[VOCl_3(bipy)]$ complex, suggesting that the metal centre has a six coordinate geometry, showing the possibility of coordination of two Me_3PO ligands to the metal centre. The $^{31}P\{^1H\}$ NMR spectrum shows one peak at +74 ppm, significantly to high frequency of Me_3PO itself and indicating that only one isomer is formed, with equivalent phosphine oxides, which are mutually *trans*. UV-vis spectroscopy also suggests the desired product was formed.

Using $VOCl_3$ with either one or two molar equivalents of Ph_3PO gives only the five coordinate $[VOCl_3(Ph_3PO)]$ as a red/brown solid. The $\nu(V=O)$ band at 1020 cm^{-1} in the IR spectrum is indicative of a five coordinate species – see above. The ^{51}V NMR spectrum shows a resonance at -83 ppm and the $^{31}P\{^1H\}$ NMR spectrum shows a peak at +56 ppm, to high frequency of Ph_3PO.

Reaction of $VOCl_3$ and $Ph_2P(O)CH_2P(O)Ph_2$ in a 1:1 molar ratio gives the complex $[VOCl_3\{Ph_2P(O)CH_2P(O)Ph_2\}]$ as a dark brown solid. In addition to this, a 2:1 $VOCl_3$: $Ph_2P(O)CH_2P(O)Ph_2$) reaction was carried out and produced a red/black solid assigned as the dinuclear $[(VOCl_3)_2\{Ph_2P(O)CH_2P(O)Ph_2\}]$ (although this was not obtained as an analytically pure sample the spectroscopic data are reproducible and consistent with this formula). Both complexes were analysed using IR, UV-vis, ^1H, ^{51}V and $^{31}P\{^1H\}$ NMR spectroscopy. The mononuclear $[VOCl_3\{Ph_2P(O)CH_2P(O)Ph_2\}]$ shows one band at 970 cm^{-1} and three bands between 390-320 cm^{-1}, consistent with a V=O stretch and three V-Cl stretches respectively on a six coordinate vanadium(V) centre. Additionally, the two bands at 1164 and 1080 cm^{-1} are assigned as ν(P=O) in an unsymmetrical isomer (one P=O *trans* oxo and one P=O *trans* Cl and *mer* Cl atoms). The proposed structure for this complex can be seen in Figure 2.8.

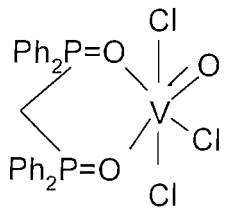

Fig 2.8 Proposed structure of $[(VOCl_3)_2\{Ph_2P(O)CH_2P(O)Ph_2\}]$

In contrast the dinuclear $[(VOCl_3)_2\{Ph_2P(O)CH_2P(O)Ph_2\}]$ shows only one ν(V=O) band at 1023 cm^{-1}, consistent with five coordination. The P=O stretching vibration is at 1094 cm^{-1}. The $^{31}P\{^1H\}$ NMR spectrum of the $[VOCl_3\{Ph_2P(O)CH_2P(O)Ph_2\}]$ shows two phosphorus environments, δ = 48.2 and 34.5 ppm, with P-P coupling of 12 Hz, both to high frequency of free $Ph_2P(O)CH_2P(O)Ph_2$ (25 ppm) and hence consistent with bidentate coordination with one phosphine oxide group *trans* oxo and one *trans* Cl. The ^{51}V NMR spectrum shows $\delta^{51}V$ = -81 ppm.

Attempts to isolate a complex of $VOCl_3$ with the diphosphine dioxide *o*-$C_6H_4(P(O)Ph_2)_2$, which is both more rigid and sterically larger were unsuccessful, giving complicated mixtures of P-containing products on the basis of $^{31}P\{^1H\}$ NMR spectroscopy. This may indicate that there is a size mismatch between the small V(V) and the large chelate bite of the diphosphine dioxide.

The five coordinate $[VOCl_3(Ph_3AsO)]$ was prepared by an analogous route to $[VOCl_3(Ph_3PO)]$ and isolated as a red/black solid. In the presence of traces of water the product is obtained as a dark red/black sticky solid which is identical spectroscopically to the solid. The IR spectrum shows ν(V=O) = 1016, ν(As=O) = 803 and three ν(V-Cl) in the region 390-340 cm^{-1}, and $\delta^{51}V$ = -141 ppm.

Complex	**ν(V=O)/cm^{-1a}**	**ν(V-Cl)/cm^{-1a}**
Six coordinate		
$[VOCl_3(15\text{-crown-5})]$	983	428, 395, 351
$[\{VOCl_3\}_2(18\text{-crown-6})]$	993	408(sh), 359, 306
$[VOCl_3(Me_3PO)_2]$	952	381, 367, 345
$[VOCl_3\{Ph_2P(O)CH_2P(O)Ph_2\}]$	970	395, 337, 320
Five coordinate		
$[VOCl_3(Ph_3PO)]$	1020	403, 372, 336
$[VOCl_3(Ph_3AsO)]$	1016	393, 365, 347
$[(VOCl_3)_2\{Ph_2P(O)CH_2P(O)Ph_2\}]$	1023	438, 388, 337

Table 2.10 Selected IR spectroscopic data Vanadium(V) Complexes with O- Donor Ligands.
a = Recorded as a Nujol mull.

Complex	**^{51}V (δ)/ppm**	**$w_{1/2}$/Hz**
$[VOCl_3(15\text{-crown-5})]$	-21	350
$[\{VOCl_3\}_2(18\text{-crown-6})]$	-6	2000
$[VOCl_3\{Ph_2P(O)CH_2P(O)Ph_2\}]$	-81	2500
$[\{VOCl_3\}_2\{Ph_2P(O)CH_2P(O)Ph_2)]$	-80	Broad
$[VOCl_3(Ph_3PO)]$	-83	700
$[VOCl_3(Ph_3AsO)]$	-141	400
$[VOCl_3(Me_3PO)_2]$	-92	740

Table 2.11. ^{51}V NMR spectroscopic data (CH_2Cl_2) for the Vanadium(V) Complexes with O- Donor Ligands.

Complex	$\delta^{31}P\{^1H\}$/ppm
$[VOCl_3\{Ph_2P(O)CH_2P(O)Ph_2\}]$	48, 35
$[VOCl_3(Me_3PO)_2]$	74
$[VOCl_3(Ph_3PO)]$	56

Table 2.12. $^{31}P\{^1H\}$ NMR data for the phosphine oxide complexes.

Complex	E_{max}/cm^{-1}	Solution/cm^{-1} (ε /mol^{-1}dm^{3}cm^{-1})
$[VOCl_3$(15-crown-5)]	16000, 20620	22420
$[\{VOCl_3\}_2$(18-crown-6)]	16000, 21000	22320
$[VOCl_3\{Ph_2P(O)CH_2P(O)Ph_2\}]$	17600, 22320, 29070	17980(1300), 22730(3750), 30490(2200)
$[(VOCl_3)_2\{Ph_2P(O)CH_2P(O)Ph_2\}]$	18800, 20800, 25000	17240(sh), 21740, 28990
$[VOCl_3(Ph_3PO)]$	15900, 19400, 21900, 32000	17000(110), 23250(500), 31000(15000)
$[VOCl_3(Ph_3AsO)]$	15500, 19840, 21750, 29760	16000(sh)(~200), 21550(3100), 30490(2295)
$[VOCl_3(Me_3PO)_2]$	17240, 19840, 21930, 28100	17240, 18380, 23580, 33000

Table 2.13. UV-vis spectroscopic data for Vanadium(V) Complexes with O- Donor Ligands.

2.2.4 Vanadium(V) Complexes with S- Donor Ligands

Neutral thioether S-donor ligands are generally considered to be soft, weakly donating ligands (see Chapter 1) and hence are not usually expected to form complexes with small, hard metals such as vanadium(V). In this work we have investigated reaction of the $VOCl_3$ with a range of S-donor ligands, including Me_2S, Ph_2S, $MeSCH_2CH_2SMe$, $EtSCH_2CH_2SEt$, $PhSCH_2CH_2SPh$ and $MeSCH_2CH_2CH_2SMe$. The reaction of $VOCl_3$ with Me_2S, Ph_2S, $PhSCH_2CH_2SPh$ and $MeSCH_2CH_2CH_2SMe$ in anhydrous CH_2Cl_2 solution gave dark solutions which even at low temperature became blue-green in a few seconds. This behaviour is indicative of reduction of the V(V) to V(IV) and/or V(III), with probable oxidation of the thioether to sulfoxide and even at low temperature we were not

able to isolate a V(V) thioether adduct with these particular ligands. The reaction schemes can be seen in Figure 2.9.

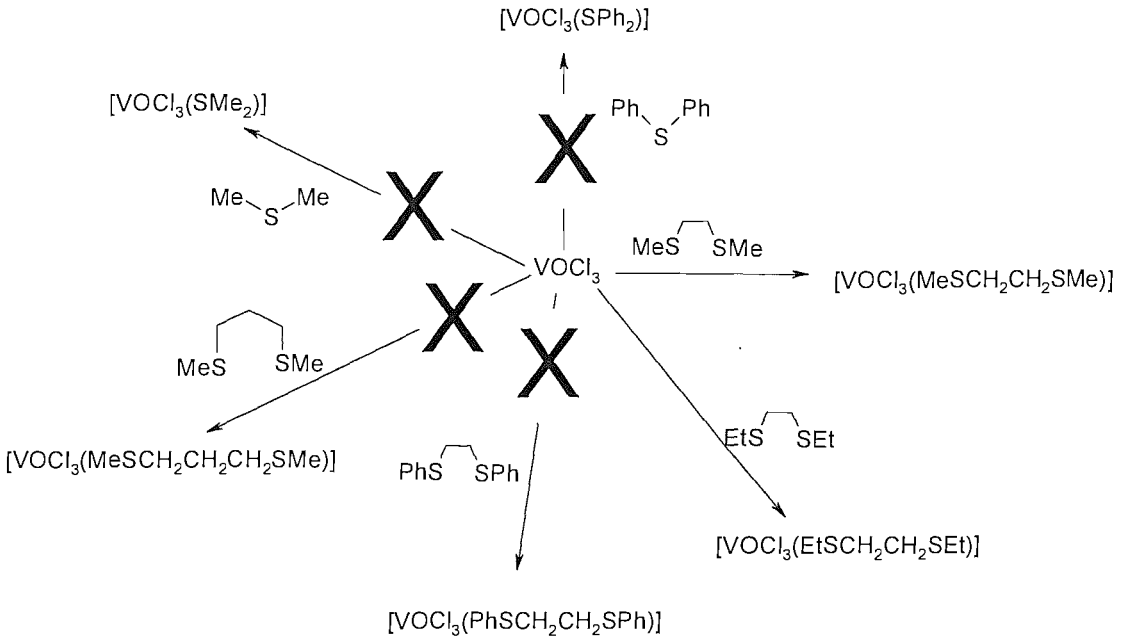

Fig 2.9 Schemes for V(V) complexes with S-Donor Ligands

However, the V(V) thioether complex $[VOCl_3(MeSCH_2CH_2SMe)]$ was successfully prepared from $VOCl_3$ and 1 molar equivalent of $MeSCH_2CH_2SMe$ in dry CH_2Cl_2. The complex was obtained as a red/black solid in good yield by precipitation with n-hexane. The product undergoes significant decomposition in solution over a period of 2 to 3 hours and also decomposes in the solid at room temperature when stored in the glove box in the dark, producing a dull purple-black solid which is insoluble in chlorocarbons. For this reason all spectroscopic measurements were undertaken using freshly prepared samples. The $[VOCl_3(MeSCH_2CH_2SMe)]$ complex was analysed by microanalysis and IR spectroscopy shows a V=O stretch at 976 cm^{-1}, with the V-Cl stretches at 376, 350, 327 cm^{-1} as well as weak features from the ligand. The diffuse reflectance and solution (CH_2Cl_2) UV-vis spectra show intense broad features in the range 18000-25000 cm^{-1} with low energy shoulders, assigned as Cl→V and S→V charge transfer bands. In contrast, the diffuse reflectance spectrum of the decomposed solid shows broad ill-defined absorptions across the visible region, probably attributable to mixed valence species formed in the decomposition. The room temperature ^1H NMR spectrum (CD_2Cl_2) shows singlet CH_3 and

CH_2 resonances, but cooling to -80°C gives rise to four CH_3 resonances of unequal intensities and the methylene region becomes a complex multiplet. This is consistent with the slowing of pyramidal inversion at the coordinated sulfur. The probable structure containing *fac*-Cl's and S *trans* Cl would give rise to three diastereoisomers with a total of four methyl resonances. The ^{51}V NMR spectrum is a singlet at δ -14 ppm; on cooling the resonance sharpens but is unshifted, consistent with one geometric isomer (it is unlikely that the diastereoisomers would be observed in the ^{51}V NMR due to the broad lines). Addition of $VOCl_3$ to the solution gives a single resonance at 25°C, due to fast exchange but on cooling below ca. -70°C separate resonances are resolved for the complex and $VOCl_3$. Traces of water cause rapid hydrolysis and the formation of $[VOCl_4]^-$ (δ = +48 ppm) and $[VO_2Cl_2]^-$ (δ = -362 ppm).

$[VOCl_3(EtSCH_2CH_2SEt)]$ was prepared by an analogous route to $[VOCl_3(MeSCH_2CH_2SMe)]$, although the almost black solid was best obtained by using an excess of $VOCl_3$ and pumping the reaction mixture to dryness. The freshly prepared complex is soluble in CH_2Cl_2 and $CHCl_3$. However it is even less stable than the Me-substituted analogue above, producing an insoluble dark purple solid after only a few hours even in the glove box. The spectroscopic features of the freshly prepared $[VOCl_3(EtSCH_2CH_2SEt]$ are very similar to the Me-substituted analogue, although the instability of the complex makes obtaining reliable solution data more difficult. These two complexes represent the first examples of vanadium(V) thioethers and show that the small, hard V(V) centre may be combined with soft thioether ligands depending upon the denticity of the ligand, the resulting chelate ring size and the nature of the terminal substituents on the S atoms. Several attempts to grow crystals of $[VOCl_3(MeSCH_2CH_2SMe)]$ were unsuccessful, probably owing to the inherent instability of the compound which partially decomposes during the crystallisation.

In an attempt to probe the possible coordination of the analogous selenoether ligands to V(V), $VOCl_3$ was combined with $MeSeCH_2CH_2SeMe$ in anhydrous CH_2Cl_2 solution at 78°C. This led to immediate formation of a green solution indicative of reduction to V(IV)/(III). This is consistent with the increased ease of oxidation of the selenoether

compared to the thioether groups. Similar results were obtained using *o*-$C_6H_4(AsMe_2)_2$ and $VOCl_3$.

Complex	ν(V=O)/cm^{-1a}	ν(V-Cl)/cm^{-1a}
[$VOCl_3$(MeSCH$_2$CH$_2$SMe)]	976	376, 350, 327
[$VOCl_3$(EtSCH$_2$CH$_2$SEt)]	977	366, 349, 323

Table 2.14 Selected IR spectroscopic data Vanadium(V) Complexes with S- Donor Ligands.

a = Recorded as a Nujol mull.

Complex	^{51}V (δ)/ppm	$w_{1/2}$/Hz
[$VOCl_3$(MeSCH$_2$CH$_2$SMe)]	-14	800
[$VOCl_3$(EtSCH$_2$CH$_2$SEt)]	-7.5	700

Table 2.15. ^{51}V NMR spectroscopic data for the Vanadium(V) Complexes with S- Donor Ligands.

2.2.5 Attempted Preparations of Vanadium(IV) Thioether Complexes

In view of the results obtained with V(V) in this work we were interested to explore the chemistry of the intermediate V(IV) oxidation state with thioether ligands. The [$VOCl_2$(thf)$_2$] complex reported in the literature was identified as a useful precursor since it was expected that the thf might be substituted by the thioether ligand and it should be easily removed under vacuum. The preparation of [$VOCl_2$(thf)$_2$] was attempted using the method outlined by Davies *et al.*, by bubbling moist air through a thf solution of [VCl_3(thf)$_3$].[45] On the basis of IR and UV-vis spectroscopy this seemed to contain the dihydrate [$VOCl_2$(thf)$_2$].2H_2O and the reaction appeared to produce the expected complex with water molecules bound to the desired product, except it was not the desired colour. However, the [$VOCl_2$(thf)$_2$].2H_2O was combined with [9]aneS_3 in thf solution, producing a pale blue solid which was collected by filtration, washed with thf and dried under vacuum. Spectroscopic analysis showed that this was the same as the [$VOCl_2$([9]aneS_3)] complex made previously and crystallographically characterised by Willey *et al.*, albeit as a hydrolysis product from the attempted synthesis of [VCl_3([9]aneS_3)].[46] The IR spectrum showed the expected V=O stretch at 957 cm^{-1} and two V-Cl stretches at 352 and 300 cm^{-1}. The UV-vis spectrum (diffuse reflectance) contained four bands at 30490, 26600, 14530

$MeSCH_2CH_2SMe$ in dry CH_2Cl_2. This produced a black waxy product which did not show any evidence for thioether coordination, and the IR spectrum showed strong bands due to the presence of substantial water (3500, 1625 cm^{-1}). This is consistent with [9]aneS_3 being a superior ligand to $MeSCH_2CH_2SMe$, the macrocycle competing successfully with the H_2O present. It was decided at this point to move the direction of the project towards vanadium(III) chemistry (Chapter 3).

2.3 Conclusion

In this chapter a series of vanadium(V) complexes have been obtained of the form $[VOCl_3(L)]$, $[VOCl_3(L)_2]$ and $[VOCl_3(L\text{-}L)]$ involving a range of ligand types including N-heterocycles, amines, crown ethers, phosphine oxides, arsine oxide and the first examples involving thioethers. The compounds have been characterised by microanalysis, IR, UV-vis, variable temperature ^1H, $^{31}P\{^1H\}$ and ^{51}V NMR spectroscopy as appropriate. The coordination number (5 or 6) has been established spectroscopically and seems to be at least partly dependent upon the steric requirements of the ligand compared to the small vanadium(V) ion. The ^{51}V NMR spectroscopy shows that the complexes are usually dynamic in solution, probably a consequence of reversible ligand dissociation. As expected the bidentate ligands with hard donor atoms (bipy, phen) form among the more stable complexes

The complexes were found to be highly moisture sensitive and this hindered attempts to obtain crystallographic data. The crystal structure of one hydrolysis product, $[VOCl_2(bipy)_2(\mu\text{-}O)]$ was determined and shows the dinuclear structure composed of distorted octahedral $VOCl_2(bipy)$ units linked by a bridging oxo ligand.

It has been found that with soft ligands such as thioethers, selenoethers and arsines, reduction of the vanadium to the +4 and +3 oxidation states becomes important. However, for the $RSCH_2CH_2SR$ (R = Me or Et) it is possible to isolate and characterise species of the form $[VOCl_3(RSCH_2CH_2SR)]$, under rigorously anhydrous conditions.

2.4 Experimental

2.4.1 General

Infrared spectra were recorded as Nujol mulls between CsI discs using a Perkin-Elmer 983G spectrometer over the range 4000-180cm^{-1}. ^{1}H NMR spectra were recorded using a Bruker AM300 spectrometer at 298 K unless otherwise stated. ^{51}V{^{1}H} and ^{31}P {^{1}H} NMR were recorded using a Bruker DPX400 spectrometer operating at 105.22 and, 161.98 MHz respectively and are referenced to external neat $VOCl_3$ and external 85% phosphoric acid respectively. UV-visible spectra were obtained in diffuse reflectance mode from powdered samples diluted with $BaSO_4$, using a Perkin Elmer Lambda19 spectrometer, or as solutions in CH_2Cl_2 using quartz cells (1 cm path length). Microanalyses were performed by the University of Strathclyde microanalytical service.

All glassware was dried in an oven overnight prior to use. Solvents were dried using standard procedures prior to use.[47] CH_2Cl_2 was dried using calcium hydride, hexane and ether were dried using sodium/benzophenone. All preparations were undertaken using standard Schlenk techniques under a N_2 atmosphere. Pyridine was distilled from sodium at 130°C. 1,10-phenanthroline was heated to just over 100°C for an hour, while under vacuum. 2,2'-dipyridyl was stored in a desiccator under vacuum overnight and an IR spectrum was obtained which showed that the solid was dry. Tetraphenylarsonium chloride was heated to 110°C for an hour under vacuum. Triphenylphosphine oxide was heated to 110°C for an hour under vacuum. $Ph_2P(O)CH_2P(O)Ph_2$ was heated to 110°C under vacuum for about 2 hours. Trimethylphosphine oxide was heated to 110°C under vacuum and sublimed onto a cold finger. 18-crown-6 and 15-crown-5 were each dissolved in CH_2Cl_2 and had thionylchloride added dropwise, refluxed for an hour at 60°C and then pumped to dryness. A glovebox was used for making up samples for analysis and for storage of particularly hydroscopic starting materials; also it was used for the storage of all products.

$VOCl_3$ was obtained from Aldrich and used as received. Bipy, phen, 18-crown-6 and 15-crown-5 were also obtained from Aldrich but were dried as above. Ph_4AsCl and Ph_3PO (Fluka). Pyridine (Aldrich) and tmen (Fluka) was distilled from sodium

2.4.2 Vanadium(V) Anion Complexes

Preparation of $[Ph_4As][VOCl_4]$ [33]

To a suspension of Ph_4AsCl (1 g, 5.3 mmol) in ethanol (1-2 mL) was added a solution of $VOCl_3$ (0.5 g, 2.9 mmol) in HCl_{conc} (saturated with hydrogen chloride gas, 9 mL) which had been cooled to 0°C. This produced a dark red precipitate. On filtering *in vacuo* a brown/red solid was obtained. The solid was filtered, washed with ether (~9 mL) and dried *in vacuo* for 30 minutes. This procedure was based on one that was reported in the literature by Drake *et al.*[33] ^1H NMR ($CDCl_3$): δ 7.75 (m) [20H] (Ph) ppm. ^{51}V NMR ($CDCl_3$): δ 48 (s, $w_{1/2}$ = 300 Hz), (major $[VOCl_4]^-$), -362 (s, $w_{½}$ = 1500 Hz) (minor $[VO_2Cl_2]^-$) ppm. IR (Nujol)/cm^{-1}: 1376(s), 1335(sh), 1310(w), 1183(w), 1160(w), 1083(m), 1025(m), 997(m), 967(m), 957(m), 920(w), 743(s), 688(m), 600(w), 490(w), 475(m), 462(m), 432(mw), 373(m), 351(w) cm^{-1}. UV-vis (solid-$BaSO_4$): 15240, 20000, 26320, 33330 cm^{-1}.

Preparation of $[Ph_4As][VOCl_4]$ [31]

To a solution of $VOCl_3$ (0.415g, 2.39 mmol) and anhydrous acetonitrile (10 mL), Ph_4AsCl (1.00 g, 2.39 mmol) dissolved in acetonitrile (10 mL) was added dropwise over a period of 15 minutes. A dark red/brown colour was noted and the mixture was left to stir for 30 minutes. The solution was then concentrated *in vacuo* and hexane (15 mL) was added. The resulting dark red precipitate was stirred vigorously for 20 minutes. Hexane (15 mL, dry) was added producing a dark brown solid and then filtered *in vacuo*. A dark brown/red solid was collected (1.8g, 89%). This procedure was based on the method that was reported by Wolfgang *et al.*[31] ^{51}V NMR ($CDCl_3$): δ 48 (s, $w_{½}$ = 300 Hz) ppm. IR (Nujol)/cm^{-1}: 3419(w), 1660(w), 1381(m), 1335(w), 1314 (w), 1263(m), 1191(w), 1162(w), 1099(sh), 1085(s), 1024(m), 995(m), 962(m), 956(s), 919(w), 812(m), 744(s), 688(s), 482(sh), 475(m), 460(m), 437(m), 393(w), 372(w) cm^{-1}. UV-vis (solid-$BaSO_4$): 15240, 18120(sh), 19840, 25000, 30490

Preparation of $[Ph_4As][VO_2Cl_2]$ [32]

A solution of Ph_4AsCl (0.93 g, 2.05 mmol) dissolved in water (1 mL) was added dropwise to a solution of sodium metavanadate (0.25 g, 2.05 mmol) dissolved in HCl (3 mL, 25%).

The contents were stirred vigorously to produce a green/yellow solution and a yellow precipitate. The solid was filtered in air and washed with diethyl ether (2 x 1 mL) and dried *in vacuo*. A yellow/green solid was obtained (0.19 g, 16%). This method was based on the procedure reported by Ahlborn *et al.*[32] ^{51}V NMR ($CDCl_3$): δ –362 (s, $w_{½}$ = 158 Hz) ppm. IR (Nujol)/cm^{-1}: 1649(w), 1480(sh), 1377(m), 1336(m), 1309(w), 1185(w),1164(w), 1081(s), 1020(w), 996(s), 967(s), 957(s), 922(w), 849(w), 742(s), 687(s), 613(w), 475(s), 459(s), 431(s), 352(s), 321(w), 235(w) cm^{-1}. UV-vis (solid-neat): 24630, 33000, 37040, 45050 cm^{-1}; (solution–CH_2Cl_2): (ε_{mol}/ 245 $mol^{-1}dm^3cm^{-1}$) 25000 (245), 35090 (1260) cm^{-1}.

2.4.3 Vanadium(V) Neutral Complexes

[$VOCl_3$(bipy)]

A solution of $VOCl_3$ (0.23 g, 1.3 mmol) in dry CH_2Cl_2 (5 mL) was added to a solution of bipy (0.2 g, 1.3 mmol) in dry CH_2Cl_2 (10 mL). The dark red solution was concentrated to *ca* 5 mL in vacuum, dry hexane (5 mL) was added and the red-black solid isolated by filtration, and dried *in vacuo*. (0.30 g, 70%). Anal: Calc. for $C_{10}H_8Cl_3N_2OV$: C, 36.5; H, 2.5; N, 8.5; Found: C, 37.1; H, 2.1; N, 8.2%. ^{1}H NMR ($CDCl_3$): 7.6 (m) [2H], 8.5 (m) [4H], 9.35 (s) [H], 9.7 (s) [H] ppm. ^{51}V NMR (CH_2Cl_2): -103 ($w_{½}$ = 370 Hz) ppm. IR (Nujol)/cm^{-1}: 1314(m), 1261(m), 1157(w), 1104(w), 1026(m), 978(s), 802(m), 763(s), 658(m), 381(s), 358(s), 348(s) cm^{-1}. UV-vis (solid-$BaSO_4$): 17200(sh), 19120(sh), 21370, 32260 cm^{-1};(solution-CH_2Cl_2): (ε_{mol}/ $cm^{-1}dm^3mol^{-1}$) 19250(sh), 21550 (1325), 22730 (1300), 26310(sh), ~33000(~ 20000) cm^{-1}.

[$VOCl_3$(phen)]

The complex was made similarly from $VOCl_3$ (0.29 g, 1.6 mmol) and phen (0.29 g, 1.6 mmol). A dark red-brown solid (0.32 g, 55%) was isolated. Anal: Calc. for $C_{12}H_8Cl_3N_2OV$: C, 40.7; H, 2.3; N, 7.9; Found: C, 39.8; H, 2.0; N, 7.5 %. ^{1}H NMR ($CDCl_3$): 8.00(m) [4H], 8.65(s) [2H], 9.75(s) [1H], 9.95(s) [1H] ppm. ^{51}V NMR (CH_2Cl_2): -108 ($w_{½}$ = 560 Hz) ppm IR (Nujol)/cm^{-1}: 1308(w), 1258(w), 1171(m), 1140(s), 1023(w), 973(s), 839(s), 776(m), 431(m), 386(s), 347(s), 319(sh). UV-Vis (solid-$BaSO_4$): 18000(sh), 22220, 32895 cm^{-1}; (solution-CH_2Cl_2): (ε_{mol}/ $cm^{-1}dm^3mol^{-1}$) 18200(sh), 21505 (1680), 22730 (1730), ~33000 (~ 15000) cm^{-1}.

[$VOCl_3$(py)]

A solution of pyridine (0.2 g, 2.5 mmol) in CH_2Cl_2 (5 mL) was added to $VOCl_3$ (0.84 g, 4.8 mmol) in CH_2Cl_2 (25 mL) producing an immediate precipitate. The solution was stirred for 30 minutes and then pumped to dryness *in vacuo* at room temperature. The dark brown powder produced was rinsed with hexane (5 mL), the solid filtered off and dried *in vacuo.* (0.40 g, 64%). Anal: Calc. for $C_5H_5Cl_3NOV$: C, 23.8; H, 2.0; N, 5.6; Found: C, 23.1; H, 2.1; N, 5.4 %. ^{1}H NMR ($CDCl_3$): 7.5(s) [2H], 8.0(s) [H], 8.9(s) [2H] ppm. ^{51}V NMR (CH_2Cl_2): -36 ($w_{½}$ = 800 Hz) ppm. IR (Nujol)/cm^{-1}: 1604(w), 1361(m), 1250(w), 1236(w), 1158(m, 1071(m), 1020(s), 964(w), 869(m) 757(s), 734(s), 687(s), 642(m), 419(s), 385(s), 344(s). UV-Vis (solid-$BaSO_4$): 16024(sh), 20900, 33000 cm^{-1}; (solution-CH_2Cl_2): 21500,29110 cm^{-1}.

[$VOCl_3$(py)$_2$]

A solution of pyridine (0.4 g, 5.0 mmol) in CH_2Cl_2 (5 mL) was added to $VOCl_3$ (0.21 g, 1.2 mmol) in CH_2Cl_2 (5 mL) producing an immediate precipitate. The mixture was stirred briefly, concentrated *in vacuo* to small volume and hexane (5 mL) added. The red solid was filtered off rinsed with hexane, and dried *in vacuo.* (0.23 g, 51%). Anal: Calc. for $C_{10}H_{10}Cl_3N_2OV$: C, 36.2; H, 3.0; N, 8.5; Found: C, 36.3; H, 3.9; N, 8.3 %. ^{1}H NMR ($CDCl_3$): 7.3-7.5(m) ppm. ^{51}V NMR (CH_2Cl_2): -58 ($w_{½}$ = 300 Hz) ppm. IR (Nujol)/cm^{-1}: 1604(m), 1375(m), 1325(w), 1263(w), 1161(w), 1054(m), 978(s), 800(s), 750(s), 671(s), 426(s), 393(m), 372(m), 347(m). UV-Vis (solid-$BaSO_4$): 20240(vbr), 27940 cm^{-1} ;(solution-CH_2Cl_2): 19800(sh), 21740, 28730 cm^{-1}.

[$VOCl_3$(tmen)]

An ice cold solution of tmen (0.5 mL, 4.0 mmol) in CH_2Cl_2 (5 mL) was added to an ice cold solution of $VOCl_3$ (0.84 g, 4.0 mmol) in CH_2Cl_2 (5 mL) to produce a dark red colour, with a dark brown precipitate. The reaction mixture was then pumped to dryness to produce a brown solid (1.3 g, 93%). Anal: Calc. for $C_6H_{16}Cl_3N_2OV$: C, 24.9; H, 5.5; N, 9.7%; Found: C, 18.41; H, 4.31; N, 6.36%. ^{1}H NMR ($CDCl_3$): 0.8 (s) [4H], 1.2 (s) [6H] ppm. ^{51}V NMR ($CDCl_3$): 7.5 (w½ = 1800Hz) ppm. IR (Nujol)/cm^{-1}: 1376(s), 1260(m),

1172(s), 1096(m), 1037(w), 990(s), 802(s), 668(w), 477(w), 434(w), 382(sh), 340(s), 310(sh). UV-vis (solid – $BaSO_4$): 15430, 20490, 33330, 43480 cm^{-1}.

[$VOCl_3$(15-crown-5)]

$VOCl_3$ (0.14 g, 0.8 mmol) in dry CH_2Cl_2 (5 mL) was added to 15-crown-5 (0.17 g, 0.77 mmol) in dry CH_2Cl_2 (10 mL) and the solution pumped to dryness in vacuum. The solid was filtered off and dried *in vacuo*. (0.2 g, 64 %) . Analysis: Calcd. for $C_{10}H_{20}Cl_3O_6V$: C, 30.5; H, 5.2. Found: C, 29.4; H, 5.7 %. ^1H NMR ($CDCl_3$): 3.6 (br,s) ppm. ^{51}V NMR (CH_2Cl_2, 223K): -21 ($w_{½}$ = 350 Hz) ppm. IR (Nujol)/cm^{-1}: 1304(w), 1261(m), 1098(vs), 1022(s), 983(m), 940(m), 802(s), 610(w), 428(m), 395(m), 351(m). UV-vis/cm^{-1} (solid-$BaSO_4$): 16000(sh), 20620 cm^{-1} ;(solution-CH_2Cl_2): 22420 cm^{-1}.

[{$VOCl_3$}$_2$(18-crown-6)]

Excess $VOCl_3$ (0.42 g, 2.4 mmol) in dry CH_2Cl_2 (5 mL) was added to 18-crown-6 (0.2 g, 0.76 mmol) in dry CH_2Cl_2 (10 mL) and worked up as described for [$VOCl_3$(15-crown-5)]. Red-brown solid (0.2 g, 30%). Analysis: Calcd. for $C_{12}H_{24}Cl_6O_8V_2$: C, 23.6; H, 4.0. Found: C, 24.3; H, 4.6 %. ^1H NMR ($CDCl_3$): 3.66 (s) ppm. ^{51}V NMR (CH_2Cl_2, 203K): -6 ($w_{½}$ = 2000 Hz) ppm. IR (Nujol) cm^{-1}: 1300(w), 1260(m), 1146(w), 1098(vs), 1027(s), 993(m), 927(m), 803(s), 563(m), 408(sh), 359(s), 306(m). UV-vis(solid-$BaSO_4$): 16000(sh), 21000(vbr) cm^{-1} ;(solution-CH_2Cl_2): 22320 cm^{-1}.

[$VOCl_3$(Ph_3PO)]

A solution of triphenylphosphine oxide (0.56 g, 2.0 mmol) in CH_2Cl_2 (5 mL) was added to $VOCl_3$ (0.35 g, 2.0 mmol) in CH_2Cl_2 (5 mL), the dark solution stirred briefly and then concentrated *in vacuo*. The solution was treated with hexane (5 mL) and refrigerated to give a red-brown solid, which was filtered off and dried *in vacuo*. (0.53 g, 58%). Anal: Calc. for $C_{18}H_{15}Cl_3O_2PV$: C, 47.9; H, 3.3; Found: C, 48.5; H, 3.3 %. ^1H NMR ($CDCl_3$): 7.4-7.8(m) ppm. ^{51}V NMR (CH_2Cl_2, 200K): -83 (w½ = 700 Hz) ppm. $^{31}P\{^1H\}$ NMR (CH_2Cl_2): 56 ppm. IR (Nujol)/cm^{-1}: 1312(w), 1260(m), 1182(m), 1119(s), 1050(s){PO}, 1020(s), 992(m), 749(s), 688(s), 535(vs), 432(m), 403(m), 372(m), 336(m), 311(m).

UV-Vis (solid-$BaSO_4$): 15900(sh), 19400, 21900(sh), 32000 cm^{-1} ;(solution-CH_2Cl_2): (ε_{mol}/ $cm^{-1}dm^3mol^{-1}$) 17000 (110), 23250(500), 31000 (15000) cm^{-1}.

[$VOCl_3(Me_3PO)_2$]

A solution of trimethylphosphine oxide (0.09 g, 1.0 mmol) in CH_2Cl_2 (5 mL) was added to $VOCl_3$ (0.09 g, 0.5 mmol) in CH_2Cl_2 (5 mL), the dark brown solution which was stirred briefly, filtered, and evaporated to dryness *in vacuo*. (0.16 g, 88%). Anal: Calc. for $C_6H_{18}Cl_3O_3P_2V$: C, 20.1; H, 5.0; Found: C, 20.6; H, 5.3%. ^1H NMR ($CDCl_3$): 2.0(br) ppm. ^{51}V NMR (CH_2Cl_2): -92 ($w_{½}$ = 740 Hz) ppm. $^{31}P\{^1H\}$ NMR (CH_2Cl_2): 74 ppm; essentially unchanged on cooling to 210 K. IR(Nujol)/ cm^{-1}: 1297(s), 1260(m), 1085(vs){PO}, 1016(s), 952(s), 863(m), 801(m), 757(w), 608(w), 468(sh), 431(m), 381(sh), 367(m), 345(sh). UV-Vis (solid-$BaSO_4$): 17240(sh), 19840(sh), 21930, 28100 cm^{-1}; (solution-CH_2Cl_2): 17240sh, 18380, 23580, 33000 cm^{-1}.

[$VOCl_3\{Ph_2P(O)CH_2P(O)Ph_2\}$]

A solution of the diphosphine dioxide (0.27 g, 0.65 mmol) in CH_2Cl_2 (10 mL) was added to $VOCl_3$ (0.11g, 0.65 mmol) in CH_2Cl_2 (5 mL), and the dark solution stirred briefly. Hexane (5 mL) was added and the dark-brown precipitate filtered off and dried *in vacuo*. (0.175 g, 46%). Anal: Calc. for $C_{25}H_{22}Cl_3O_3P_2V$: C, 50.9; H, 3.8; Found. C, 50.9; H, 3.5%. ^1H NMR ($CDCl_3$): 7.4-7.9(m), 3.95(br,s) ppm; no change at 210 K. ^{51}V NMR (CH_2Cl_2, 200 K): -81 ($w_{½}$ = 2500 Hz) ppm. $^{31}P\{^1H\}$ NMR (CH_2Cl_2, 223 K): 48 (br), 35 (br) ppm; 200 K: 48.2(d, $^2J_{P\text{-}P}$ = 12 Hz), 34.5 (d, $^2J_{P\text{-}P}$ = 12 Hz) ppm. IR (Nujol)/cm^{-1}: 1260(m), 1164(s) {PO}, 1125(s), 1099(m), 1080(m){PO}, 1055(m), 1025(m), 970(w), 777(s), 687(s), 517(s), 395(m), 337(s), 320(sh). UV-Vis (solid-$BaSO_4$): 17600(sh), 22320, 29070 cm^{-1} ;(solution-CH_2Cl_2): (ε_{mol}/ $cm^{-1}dm^3mol^{-1}$): 17980 (1300), 22730 (3750), 30490 (2200) cm^{-1}.

[$(VOCl_3)_2\{Ph_2P(O)CH_2P(O)Ph_2\}$]

$VOCl_3$ (0.19 g, 1.08 mmol) was added to a solution of $Ph_2P(O)CH_2P(O)Ph_2$ (0.30 g, 0.72 mmol) in CH_2Cl_2 (5 mL) to produce a red solution. The solution was pumped to dryness *in vacuo*. A red/black solid was produced (2.35 g, 77%). Microanalysis: Anal: Calc. for

$C_{25}H_{22}Cl_6O_4P_2V_2$: C, 39.0; H, 2.9; Found: C, 43.1; H, 2.9%. ^1H NMR ($CDCl_3$): 4.2 (s), 4.25 (s), 7.2-8.2 (broad m) ppm; (323 K): 4.2 (s), 4.25 (s), 7.2-8.2 (broad m) ppm. ^{51}V NMR ($CDCl_3$, 183 K): -80 (broad s) ppm; shifts gradually to low frequency on cooling. $^{31}P\{^1H\}$ NMR (CH_2Cl_2, 183 K): no resonance observed. IR (Nujol)/cm^{-1}: 1589(w), 1376(s), 1260(m), 1123(m), 1094(m) {PO}, 1081(m), 1023(m), 995(w), 927(w), 872(w), 789(m), 687(m), 637(w), 609(w), 572(w), 503(w), 503(m), 438(m), 388(m), 337(m). UV-vis (solid-$BaSO_4$): 15620, 18800, 20800(sh), 25000, 32900 cm^{-1}; (solution – CH_2Cl_2): 17240 (sh), 21740, 28990 cm^{-1}

[$VOCl_3(Ph_3AsO)$]

Triphenylarsine oxide (0.32 g, 1.0 mmol) was melted *in vacuo* † and after 20 minutes the melt was cooled to room temperature, dissolved in dry CH_2Cl_2 (10 mL) and added to $VOCl_3$ (0.35 g, 2.0 mmol) dissolved in CH_2Cl_2 (5 mL). The dark solution stirred briefly and then concentrated *in vacuo*. The solution was treated with hexane (5 mL) to give a red-black solid, which was filtered off and dried *in vacuo*. (0.40 g, 80%). Anal: Calc for $C_{18}H_{15}AsCl_3O_2V.CH_2Cl_2$: C, 39.3; H 3.0; Found: C, 39.6; H, 2.7%. ^1H NMR ($CDCl_3$): 7.4-7.8(m), 5.4 (CH_2Cl_2) ppm. ^{51}V NMR (CH_2Cl_2): -142 (w½ = 400 Hz) ppm. IR (Nujol)/cm^{-1}: 1363(m), 1260(m), 1087(s), 1016(s), 803(m) {AsO}, 735(s), 684(m), 530(w), 461(m), 393(m), 365(m), 347(sh). UV-Vis (solid-$BaSO_4$): 15500(sh), 19840, 21750, 29760 cm^{-1} ;(solution-CH_2Cl_2):(ε_{mol}/ $cm^{-1}dm^3mol^{-1}$) 16000(sh) (~200), 21550(3100), 30490(2295) cm^{-1}.

† Unless rigorously dried this reaction gives the product as a black oil which appears spectroscopically identical to the solid complex.

[$VOCl_3(MeSCH_2CH_2SMe)$]

A solution of $VOCl_3$ (0.23 g, 1.3 mmol) in dry CH_2Cl_2 (5 mL) was added to a solution of 2,5-dithiahexane (0.16 g, 1.3 mmol) in dry CH_2Cl_2 (20 mL). The dark red solution was concentrated to *ca* 5 mL *in vacuo*, dry n-hexane (5 mL) added and the red-black solid isolated by filtration, and dried *in vacuo* (0.18 g, 46%). Anal: Calc. for $C_4H_{10}Cl_3OS_2V$: C, 16.3; H, 3.4; Found: C, 16.1; H, 3.6%. ^1H NMR (CD_2Cl_2): 2.35 (s) [3H], 3.0 (s) [2H] ppm; 193 K: 2.36 (s), 2.39 (s), 2.47 (s), 2.60 (s) (Me), 3.15-3.33 (CH_2 v br) ppm. ^{51}V NMR (CH_2Cl_2): -14 (w½ = 800 Hz) ppm; sharpens on cooling but shift unchanged. IR

(Nujol)/cm^{-1}: 1376(s), 1309(w), 1261(m), 1165(w), 1068(m), 1023(m), 976(s), 952(sh), 884(w), 864(w), 833(w), 806(w), 648(w), 638(w), 612(w), 450(w), 376(s), 350(s), 327(s), 225(m). UV-Vis (solid- $BaSO_4$): 14 200(br, sh), 18 880, 21 500(sh), 27 000(sh), 34 500 cm^{-1}; (solution-CH_2Cl_2): (ε_{mol}/ $cm^{-1}dm^3mol^{-1}$) 17 120(sh), 20 160 (930), 21 050 (1150), 25 600 (1500), 31 050(sh), 33 330 (2700) cm^{-1}.

[$VOCl_3(EtSCH_2CH_2SEt)$]

A solution of $VOCl_3$ (0.35 g, 2.0 mmol) in dry CH_2Cl_2 (5 mL) was added to a solution of $EtSCH_2CH_2SEt$ (0.30 g, 2.0 mmol) in dry CH_2Cl_2 (5 mL). The dark red solution was concentrated to *ca* 5 mL in vacuum, dry n-hexane (10 mL) added and the black solid isolated by filtration, and dried *in vacuo* (0.1 g, 45%). IR (Nujol)/cm^{-1}: 1377, 1253, 1037, 977, 918, 799, 667, 476, 434, 366, 349, 323. ^{51}V NMR (CH_2Cl_2): -7 ($w½$ = 1180Hz) ppm; 223 K: -7.5 ($w_{1/2}$ = 700 Hz) ppm. ^1H NMR (CD_2Cl_2,): 1.46 (s) [3H], 2.96 [2H], 3.20 [2H] ppm. UV/Vis (solid- $BaSO_4$)15000(sh), 20800, 27800(s)cm^{-1}.

[$VOCl_2([9]aneS_3)$]

A solution of $VOCl_2(thf)_2$ (0.16 g, 0.55 mmol) in CH_2Cl_2(30 mL) was added to $[9]aneS_3$ (0.10 g, 0.55 mmol) to produce a blue/green precipitate. The solid was filtered and dried under vacuum and washed with thf (5mL) and diethyl ether (5mL). A blue solid was obtained. (0.1g, 57%). IR (Nujol)/cm^{-1}: 1377(s), 1299(w), 1263(w), 1177(w), 1132(w), 959(s), 935(m), 901(s), 831(m), 673(w), 626(w), 437(m), 352(s), 300(sh). UV-vis (solid – $BaSO_4$): 12630, 14530, 26600, 30490 cm^{-1}; (solution-CH_2Cl_2): (ε_{mol}/ $cm^{-1}dm^3mol^{-1}$): 12650(216), 14730(378), 26390(283).

2.4.4 X-Ray Data

The X-ray data were obtained on a Nonius Kappa CCD diffractometer. The data were collected at 120 K using graphite monochromated M_o-K_α X-ray radiation (λ= 0.71073 Å). The structure, solution and refinement used routine methods.[48,49]

2.5 References

[1] F. A. Cotton, G. Wilkinson, C. A. Murillo, M. Bochmann, *"Advanced Inorganic Chemistry"*, 6th Edition, John Wiley & Sons, New York, (**1999**).

[2] K. Sharpless, A. Teranishi and J. Backvall, *J. Am. Chem. Soc.*, 99, (**1977**), 3120.

[3] G. Cook and J. Mayer, *J. Am. Chem. Soc.*, 116, (**1994**), 1855.

[4] D. C. Crans, J. J. Smee, *Comprehensive Coordination Chemistry*, 11, J. A. McCleverty, T.J. Meyer (eds.), 4, (**2004**), 175; R. Weaver, K. Kustin, *Advan. Inorg. Chem.*, 35, (**1990**), 81.

[5] G. Maciejewska, M. Nosek, T. Glowiak, J. Starosta and M. Cieslak-Golonka, *Polyhedron,* 22, (**2003**), 1415.

[6] M. Ksibi, E. Elaloui, A. Houas, N. Moussa, *Applied Surface Science,* 220, (**2003**), 105

[7] M. Stanciulescu, M. Ikura, *U. S. Pat. Appl. Publ.*, 2003075483, (**2003**).

[8] H. Hagen, C.Bezemer, J. Boersma, H. Kooijman, M. Lutz, A. L. Spek and G. van Koten, *Inorg. Chem.*, 39, (**2000**), 3970.

[9] D. Rehder, H. Holst, W. Priebsch and H. Vilter, *J. Inorg. Biochem.*, 41, (**1991**), 171.

[10] S. Brownstein, *J. Fluorine Chem.*, 15, (**1980**), 539.

[11] C. Weidemann and D. Rehder, *Inorg. Chim. Acta,* 120, (**1986**), 15.

[12] W. Priebsch, D. Rehder, *Inorg. Chem.*, 24, (**1985**), 3058.

[13] D. Rehder, *Z. Naturforsch., Teil* B, 32, (**1977**), 771.

[14] J. C. Daran, A. Gourdon, Y. Jeanin, *Acta Crystallogr., Sect B*, 36, (**1980**), 309

[15] A. Gourdon, Y. Jeannin, *Acta Crystallogr., Sect B*, (**1980**), 304.

[16] J.C Daran, Y. Jeannin, G. Constant, R. Morancho, *Acta Crystallogr., Sect B*, 31, (**1975**), 1833.

[17] C. D. Abernethy, G. M. Codd, M. D. Spicer, M. K. Taylor, *J. Am. Chem. Soc.*, 125, (**2003**), 1128.

[18] T. Wistuba, C. Limburg, H. Pritzkow, *Z. Anorg. Allgem. Chem.*, 628, (**2002**), 2340.

[19] T. A. Kabanos, A. D. Keramidas, A. Papaioannou, A. Terzis, *Inorg. Chem.*, 33, (**1994**), 845.

[20] U. Kynast, S. G. Bott, J. L. Atwood, *J. Coord. Chem.*,17, (**1988**), 53

[21] H. L. Krauss, G. Gnatz, *Chem. Ber.*, 95, (**1962**),1023; K. Behzadi, A. Thompson, *J. Less Common Met.*, 132, (**1987**), 49; R. C Paul, N. C. Sharma, Y .P. Sahi, S .L. Chadha, K. Ashok, *Ind. J. Chem.*,13, (**1975**), 1191.

[22] K. L. Baker, D. A. Edwards, G. W. A. Fowles and R. G. Williams, *J. Inorg. Nucl. Chem.*, 29, (**1967**), 1881.

[23] E. Rosenthal, H. Cui, J. Koch, P. Gaede, M. Hummert and S. Dechert, *J. Chem. Soc., Dalton Trans.*, (**2005**), 3108.

[24] H. Hagen, C.Bezemer, J. Boersma, H. Kooijman, M. Lutz, A. L. Spek and G. van Koten, *Inorg. Chem.*, 39, (**2000**), 3970.

[25] S. J. Miles and J. D. Wilkins, *J. Inorg. Nucl. Chem.*, 37, (**1975**), 2271.

[26] H. Funk, W. Weiss and M. Zeising, *Z. Anorg. Allg. Chem.*, 296, (**1958**), 42.

[27] C. Dijkgraaf, *J. Phys. Chem.*, 69, (**1965**), 660.

[28] M. C. Chakravorti and A. R. Sarkar, *J. Fluorine Chem.*, 8, (**1976**), 421.

[29] R. C. Hibbert, *J. Chem. Soc., Dalton Trans.*, (**1986**), 751.

[30] D. Nicholls and K. R. Seddon, *J.Chem. Soc. Dalton Trans.*, (**1973**), 2751

[30a] M. F. Gómez, A. Navarro, S. A. Brandón, C. Scolsky, A. B. Altabef, E. L. Veretti, *J. Mol. Struc.*, 626, (**2003**), 101.

[31] G. Beindorf, J. Strahle, W. Liebelt and K. Dehnicke, *Z. Naturforsch., Teil* B, 35, (**1980**), 521.

[32] E. Ahlborn, E. Diemann and A. Muller, *J. Chem. Soc., Chem. Comm.*, (**1972**), 378.

[33] J. E. Drake, J. E. Vekris and J. S. Wood, *J. Chem. Soc., Dalton Trans.*, (**1969**), 345.

[34] D. Fenske, A. F. Shihada, H. Schwab, K. Dehnicke, *Z. Anorg. Allgem. Chem.*, 471, (**1980**), 140.

[35] W. Levason, B. Patel and G. Reid, *Inorg. Chim. Acta*, 357, (**2004**), 2115.

[36] S. J. A. Pope, N. R. Champness and G. Reid, *J. Chem. Soc., Dalton Trans.*, (**1997**), 1639.

[37] M. B. Hursthouse, W. Levason, R. Ratnani and G. Reid, *Polyhedron*, 23, (**2004**), 1915.

[38] M. D. Brown, M. B. Hursthouse, W. Levason, R. Ratnani and G. Reid, *J. Chem. Soc., Dalton Trans.*, (**2004**), 2487.

[39] R. Hart, W. Levason, B. Patel and G. Reid, *Eur. J. Inorg. Chem.*, (**2001**), 2927.

[40] J. Hanich and M. Krestel, *Z. Naturforsch.,Teil* B, 39, (**1984**), 1686.

[41] J. C. Daran, A. Gourdon, Y. Jeannin, *Acta Crystallogr., Sect. B,* 36, (**1980**), 309.

[42]A. Gourdon, Y. Jeannin, *Acta Crystallogr. Sect. B,* 36, (**1980**), 304.

[43] A. Noll, S. Rabe, U. Mueller, *Z. Naturforsch. Teil* B, 54, (**1999**), 591

[44] F. A. Cotton, S. A. Duraj, G. L. Powell, W. J. Roth, *Inorg. Chim. Acta*, 113, (**1986**), 81.

[45] S. Davies, M. Durrant, D. Hughes, C. LeFloc'h, S. Pope, G. Reid, R. Richards and J. Saunders, *J. Chem. Soc., Dalton Trans.,* (**1998**), 2191.

[46] G. R. Willey, M. T. Lakin, A. W. Alcock, *J. Chem. Soc., Chem. Comm.*, (**1991**), 1414.

[47] R. J. Errington, *Advanced Practical Inorganic and Metal Organic Chemistry*, Blackie Academic and Professional London, (**1997**).

[48] SHELXS-97, program for crystal structure, solution, G. M. Sheldrick, University of Göttingen. Germany 1997.

[49] SHELXS-97, program for crystal structure, refinement, G. M. Sheldrick, University of Göttingen. Germany 1997.

Chapter 3

Chromium(III) and Vanadium(III) Chemistry

3.1 Introduction

Crown ether coordination chemistry has been dominated by group 1 and 2 metals as well as lanthanides.[1,2,3] There are two main types of metal-crown coordination; primary and secondary. Primary coordination is a direct bond between the metal and the crown ether oxygen atoms in complexes such as $[ScCl_2(15\text{-crown-}5)][SbCl_6]$.[4] Secondary coordination involves the crown being bound to the metal via hydrogen bonding from water molecules in complexes such as $[ScCl_3(H_2O)_3]$.18-crown-6.[4] Both forms of coordination can be seen in Fig 3.1.

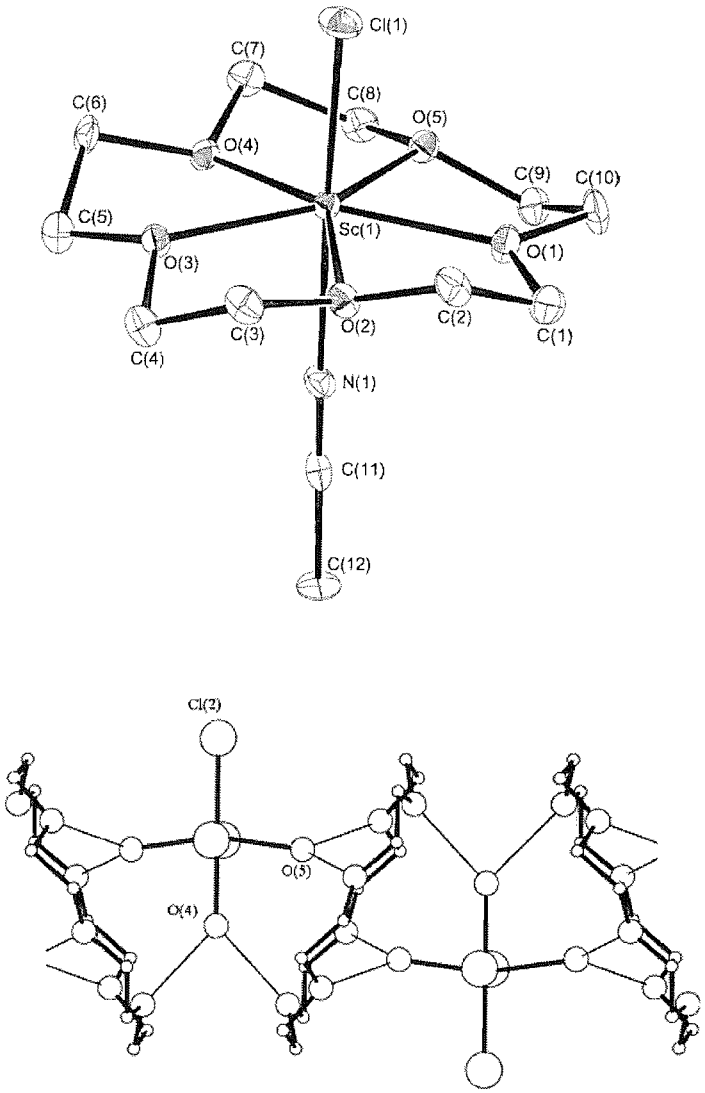

Fig 3.1 Complexes showing primary coordinated $[ScCl(MeCN)(15\text{-crown-}5)][SbCl_6]_2.MeCN$ and secondary coordination $[ScCl_3(H_2O)_3].(18\text{-crown-}6)]$.[4]

This chapter will be exploring the coordination of macrocycles to V(III) or Cr(III) metals. The complexes $[CrCl_3(thf)_3]$ and $[VCl_3(thf)_3]$ both possess octahedral geometry.[5] This has been confirmed by single crystal X-ray diffraction (Fig 3.2). [6]

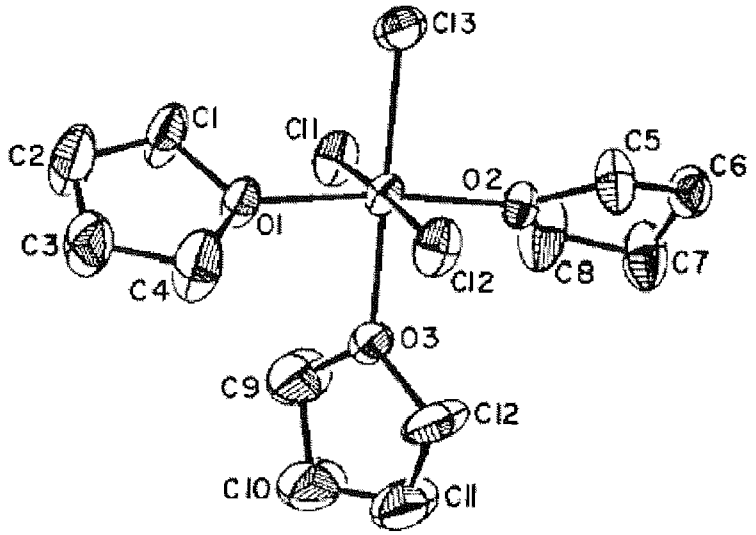

Fig 3.2 Diagram showing the crystal diagram of $[MCl_3(thf)_3]$ (where M=Cr and V).[6]

While Ti(III), V(III) and Cr(III) have all previously been used to produce a number of complexes which have been analysed structurally, such as $[MCl_3(H_2O)(18\text{-crown-}6)]$ (M=Ti or V), [7, 8] $[VCl_2(15\text{-crown-}5)][VOCl_4]$, [9] $[CrCl_3(H_2O)(15\text{-crown-}5)]$ [10] and $[CrCl_3(H_2O)_3].(15\text{-crown-}5)$ [11], no systematic study has been produced. Titanium (IV) halides have been used to synthesise κ^2-coordinated complexes with a selection of crown ethers to produce the moisture sensitive complexes $[TiX_4(\kappa^2\text{-crown})]$ (X=Cl, Br; crown= 12-crown-4, 15-crown-5 and 18-crown-6) as well as $[TiCl_3(15\text{-crown-}5)(MeCN)][SbCl_6]$. Hydrolysed analogues of the species have also been synthesised such as $[Ti_2Cl_6(\mu\text{-}O)(18\text{-crown-}6)_2]$, (fig. 3.3) and $[Ti_4(\mu\text{-}O)_4Cl_8(15\text{-crown-}5)_4]$. These have all been characterised by single crystal X-ray diffraction.[12,13,14]

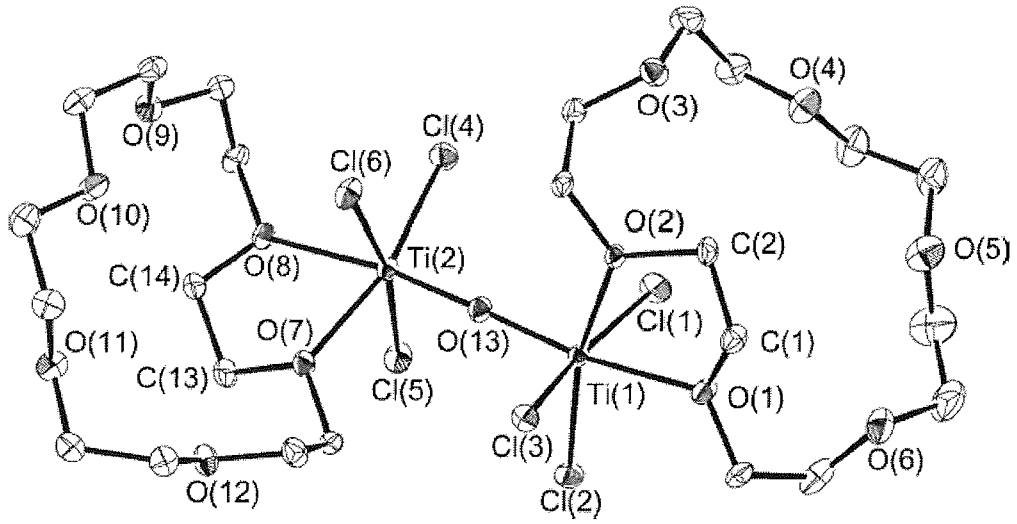

Fig 3.3 Crystal structure of $[(18\text{-crown-6})Cl_3Ti(\mu\text{-}O)TiCl_3(18\text{-crown-6})]$. H atoms are omitted for clarity and the ellipsoids are shown with 50% probability.[13]

There have been many examples of chromium(III) complexes with the harder ligands which incorporate hard donor atoms such as nitrogen and oxygen. $[CrCl_3(NMe_3)_2]$[15]and $[CrCl_3(H_2O)(15\text{-crown-5})]$ have been synthesised[10] but there are few examples with the softer ligands such as thioethers. However, one example is $[CrCl_3([18]aneS_6)]$, the structure published is seen in Section 3.1.2 (Chromium (III) chemistry).[16] Chemistry of vanadium(III) is also limited to the hard ligands rather than the soft thioether ligands, but one example with thioether coordination is $[VCl_3([9]aneS_3)]$.[17]

The effect of combining these soft thioether ligands with hard metals has also been investigated during this work. Previous work on this has also been achieved synthesising complexes such as $[MX_3(L)]$ (X=Cl or Br; L=[9] $aneS_3$, [10]$aneS_3$ and [18]$aneS_6$) as well as cationic species $[CrX_2([n]aneS_4)]PF_6$ (X=Cl or Br; n = 14 or 16).[16,17,18] As well as this, crystallographic data have been obtained on $[CrCl_3\{RS(CH_2)_2NH(CH_2)_2SR\}]$ (R=Me, Et and n-decyl). Fig. 3.4 shows the crystal structure obtained for $[[CrBr_2([14]aneS_4)]PF_6]$, this shows that the Cr metal centre has an octahedral geometry. This further investigation has shown that when the Cr(III) complexes are combined with methylaluminoxane they produce the selective trimerisation of ethene to produce 1-hexene.[19,20]

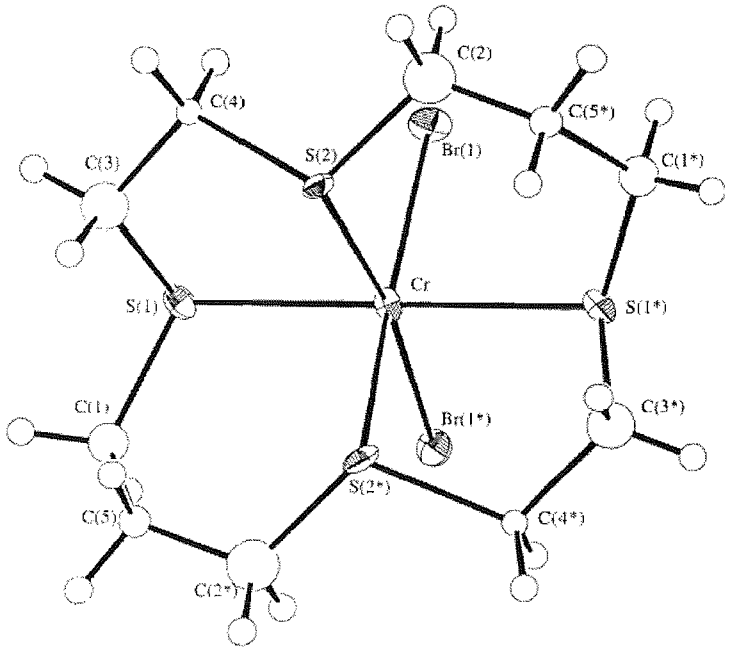

Fig 3.4 Crystal structure of *cis*-$[CrBr_2([14]aneS_4)]PF_6$. H atoms are omitted for clarity and the ellipsoids are shown with 50% probability.[16]

Thioether macrocyclic ligands have also been of interest due to their ability to stabilise unusual oxidations states. This has brought about their use with hard metals. The macrocycles are found to be flexible and possess multiple binding sites, which all aid the stability of the hard metal within the complex.[21] There has also been a keen interest in the use of mixed macrocyclic ligands such as $[18]aneS_3O_3$. This is due to the macrocycle containing hard and soft donor atoms therefore stabilising the metal centre. This has potential applications such as being used as an extractor of metals within the body.[8]

3.1.1 Vanadium (III) Chemistry

$[VCl_3(thf)_3]$ is synthesised by refluxing VCl_3 in thf, and the crystal structure of this complex has been obtained. (Fig. 3.2)[22,23] There is interest in the binding of vanadium to sulfur ligands due to the need to extract sulfur impurities from crude oil. Complexes have been synthesised using both hard and soft macrocyclic ligands. For example, $[VCl_3([9]aneS_3)]$ has been synthesised previously by Davies *et al.*[17] A crystal structure has been obtained (Fig. 3.5).

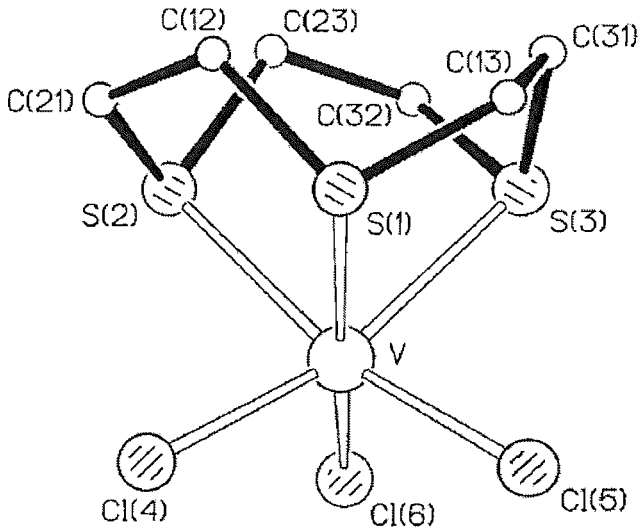

Fig 3.5 Diagram showing the crystal obtained of $[VCl_3([9]aneS_3)]$[17]

The vanadium metal centre is seen to have a distorted octahedral geometry and is bound to three sulfur atoms within the thioether ligand. The complex is found to be hydrolytically stable unlike some other complexes such as $[VCl_3(H_2O)(18\text{-crown-}6)]$. This complex has been synthesised by Kynast *et al.*[8] and is found to be the hydrated form. It appears from the literature that the anhydrous V(III) crown complexes are harder to obtain than the V(III) complexes with the thioether ligands. This was the basis of the investigations in this Chapter, to see how the different O- and S-donor macrocycles bind to the metal centre. Vanadium (IV) crown complexes have also been formed such as $[VOCl_2([9]aneS_3)]$, the crystal data shows the metal has three facially bound sulfurs.[24]

3.1.2 Chromium (III) Chemistry

$[CrCl_3(thf)_3]$ is synthesised by reacting chromium(III) chloride with thf in the presence of zinc powder using a soxhlet apparatus.[25] Cr(III) possesses similar properties to V(III) but tends to be more hydrolytically stable. Cr(III) was therefore used within this chapter to help support or contrast the concept of how the hard metal centres bound with various macrocyclic complexes.

The complex $[CrCl_3([9]aneS_3)]$ has been achieved and partially analysed but no crystal structure has been achieved.[26] It was found that the softer ligand $[9]aneS_3$ bound more readily to the metal centre than the harder ligand $[9]aneN_3$. This was not the expected outcome due to the principles of HSAB theory.

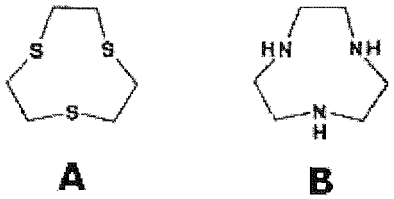

Fig 3.6 Structures of A = $[9]aneS_3$ and B = $[9]aneN_3$ [26]

Crystallographic and spectroscopic data were obtained on the complex $[CrCl_3([18]aneS_6)]$[27] and this showed an octahedral Cr(III) metal centre *via* three facial Cl atoms and three adjacent S atoms. $[CrCl_3(H_2O)(15\text{-crown-5})]$ has been analysed by Junk *et al.*, although the spectroscopic analysis is limited.[11]

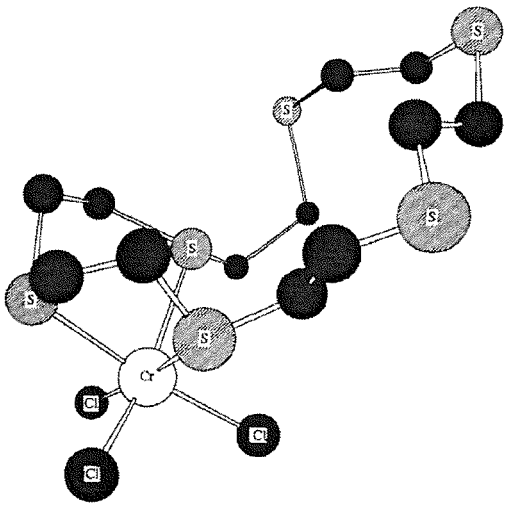

Fig 3. 7 Crystal structure of $[CrCl_3([18]aneS_6)]$.[27]

3.1.3 Other mixed ligand complexes

Other hard metals have been reacted with macrocyclic ligands, such as Ti(III)[21], and Sc(III)[4]. Complexes such as $[ScCl_2(15\text{-crown-5})][SbCl_6]$ [4]

$[ScCl_2(15\text{-crown-5})(MeCN)][SbCl_6]$[4], $[ScCl_2(18\text{-crown-6})][SbCl_6]$[4], $[Sc(12\text{-crown-4})_2]^{3+}$[4] and $[TiCl_4(\kappa^2\text{-crown})]$[21], (where crown= 12-crown-4, 15-crown-5 and 18-crown-6) have all been synthesised. Each of these complexes shows that there are many examples of hard metals bound to hard macrocyclic ligands rather than the softer analogues. $[(TiF_4)_2(18\text{-crown-6})]$ has been synthesised by Cameron *et al.*[28] It was found to be hydrolytically stable and the metal centre is in an octahedral geometry.

Soft metals have been used with mixed donor ligands, such as $[PdCl_2([18]aneS_2O_4)]$. A crystal structure of $[PdCl_2([18]aneS_2O_4)]$ was obtained by Blake *et al.*[29]

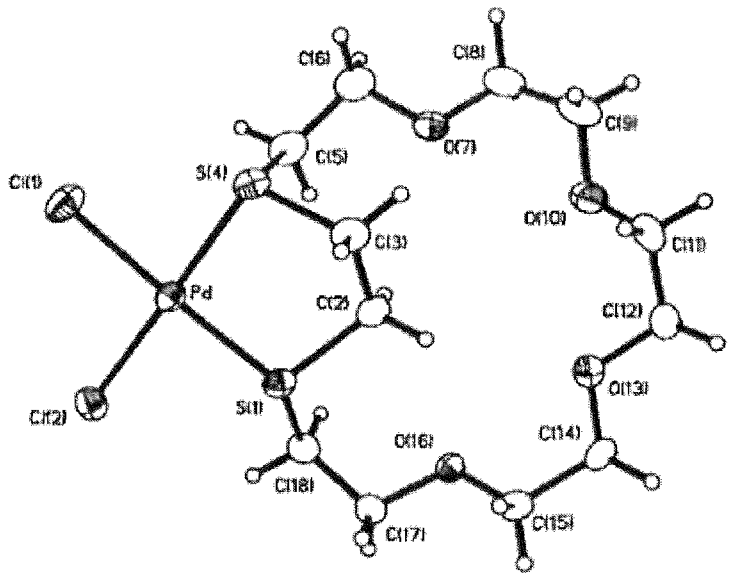

Fig 3.8 Crystal structure of $[PdCl_2([18]aneS_2O_4)]$ with thermal ellipsoids at 30% probability. The hydrogens have been emitted for clarity.[29]

It is seen from the diagram (Fig. 3.8) that as expected the soft metal centre easily binds to the softer sulfur atoms rather than the harder oxygen atoms.[29]

3.1.4 Aims for this chapter

The aim of this work was to investigate the coordination chemistry of V(III) and Cr(III) with a series of macrocyclic ligands incorporating ether and/or thioether functions. As well as extending considerably the range of such complexes, we were also interested to

probe competitively thioether *vs* ether coordination on these metals. Complexes of the form $[MCl_3(\kappa^3\text{-crown})]$ (M = Cr or V; crown = 12-crown-4, 15-crown-5, 18-crown-6, [12]aneS$_4$, [15]aneS$_5$, [9]aneS$_2$O, [15]aneS$_2$O$_3$ and [18]aneS$_3$O$_3$), $[MCl_3(H_2O)(\kappa^2\text{-crown})]$ (crown = 15-crown-5, 18-crown-6) and the dinuclear $[(MX_3)_2(\mu\text{-18-crown-6})]$ were obtained *via* the synthetic routes outlined below (Fig. 3.9 and 3.10).

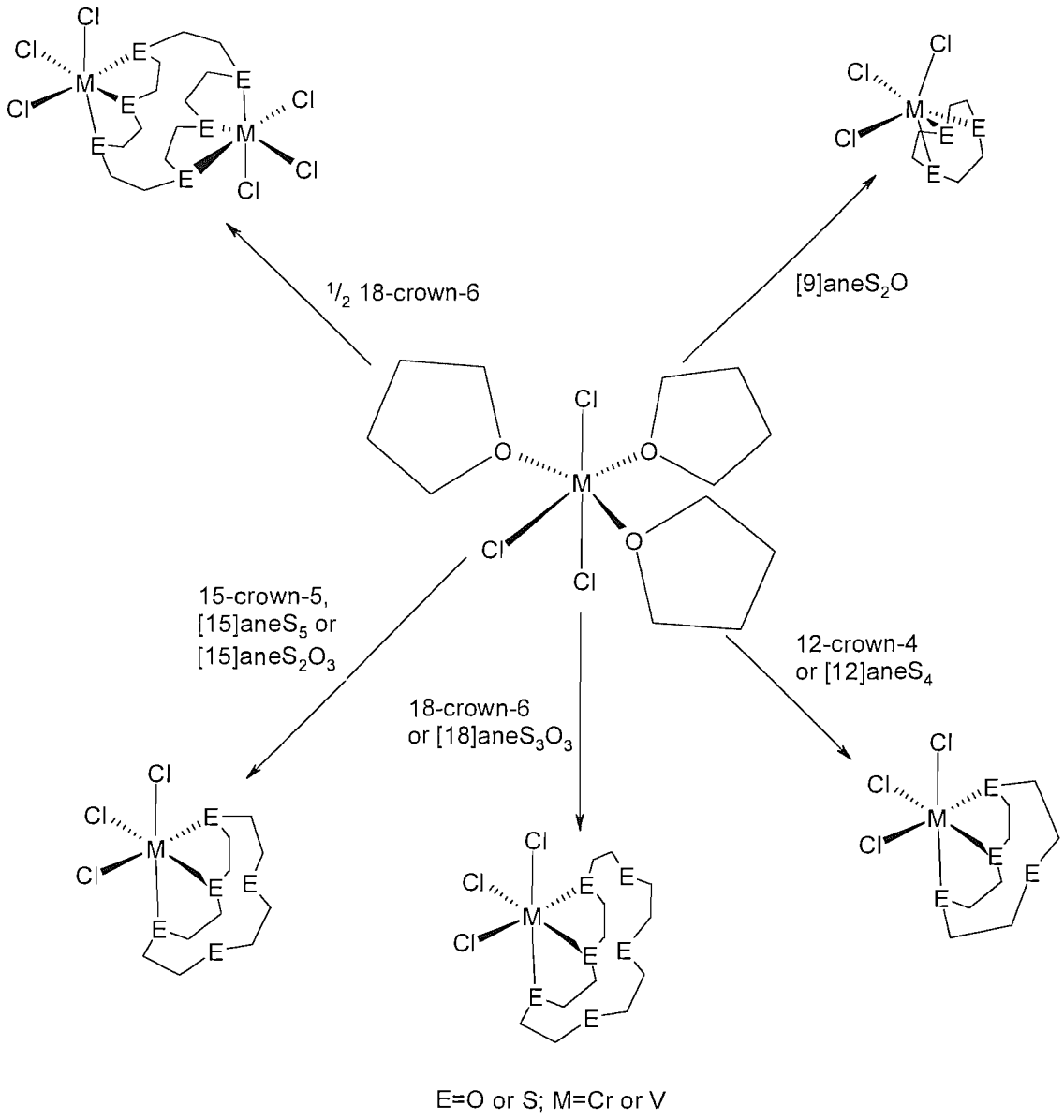

Fig 3.9 Scheme showing the anhydrous Cr(III) and V(III) complexes investigated in this work.

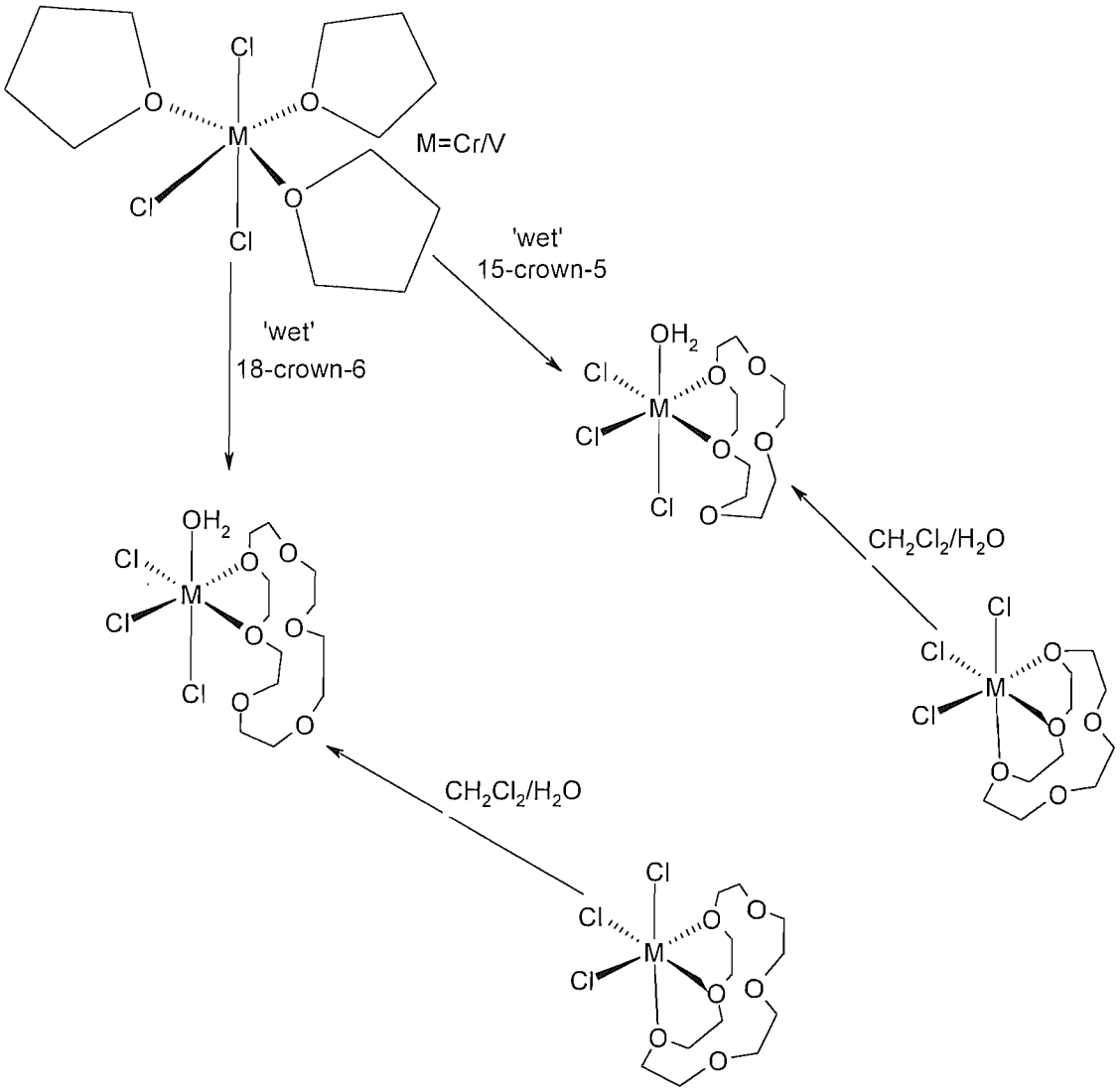

Fig 3.10 Scheme showing the hydrated Cr(III) and V(III) crown ether complexes investigated in this work.

3.2 Results and Discussion

Within this chapter both the hard vanadium(III) and chromium(III) metal centres have been combined with a series of macrocycles containing (i) hard ether oxygen donor atoms, (ii) soft thioether sulfur donor atoms and (iii) mixed ether/thioether macrocycles to test the boundaries of hard soft acid base theory (Chapter 1).

3.2.1 Chromium(III) Crown Ether Complexes

The crown ethers were treated *via* two methods; the first involved dissolving the crown ethers in anhydrous CH_2Cl_2 and refluxing with $SOCl_2$ for *ca.* an hour, before isolating the anhydrous crown under vacuum. The second involved drying the crown ethers under vacuum for *ca.* an hour. This method did not fully remove the excess water associated with the crown ethers. The thioether macrocycles and mixed thia/oxa macrocycles had a lower affinity for water and so were pre-treated by drying under vacuum *ca.* an hour.

$[CrCl_3(12\text{-crown-4})]$ was prepared from $[CrCl_3(thf)_3]$ combined with 1 molar equivalent of anhydrous 12-crown-4, in dry CH_2Cl_2. The complex was obtained as a pink solid and was pure by microanalysis. $[CrCl_3(15\text{-crown-5})]$ was prepared by an analogous route to $[CrCl_3(12\text{-crown-4})]$ to produce a purple solid of good yield. $[CrCl_3(18\text{-crown-6})]$ was prepared by the reaction of $[CrCl_3(thf)_3]$ and 1 molar equivalent of anhydrous 18-crown-6. The complex was obtained as a pink solid by precipitation with *n*-hexane. The dinuclear $[\{CrCl_3\}_2(18\text{-crown-6})]$ was prepared by reaction of anhydrous 18-crown-6 with *ca.* 2 molar equivalents of $CrCl_3$ in dry CH_2Cl_2. The pink solid was obtained by precipitation with *n*-hexane.

The *fac*-$[CrCl_3(\kappa^3\text{-crown})]$ complexes have approximate C_{3v} local symmetry, hence two Cr-Cl stretching vibrations are expected (A_1 and E). The IR spectra typically show two bands present in the region 370-320 cm^{-1}(Table 3.1). The UV-Vis spectra (Table 3.2) show the three expected bands associated with octahedral chromium d^3 metal centres. The bands correspond to $^4A_{2g}\rightarrow{}^4T_{2g}$, $^4A_{2g}\rightarrow{}^4T_{1g}(F)$ and $^4A_{2g}\rightarrow{}^4T_{1g}(P)$ d-d transitions. This helps support the expected six-coordinate metal centre binding to three oxygen atoms in the macrocycle. Similar trends were seen with all the anhydrous complexes produced.

It was predicted that there would be two bands in the IR spectrum of the dinuclear [{$CrCl_3$}$_2$(18-crown-6)]. Indeed this was the case with bands present at 352 and 367 cm^{-1} indicating a six-coordinate metal centre. Two bands were seen in the UV-vis spectrum at 13400 cm^{-1}($^4A_{2g}\rightarrow{}^4T_{2g}$) and 19450 cm^{-1}($^4A_{2g}\rightarrow{}^4T_{1g}(F)$) with the third band probably being obscured by the charge transfer band associated with Cl→Cr. This supports the theory of κ^3- coordination of the macrocycle to the $CrCl_3$.

Complexes of the form [$CrCl_3$(κ^3-crown)] (where crown=15-crown-5, 18-crown-6) were seen to be highly moisture sensitive. It was observed that the anhydrous [$CrCl_3$(κ^3-18-crown-6)] complex was more moisture sensitive than the similar [$CrCl_3$(κ^3-15-crown-5)] complex, which in turn was more moisture sensitive than [$CrCl_3$(κ^3-12-crown-4)]. It can therefore be suggested that the water is first associated with the uncoordinated O atoms of the crown and then transferred to the metal due to the close proximity of the molecules. This is further supported by the absence of the [$CrCl_3(H_2O)$(κ^2-12-crown-4)] species being formed due to the smaller ring of the macrocycle.

A sample of [$CrCl_3$(15-crown-5)] was placed on a watch glass and monitored over a period of time to determine the time in which the complex took water on and whether there was a noticeable trend. The complex showed a gradual, but significant weight increase over a period of minutes, and became sticky in appearance. However, the percentage weight increase did not correspond to formation of a single hydrated species (Figure 3.11).

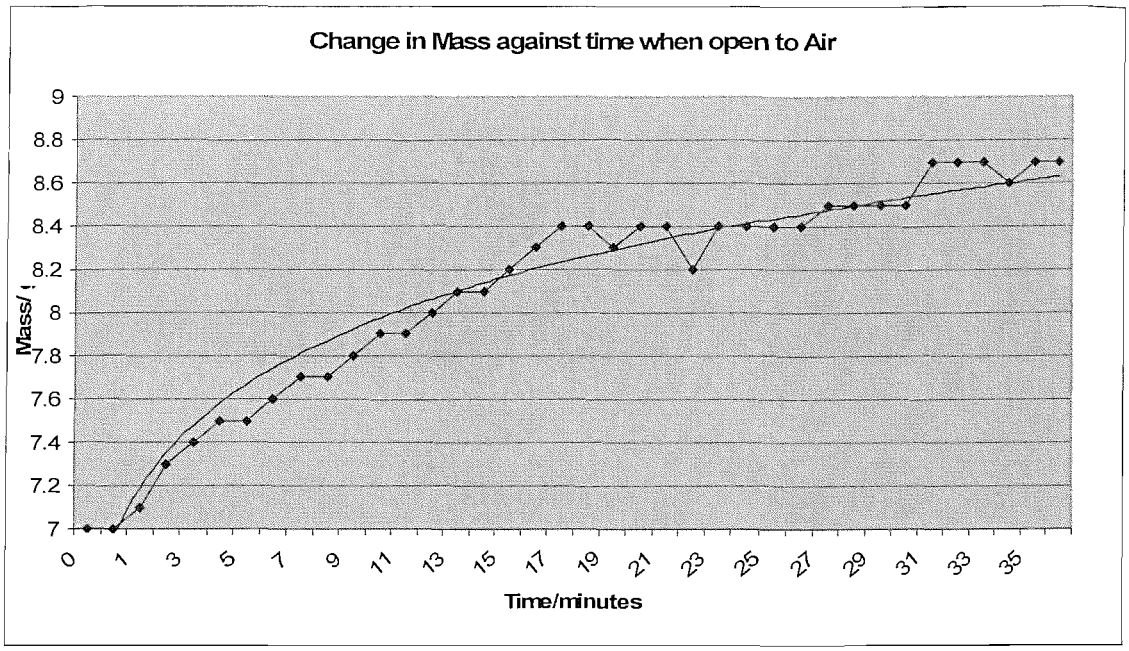

Fig 3.11 Showing the results of leaving [($CrCl_3$)(15-crown-5)] in the air for a set period of time.

On the basis of these observations, and the crystal structures of [$CrCl_3(H_2O)$(15-crown-5)] and [$VCl_3(H_2O)$(18-crown-6)] reported by Plate *et al.* and Junk *et al.* respectively,[11,12] It was then decided to attempt the preparation of the hydrated species [$MCl_3(H_2O)$(crown ether)] (M = Cr, V; crown ether = 15-crown-5 and 18-crown-6) to provide comparisons with the anhydrous species [MCl_3(crown ether)].

[$CrCl_3(H_2O)$(15-crown-5)] was obtained as a pink solid by direct reaction of [$CrCl_3(thf)_3$] with 15-crown-5 (pre-treated simply by drying the crown *in vacuo*) in anhydrous CH_2Cl_2 solution. The same product was isolated by stirring a suspension of [$CrCl_3(\kappa^3$-15-crown-5)] in CH_2Cl_2 with *ca.* one molar equivalent of water added. The compound was characterised by microanalyses, IR spectroscopy and UV-vis spectroscopy.

[$CrCl_3(H_2O)$(18-crown-6)] was prepared by reaction of [$CrCl_3(thf)_3$] with 18-crown-6 in anhydrous CH_2Cl_2 to produce a pink solid which was precipitated with *n*-hexane. The aqua complexes [$CrCl_3(H_2O)(\kappa^2$-crown)](where crown = 15-crown-5 and 18-crown-6) contain a six-coordinate metal centre with κ^2- coordination to the macrocycle. The IR spectrum showed two bands which corresponded to Cr-Cl stretches between 321-360 cm^{-1}

(Table 3.1). This supports the presence of the Cr metal centre in a six-coordinate geometry. $[CrCl_3(H_2O)(15\text{-crown-5})]$ was prepared and fully characterised by Ernst *et al* and a crystal structure was also obtained.[10] IR data obtained by Ernst *et al.* showed two Cr-Cl stretches (365, 340 cm^{-1}) and one Cr-O(H_2O) stretch at 505 cm^{-1}.[10] These data were found to be in good agreement with the data obtained in this thesis. The UV-vis spectra obtained on complexes of the form $[CrCl_3(H_2O)(\kappa^2\text{-crown})]$ possessed three d-d transitions bands (Table 3.2). Furthermore, when the spectra of $[CrCl_3(H_2O)(15\text{-crown-5})]$ and the $[CrCl_3(15\text{-crown-5})]$ were compared, significant differences in the fingerprint region and the far IR region were evident (and bands due to water were present in the former only) (Fig. 3.12).

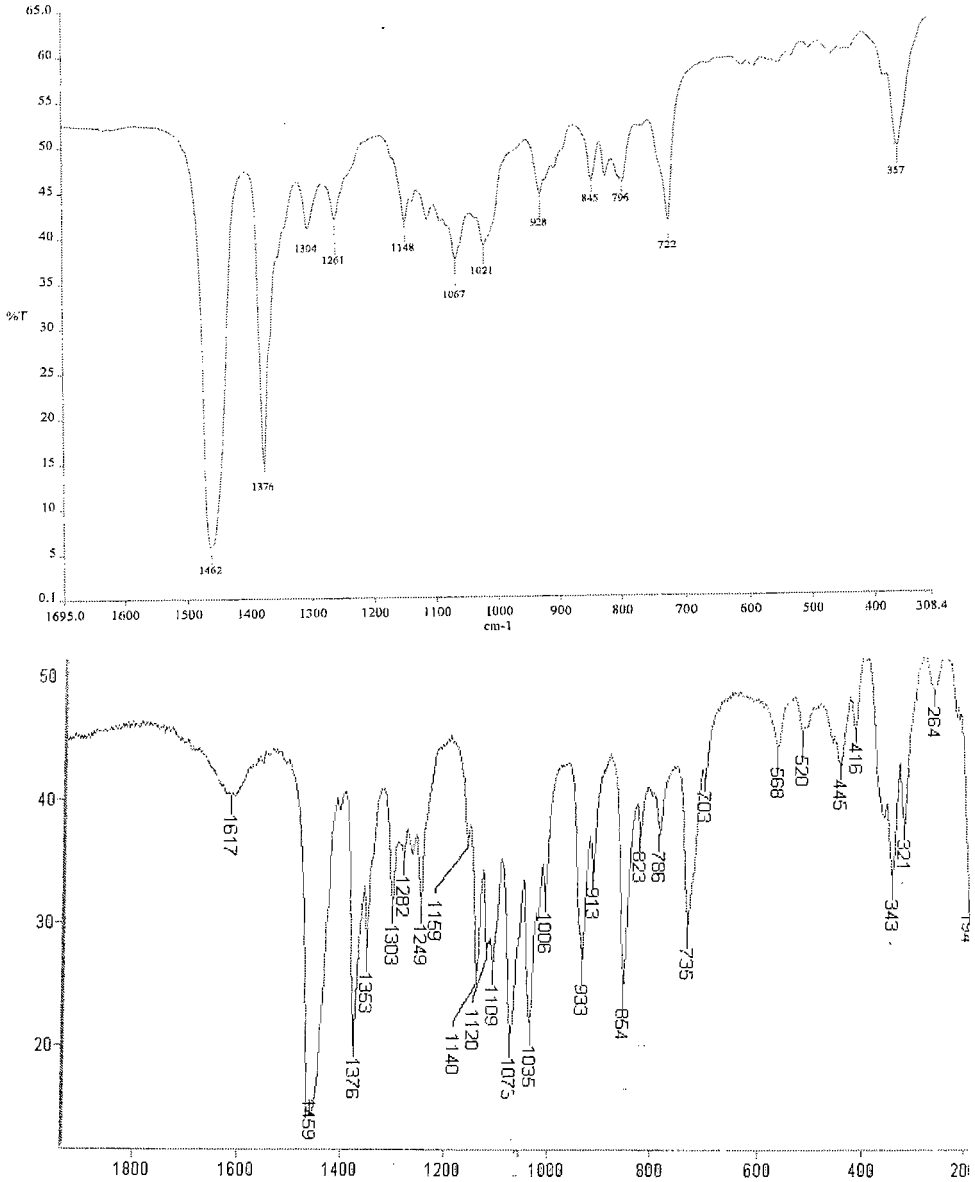

Fig 3.12 Shows the finger print region of $[CrCl_3(15\text{-crown-5})]$ and $[CrCl_3(H_2O)(15\text{-crown-5})]$ respectively.

Complex	ν(Cr-Cl)/cm^{-1a}
[$CrCl_3$(12-crown-4)]	362, 356, 341
[$CrCl_3$(15-crown-5)]	377, 357, 335
[$CrCl_3(H_2O)$(15-crown-5)]	321, 343, 365
[$CrCl_3$(18-crown-6)]	303, 351, 377
[$CrCl_3(H_2O)$(18-crown-6)]	323, 356
[$(CrCl_3)_2$(18-crown-6)]	352, 367

Table 3.1 Selected IR spectroscopic data for the chromium(III) crown ether complexes.

a= Recorded as a nujol mull supported between CsI plates

Complex	$^4A_{2g}\rightarrow{}^4T_{2g}$	$^4A_{2g}\rightarrow{}^4T_{1g}(F)$	$^4A_{2g}\rightarrow{}^4T_{1g}(P)$
$CrCl_3$(12-crown-4)	13510	19050	
$CrCl_3$(15-crown-5)	13195	19230	27930
$CrCl_3(H_2O)$(15-crown-5)	13660	19650	29250(sh)
$CrCl_3$(18-crown-6)	13200(sh), 13500	19380	28900(sh)
$CrCl_3(H_2O)$(18-crown-6)	13570	19685	29270(sh)
$(CrCl_3)_2$(18-crown-6)	13400, 13960(sh)	19450	

Table 3.2 Diffuse reflectance UV/vis spectroscopic data for chromium(III) crown ether complexes

3.2.2 Vanadium(III) Crown Ether Complexes

[VCl_3(12-crown-4)] was isolated as a pink solid and was prepared from [$VCl_3(thf)_3$] and was combined with an excess anhydrous 12-crown-4, in dry CH_2Cl_2. The purity of the crown ether complex was established by microanalysis. [VCl_3(15-crown-5)] was prepared from [$VCl_3(thf)_3$] and with 1 molar equivalent of anhydrous 15-crown-5 in dry CH_2Cl_2 to produce a pink solid of good yield. [VCl_3(18-crown-6)] was prepared by an analogous route to [VCl_3(15-crown-5)] and was isolated as a pink solid. The dinuclear [$\{VCl_3\}_2$(18-crown-6)] was prepared by combining anhydrous 18-crown-6 with *ca.* 2 molar equivalents of [$VCl_3(thf)_3$] in dry CH_2Cl_2. The pink solid was obtained in moderate yield.

The *fac*-[$VCl_3(\kappa^3$-crown)] complexes have approximate C_{3v} local symmetry, hence two V-Cl stretching vibrations are expected (A_1 and E). The IR spectra typically show two bands

present in the region 370-300 cm^{-1}(Table 3.3). The UV-Vis spectra (Table 3.4) show the two expected bands associated with octahedral vanadium d^2 metal centres. The bands correspond to $^3T_{1g} \rightarrow {}^3T_{2g}$ and $^3T_{1g} \rightarrow {}^3T_{1g}$ d-d transitions. This helps support the expected six-coordinate metal centre binding to three oxygen atoms in the macrocycle. Similar trends were seen with all the anhydrous complexes produced.

In the IR spectrum of the dinuclear [$\{VCl_3\}_2$(18-crown-6)], bands were present at 311, 341 and 365cm^{-1} indicating a six-coordinate metal centre. Two bands were seen in the UV-vis spectrum at 12320 cm^{-1}($^3T_{1g} \rightarrow {}^3T_{2g}$) and 19230 cm^{-1}($^3T_{1g} \rightarrow {}^3T_{1g}$). This supports the theory of κ^3- coordination of the macrocycle to the VCl_3.

[$VCl_3(H_2O)$(15-crown-5)] was prepared from [$VCl_3(thf)_3$] combined with 1 molar equivalent of 15-crown-5, in dry CH_2Cl_2. The complex was obtained as a pink solid. [$VCl_3(H_2O)$(18-crown-6)] was prepared by an analogous route to [VCl_3(15-crown-5)] and also produced a pink solid. The IR spectrum obtained on the complexes showed two or three bands between 320-280 cm^{-1}. The reason for the difference seen in the number of bands is due to the V-Cl region being less defined. This supports the theory of a six-coordinate vanadium(III) metal centre. Two bands were seen in the UV-vis spectrum at 13400 cm^{-1}($^3T_{1g} \rightarrow {}^3T_{2g}$) and 19800 cm^{-1}($^3T_{1g} \rightarrow {}^3T_{1g}$). This supports the theory of κ^2-coordination of the macrocycle to the VCl_3.

The hydrated and anhydrous vanadium crown ether complexes showed similar differences in the IR spectra fingerprint region mentioned previously. The [$VCl_3(H_2O)$(12-crown-4)] complex was also found to be difficult to produce, it is expected to be due to the similar reasons mentioned previously for the analogous chromium species.

Complex	ν(V-Cl)/cm^{-1a}
$[VCl_3(12\text{-crown-4})]$	305, 339, 364
$[VCl_3(15\text{-crown-5})]$	340, 372
$[VCl_3(H_2O)(15\text{-crown-5})]$	324, 334, 342
$[VCl_3(18\text{-crown-6})]$	340, 359
$[VCl_3(H_2O)(18\text{-crown-6})]$	310, 333
$[(VCl_3)_2(18\text{-crown-6})]$	311, 341, 365

Table 3.3 Selected IR spectroscopic data for the V(III) crown ether complexes.

a= Recorded as a nujol mull supported between CsI plates

Complex	$^3T_{1g} \rightarrow {}^3T_{2g}$	$^3T_{1g} \rightarrow {}^3T_{1g}$
$[VCl_3(12\text{-crown-4})]$	11870	18900
$[VCl_3(15\text{-crown-5})]$	11500sh, 12830	19380
$[VCl_3(H_2O)(15\text{-crown-5})]$	11300sh, 12690	19190
$[VCl_3(18\text{-crown-6})]$	12900	18950
$[VCl_3(H_2O)(18\text{-crown-6})]$	11900sh, 13400	19800
$[(VCl_3)_2(18\text{-crown-6})]$	12320	19230

Table 3.4 Diffuse reflectance UV-vis spectroscopic data for V(III) crown ether complexes

3.2.3 Chromium(III) Thioether and Mixed Thia/oxa Macrocyclic Complexes

$[CrCl_3([12]aneS_4)]$ was prepared from $[CrCl_3(thf)_3]$ with 1 molar equivalent of anhydrous $[12]aneS_4$, in dry CH_2Cl_2, as a blue solid. The purity of the thioether macrocyclic complex was established by microanalysis. $[CrCl_3([15]aneS_5)]$ was prepared from an analogous route to $[CrCl_3([12]aneS_4)]$ as a purple solid in a good yield.

The IR spectrum obtained on the complexes showed two bands between 370-315 cm^{-1} for each complex. This supports the theory of a six-coordinate chromium(III) metal centre. Three bands were seen in the UV-vis spectrum (Table 3.6). This supports the theory of κ^3-coordination to the macrocycle. These complexes were seen to be reasonably stable and did not seem as hydrophilic. It was decided to produce mixed donor macrocyles, containing both hard oxygen donor atoms and the soft sulfur donor atoms. These would act as a comparison to the previous complexes made.

$[CrCl_3([9]aneS_2O)]$ was obtained as a pink solid from the reaction of $[CrCl_3(thf)_3]$ with 1 molar equivalent of anhydrous of $[9]aneS_2O$, in dry CH_2Cl_2. The purity of the mixed thia/oxa macrocyclic complex was established by microanalysis. $[CrCl_3([15]aneS_2O_3)]$ was prepared from an analogous route to $[CrCl_3([9]aneS_2O)]$ as a purple solid of good yield. $[CrCl_3([18]aneS_3O_3)]$ was prepared by combining $[CrCl_3(thf)_3]$ with 1 molar equivalent of $[18]aneS_3O_3$ and the pink solid was precipitated by anhydrous Et_2O.

IR spectra obtained on the complexes were noted to have similar trends to the thioether macrocyclic complexes made previously in this work. Two IR spectra bands were seen between 370-340 cm^{-1}, consistent with a complex containing a six coordinate chromium metal centre. The $[CrCl_3([9]aneS_2O)]$ complex was analysed by UV-vis spectroscopy and the spectrum showed two bands at 14880 and 19970 cm^{-1}. This is consistent with the Cr metal centre being bound to the two sulfur atoms and oxygen atom of the macrocycle. The $[CrCl_3([15]aneS_2O_3)]$ and $[CrCl_3([18]aneS_3O_3)]$ complexes were also analysed *via* UV-vis spectroscopy showing bands consistent with the thioether complexes mentioned previously rather than the crown ether complexes as expected. It appears that the metal centre formed bonds more readily with the softer sulfur donor atoms rather than the harder oxygen atoms.

Complex	ν(Cr-Cl)/cm^{-1a}
$[CrCl_3([12]aneS_4)]$	329, 366
$[CrCl_3([15]aneS_5)]$	315sh, 340
$[CrCl_3([9]aneS_2O)]$	358, 343
$[CrCl_3([15]aneS_2O_3)]$	366, 345
$[CrCl_3([18]aneS_3O_3)]$	355, 345

Table 3.5 Selected IR spectroscopic data for Cr(III) thioether complexes and thia/oxa complexes

a= Recorded as a nujol mull supported between CsI plates

Complex	$^4A_{2g} \rightarrow {}^4T_{2g}$	$^4A_{2g} \rightarrow {}^4T_{1g}(F)$	$^4A_{2g} \rightarrow {}^4T_{1g}(P)$
$[CrCl_3([12]aneS_4)]$	14050	19840	29900sh
$[CrCl_3([15]aneS_5)]$	14290	19380	30490sh
$[CrCl_3([9]aneS_2O)]$	14880	19970	-
$[CrCl_3([15]aneS_2O_3)]$	14450	20000	30860sh
$[CrCl_3([18]aneS_3O_3)]$	14350	19660	30300

Table 3.6 Diffuse reflectance UV-vis spectroscopic data for Cr(III) thioether complexes and thia/oxa complexes

3.2.4 Vanadium(III) Thioether and Mixed Thia/oxa Macrocyclic Complexes

$[VCl_3([12]aneS_4)]$ was prepared from $[VCl_3(thf)_3]$ with 1 molar equivalent of anhydrous $[12]aneS_4$, in dry CH_2Cl_2, as a pink solid. The purity of the thioether macrocyclic complex was established by microanalysis. $[VCl_3([15]aneS_5)]$ was prepared but the complex could not be isolated in a sufficient quantity to analyse by microanalysis or perform sufficient spectroscopic analysis on.

The IR spectrum obtained on the complex $[VCl_3([12]aneS_4)]$ showed two bands at 361 and 346 cm^{-1}. This supports the theory of a six-coordinate vanadium(III) metal centre. Two bands were seen in the UV-vis spectrum (Table 3.8). This supports the theory of κ^3-coordination to the macrocycle. This complex was also seen to be reasonably stable and did not seem as susceptible to water molecules as the vanadium crown ether species. Due to similar observations noted on the chromium thioether complexes mixed macrocyclic species were also synthesised with $[VCl_3(thf)_3]$, again these would act as a comparison to the previous complex made.

$[VCl_3([9]aneS_2O)]$ was prepared from excess $[VCl_3(thf)_3]$ with anhydrous $[9]aneS_2O$, in dry CH_2Cl_2, the complex was precipitated with *n*-hexane as a pink solid. The purity of the mixed thia/oxa macrocyclic complex was established by microanalysis. $[VCl_3([15]aneS_2O_3)]$ was prepared from $[VCl_3(thf)_3]$ and 1 molar equivalent of $[15]aneS_2O_3$ to produce a pink solid. $[VCl_3([18]aneS_3O_3)]$ was prepared by combining

$[VCl_3(thf)_3]$ with 1 molar equivalent of $[18]aneS_3O_3$ and the pink solid was precipitated with anhydrous Et_2O.

Similar observations made with the chromium mixed thia/oxa macrocyclic species were seen with the vanadium analogues. The IR spectra were consistent with six-coordinate metal centres and the UV-vis spectra were more closely associated with the thioether macrocyclic complexes than the crown ethers. Unfortunately attempts to grow crystals of these complexes failed.

Complex	ν(V-Cl)/cm^{-1a}
$[VCl_3([12]aneS_4)]$	361, 346
$[VCl_3([9]aneS_2O)]$	356, 339
$[VCl_3([15]aneS_2O_3)]$	360, 322
$[VCl_3([18]aneS_3O_3)]$	355, 343

Table 3.7 Selected IR spectroscopic data for V(III) thioether complexes and thia/oxa complexes

a= Recorded as a nujol mull supported between CsI plates

Complex	$^3T_{1g} \rightarrow {}^3T_{2g}$	$^3T_{1g} \rightarrow {}^3T_{1g}$
$[VCl_3([12]aneS_4)]$	12690	18250
$[VCl_3([9]aneS_2O)]$	13440	18880
$[VCl_3([15]aneS_2O_3)]$	12940, 13400sh	19850
$[VCl_3([18]aneS_3O_3)]$	12800	19690

Table 3.8 Diffuse reflectance UV-vis spectroscopic data for the V(III) thioether complexes and thia/oxa complexes

3.2.5 Single Crystal X-Ray Structure Analysis

Small pink/purple crystals of $[CrCl_3(H_2O)(18\text{-crown-}6)]$, $[CrCl_3([15]aneS_5)]$ and $[VCl_3(H_2O)(15\text{-crown-}5)].3/4CH_2Cl_2]$ were obtained by dissolving the appropriate solid in dry CH_2Cl_2, layering with hexane, and storing in an inert atmosphere. The crystallographic data are tabulated (Table 3.9).

	$[CrCl_3(H_2O)$(18-crown-6)]	**$[CrCl_3$([15]aneS_5)]**	**$[VCl_3(H_2O)$(15-crown-5)].3/4CH_2Cl_2**
Formula	$C_{12}H_{26}Cl_3CrO_7$	$C_{10}H_{20}Cl_3CrS_5$	$C_{10}H_{22}Cl_3O_6V.0.75CH_2Cl_2$
Molecular Weight	440.68	458.91	459.26
Crystal Structure	Monoclinic	Orthorhombic	Trigonal
Space Group	$P2_1/c$	$Pna2_1$	$P3_22_1$
a/Å	15.663(3)	12.942(3)	12.153(2)
b/Å	13.0981(16)	8.4682(15)	12.153(2)
c/Å	19.216(4)	16.040(3)	22.773(3)
α/°	90	90	90
β/°	109.352(8)	90	90
γ/°	90	90	120
U/A^3	3719.5(11)	1757.8(6)	2912.9(9)
Z	8	4	6
$\mu(M_o\text{-}K_\alpha)/mm^{-1}$	1.074	1.684	1.150
Unique Reflections	8505	3972	4408
No. of parameters	428	172	209
$R1[I_o>2\sigma(I_o)]$	0.0580	0.0292	0.0681
R1[all data]	0.1402	0.0380	0.1787
$wR2[I_o>2\sigma(I_o)]$	0.1062	0.0537	0.1180
wR2[all data]	0.1314	0.0567	0.1490

Table 3.9 Crystallographic parameters

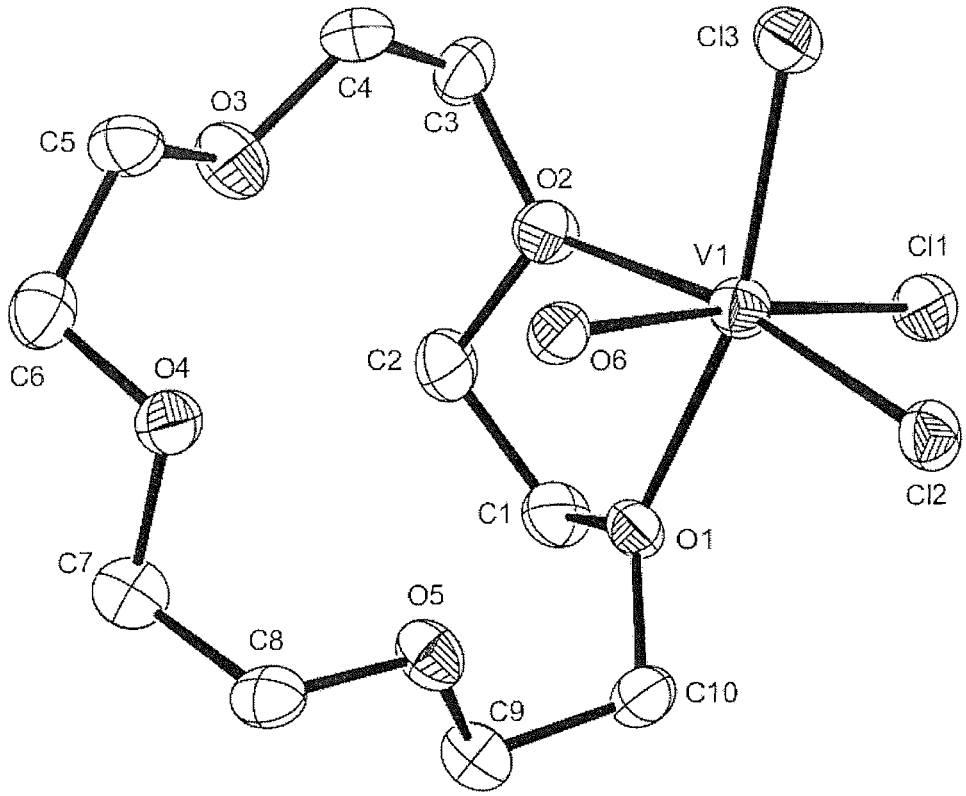

Fig 3.13 Crystal structure of $[VCl_3(H_2O)(15\text{-crown-}5)]$ with numbering scheme adopted. H atoms have been omitted for clarity and the ellipsoids are drawn at the 50% probability level.

The crystal structure shows that the vanadium metal centre is 6-coordinate with a distorted octahedral geometry. The vanadium atom is bound to three facial Cl atoms, two adjacent ether O atoms and to a water molecule. The bond distances show little difference between V-O(ether) and V-O(H_2O). The O–V–O angle within the chelate ring is 76.23(18)°. The O(5)···O(6)···O(4) angle is 102.3°. Although the H atoms bonded to the water O(6) were not convincingly identified, there are only two suitable O···O distances for O–H···O H-bonding interactions. Thus O(6)···O(5) (2.784(6) Å) is an intramolecular H-bond and O(6)···O(4)a (2.676(6) Å, a = y, x, –z) an intermolecular interaction to crown O atoms.

V(1)-O(1)	2.070(4)	V(1)-Cl(1)	2.319(2)
V(1)-O(2)	2.122(4)	V(1)-Cl(2)	2.335(2)
V(1)-O(6)	2.064(5)	V(1)-Cl(3)	2.309(2)

Table 3.10 Selected bond lengths [Å]for $[VCl_3(H_2O)(15\text{-crown-}5)]$.

These values were compared with other V(III) complexes published in literature. The $[VCl_3([9]aneS_3)]$ crystal structure has been reported and the V-Cl bond lengths were 2.277(2)-2.304(2) Å which is slightly shorter than the bonds obtained in the present structure 2.309(2)-2.335(2) Å.[17] As expected on the basis of the atom size, the V-S bonds are longer than the V-O bonds. Also, this structure is similar to that of $[VCl_3(H_2O)(18\text{-crown-6})]$ obtained by Atwood *et al.* which shows $d(V\text{-}O_{ether})$ = 2.070(4) and 2.122(4) Å.[1]

O(6)-V(1)-O(2)	82.72(9)	O(6)-V(1)-O(2)	88.12(18)
O(1)-V(1)-O(2)	76.23(18)	O(6)-V(1)-Cl(3)	89.08(14)
O(1)-V(1)-Cl(3)	166.19(4)	O(2)-V(1)-Cl(3)	92.46(14)
O(6)-V(1)-Cl(1)	172.78(14)	O(1)-V(1)-Cl(1)	90.07(15)
O(2)-V(1)-Cl(1)	89.73(14)	Cl(3)-V(1)-Cl(1)	97.90(8)
O(6)-V(1)-Cl(2)	89.08(13)	O(1)-V(1)-Cl(2)	94.00(13)
O(2)-V(1)-Cl(2)	170.10(14)	Cl(3)-V(1)-Cl(2)	96.98(8)
Cl(1)-V(1)-Cl(2)	91.89(8)		

Table 3.11 Selected bond angles [°] for $[VCl_3(H_2O)(15\text{-crown-5})]$.

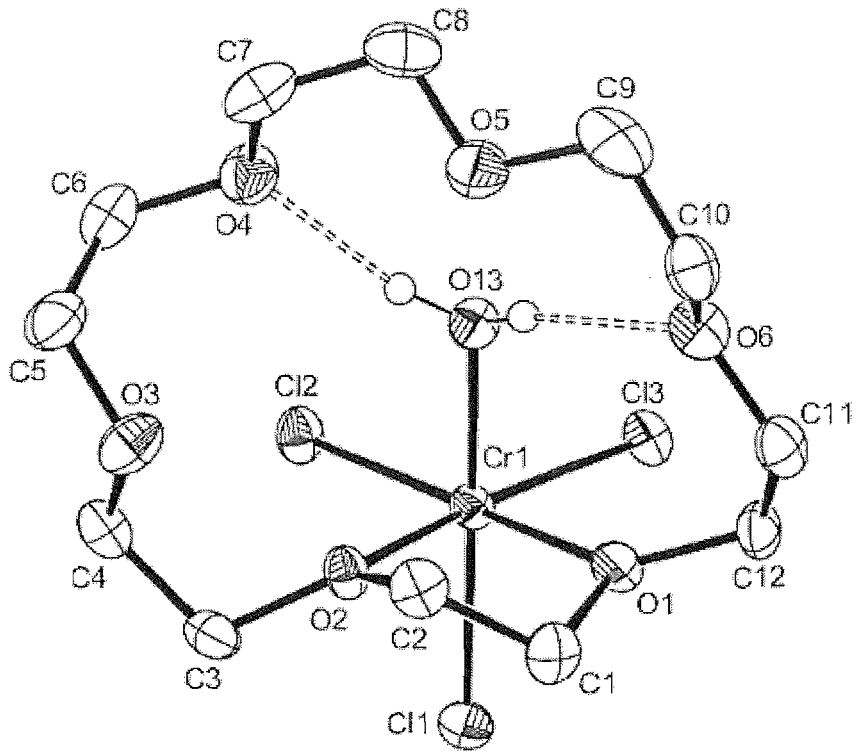

Fig 3.14 View of the structure of one of the two independent $[CrCl_3(H_2O)(18\text{-crown-6})]$ molecules with numbering scheme adopted. H atoms on C have been omitted for clarity and the ellipsoids are drawn at the 50% probability level. The other molecule is very similar.

The crystal structure of $[CrCl_3(H_2O)(18\text{-crown-6})]$ shows (Figure 3.14) that the chromium atom is 6-coordinate, with a distorted octahedral geometry, similar to that observed in the other two crystal structures reported here. The chromium is bound to three facial chlorines, two adjacent ether O atoms and a water molecule. For the Cr(1) molecule each of the O(13) H atoms is involved in an intramolecular H-bond to a crown O atom (O13···O4 2.813(4), O(13)···O(6) 2.842(4) Å). A similar situation applies to the Cr(2) containing molecule and O(14). The Cr–O distances within the crown are ~2.05 Å, while the Cr–OH_2 distances are slightly shorter in each case. The O–Cr–O angles within the chelate rings are notable at only 79.22(11) and 76.93(12)°. The structural features in this species parallel those in $[CrCl_3(H_2O)(\kappa^2\text{-15-crown-5})]$ reported by Dehnicke et al.,[9] which shows intramolecular H-

bonding interactions between the coordinated H_2O ligand and two of the uncoordinated O atoms of the crown.

Cr(1)-O(1)	2.060(3)	Cr(1)-Cl(1)	2.3047(13)
Cr(1)-O(2)	2.047(3)	Cr(1)-Cl(2)	2.2704(12)
Cr(1)-O(13)	2.034(3)	Cr(1)-Cl(3)	2.2780(12)

Table 3.12 Selected bond lengths [Å] for $[CrCl_3(H_2O)(18\text{-crown-6})]$.

O(13)-Cr(1)-O(2)	86.41(12)	O(3)-Cr(1)-O(1)	86.05(12)
O(2)-Cr(1)-O(1)	79.22(11)	O(13)-Cr(1)-Cl(2)	89.84(9)
O(2)-Cr(1)-Cl(2)	94.26(8)	O(1)-Cr(1)-Cl(2)	172.49(9)
O(13)-Cr(1)-Cl(3)	90.94(9)	O(2)-Cr(1)-Cl(3)	169.63(8)
O(1)-Cr(1)-Cl(3)	90.60(8)	Cl(2)-Cr(1)-Cl(3)	95.75(4)
O(13)-Cr(1)-Cl(1)	173.43(9)	O(2)-Cr(1)-Cl(1)	87.82(9)
O(1)-Cr(1)-Cl(1)	89.78(9)	Cl(2)-Cr(1)-Cl(1)	93.73(5)
Cl(3)-Cr(1)-Cl(1)	94.18(5)		

Table 3.13 Selected bond angles [°] for $[CrCl_3(H_2O)(18\text{-crown-6})]$.

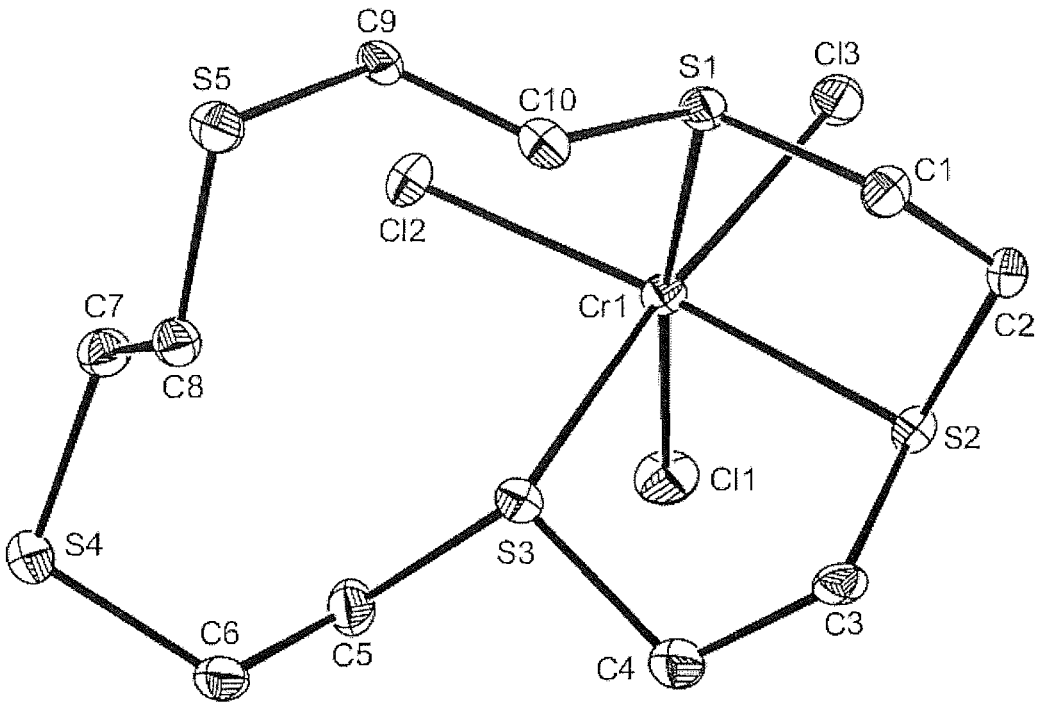

Fig 3.15 View of the structure of $[CrCl_3([15]aneS_5)]$ with numbering scheme adopted. H atoms are omitted for clarity and the ellipsoids are drawn at the 50% probability level.

The crystal structure of $[CrCl_3([15]aneS_5)]$ shows (Figure 3.15) a distorted octahedral Cr coordination environment through three facial chlorines and three facial sulfur atoms.

Cr(1)-Cl(1)	2.2849(8)	Cr(1)-S(1)	2.4942(8)
Cr(1)-Cl(2)	2.2885(9)	Cr(1)-S(2)	2.4166(9)
Cr(1)-Cl(3)	2.3028(9)	Cr(1)-S(3)	2.4261(10)

Table 3.14 Selected bond lengths [Å]for $[CrCl_3([15]aneS_5)]$.

The bond lengths in this species compare with those for $[CrCl_3([18]aneS_6)]$ previously reported published in literature which shows d(Cr-S) = 2.440(5)-2.459(3) Å.[27] These are very similar to the values obtained in this work (Table 3.14). Champness *et al.* obtained single crystal X-ray diffraction data on $[CrBr_2([14]aneS_4)]PF_6$ and $[CrCl_2([14]aneS_4)]PF_6$. Cr-S bond lengths were seen to be 2.409(3) Å and 2.394(5)Å respectively.[16] This is consistent with the data seen in Table 3.14.

Cl(1)-Cr(1)-Cl(2)	96.13(3)	Cl(1)-Cr(1)-Cl(3)	94.45(3)
Cl(2)-Cr(1)-Cl(3)	99.08(3)	Cl(1)-Cr(1)-S(2)	87.74(3)
Cl(2)-Cr(1)-S(2)	171.22(3)	Cl(3)-Cr(1)-S(2)	88.43(3)
Cl(1)-Cr(1)-S(3)	90.21(3)	Cl(2)-Cr(1)-S(3)	88.46(3)
Cl(3)-Cr(1)-S(3)	170.64(3)	S(2)-Cr(1)-S(3)	83.64(3)
Cl(1)-Cr(1)-S(1)	172.12(3)	Cl(2)-Cr(1)-S(1)	91.71(3)
Cl(3)-Cr(1)-S(1)	83.62(3)	S(2)-Cr(1)-S(1)	84.58(3)
S(3)-Cr(1)-S(1)	90.68(2)		

Table 3.15 Selected bond angles [°] for $[CrCl_3([15]aneS_5)]$.

The trends in bond angles are discussed in more detail below (section 3.2.6). The bond angles were compared to data obtained on the complex $[VCl_3([9]aneS_4)]$.[17] Data obtained by Davies *et al.* had similar bond angle to those seen in Table 3.15, bond angles between 82.34(8)- 83.03(8)° were obtained. Bond lengths were also consistent to the ones in Table 3.14, Davies *et al.* obtained three V-S bond lengths between the range 2.469(2)-2.515(2) Å.[17]

3.2.6 Analysis of structural data

From this work we have shown that the κ^3-coordinated (anhydrous) crown ether complexes may be obtained only under rigorously dry conditions, with traces of water leading to partial hydrolysis and isolation of the mono-aqua complexes. On the other hand, the thiamacrocycles readily yield S_3-coordinated species, which appear to be considerably less prone to hydrolysis. On the basis of HSAB theory, we would anticipate that the crown ethers (O-donor) would result in more stable complexes than the softer thioethers. To try to explain these results we have examined the structural parameters in these species, together with the crystallographically determined parameters in all other reported six-coordinate (octahedral) complexes of early transition metals (Sc, Ti, V and Cr) with ether and thioether ligands of the form $RE(CH_2)_2ER$ and $RE(CH_2)_2E(CH_2)_2ER$ (E = O or S; R = alkyl) and S- or O-donor macrocycles involving $-CH_2CH_2-$ linkages. The results obtained using the Cambridge Crystallographic Database[30,31] are presented in Figure 3.16 which shows histograms of the E–M–E angles within the five-membered

chelate rings for E = O (a) and for E = S (b). The average O–M–O angles in these species are 74.8°, with values ranging from 68.6–79.0°, while the average S–M–S chelate angles are 82.2°, with values ranging from 75.7–86.8°. The data obtained from the three crystal structures described in this work (above) are consistent with the data in Fig 3.16. This surprisingly large difference is consistent with the crown ether complexes being more strained, and may well explain why the κ^3-crown complexes are so readily hydrolysed – incorporating two adjacent very acute five-membered chelates leads to a very strained species which will readily pick-up another donor ligand such as H_2O and convert to κ^2-crown to relieve the strain within the coordination sphere. In contrast, the S–M–S chelate angles of ~82° are closer to the idealised 90° angle in a regular octahedron. In support of this, the O–Cr–O angles in *mer*-$[CrCl_3(thf)_3]$ are 86.0(1) and 86.5(1)° – the monodentate thf ligands remove chelate constraints as a consideration and hence presumably reflect the preferred relative positioning of the ligands.[6]

The size of the chelate angle at the metal M is a consequence of both the M–E distances and the E–C distances. The M–S distances are ~0.4 Å longer than d(M–O) in these species. The reason for the large difference in E–M–E angles presumably originates from the difference between d(O–C) (typically ~1.47 Å) *vs* d(S–C) (typically ~1.83 Å) - hence an O–C–C–O linkage is too short to accommodate idealised octahedral angles at a coordinated early transition metal without introducing significant angle strain at the O and the C atoms.

The preparation and properties of the Ti^{IV} complex $[TiCl_4(\kappa^2\text{-}[15]aneS_2O_3)]$ have been reported previously by this research group. Its ^1H NMR spectrum unexpectedly showed that coordination to Ti was via the two thioether S atoms, not the ether O atoms.[14] This result, together with the results of the present studies, suggest that the different ring strain effects introduced upon chelation of $-OCH_2CH_2O-$ compared to $-SCH_2CH_2S-$ linkages plays an important role in determining the donor set at Ti and offsets the fact that the thioethers are softer donor ligands than the ethers.

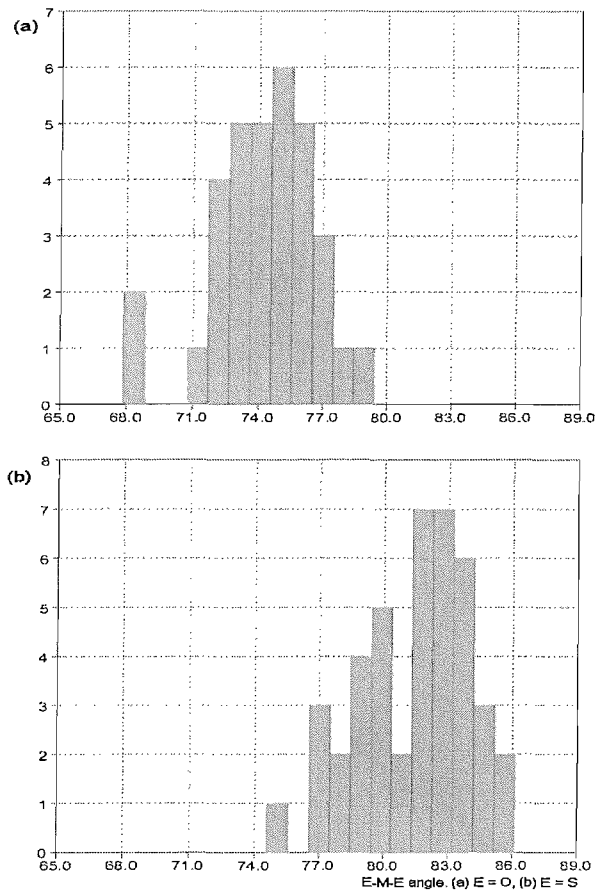

Figure 3.16 Histograms showing the crystallographically determined E–M–E angles in saturated five-membered chelate rings on an octahedral metal centre (M = Sc, Ti, V, Cr); (a) E = O, mean O-M-O angle 74.8(2.4)°. The lowest angles are for $[Sc(CH_2SiMe_3)_3(12\text{-crown-4})]$ which contains two adjacent 5-membered chelate rings [32]; (b) E = S, mean S-M-S angle 82.2(2.6)°. The lowest angles are for those complexes involving the macrocycle $[9]aneS_3$ involving three adjacent 5-membered chelate rings.

3.3 Conclusion

In this chapter a selection of complexes have been obtained of the form $[MCl_3(L)]$ and $[(MCl_3)_2(L)]$ (where M= Cr and V, L= crown ethers, thiacrowns and thia/oxa crowns). The complexes contained either the hard vanadium(III) or chromium(III) metal centre and a selection of soft and hard macrocyclic ligands. The complexes were 6-coordination at the metal centre, which was supported by the IR and UV-vis spectra.

The complexes were found to be more moisture sensitive when combined with the harder crown ether ligand rather than the softer thioether crown. This was seen more clearly within the crystal structures obtained. The bond angles of the complexes showed that the angles were more strained in the complexes with the crown ethers, where as when the hard metal was combined with the softer thioether macrocycles the angles were nearer the required 90°. The data obtained was compared with other literature examples, and the same results were found. It was then decided that the reason the anhydrous crown ether complexes were moisture sensitive was due to the strain the molecule was under when bound to three atoms of the ligand. If a water molecule was present the Cr would lose a bond to the crown ether and pick up the water molecule. However, when a complex was formed with the thioether crown the O-M-O bond angle is seen to be less strained and the complex appears more hydrolytically stable.

Unfortunately there was a limit to the amount of analysis that could be performed on the complexes as both Cr(III) and V(III) are paramagnetic. Therefore NMR analysis could not be used. There was also the issue that the anhydrous crown complexes were also found to be difficult to crystallize as only the hydrated forms were produced. The softer macrocyclic thioether complexes were slightly easier to crystallize but in this instance only one structure was obtained. The IR, microanalysis and UV analysis showed some consistencies with data published in literature helping to conclude that the expected structures had been obtained. There were also noticeable differences in the IR fingerprint region which determined the aqua complexes from the anhydrous ones.

The crystal data obtained within this chapter showed anomalies between the O-M-O bond angle within the complex $[CrCl_3(H_2O)(18\text{-crown-6})]$, compared to the S-M-S bond angle within the complex $[CrCl_3([15]aneS_5)]$. When data from the Cambridge Crystallographic Database was in corporated into a histogram to show the E-M-E angles for the five membered chelate rings produced, it was observed that the O-M-O angle was averaged at 74.8° compared to the S-M-S angle which was 82.2°. The S-M-S angle was closer to the desired 90° angle which is favoured by six coordinate metal species, this helped to explain the increased stability observed for the thioether crown complexes compared to the crown ethers, and is of vital importance as it disagrees with HSAB theory.

3.4 Experimental

3.4.1 General

Infrared spectra were recorded as Nujol mulls between CsI discs using a Perkin-Elmer 983G spectrometer over the range 4000-180cm^{-1}. UV-visible spectra were obtained in diffuse reflectance mode from powdered samples diluted with $BaSO_4$, using a Perkin Elmer Lambda 19 spectrometer, or as solutions in CH_2Cl_2 using quartz cells (1 cm path length). Microanalyses were performed by the University of Strathclyde microanalytical service.

All glassware was dried in an oven overnight prior to use. Solvents were dried using standard procedures (see chapter 2) prior to use, and all preparations were undertaken using standard Schlenk techniques under a N_2 atmosphere. The crown ethers 12-crown-4, 15-crown-5 and 18-crown-6 were obtained from Aldrich. The anhydrous crown ethers were obtained either by prolonged heating under vacuum or by refluxing the crown with thionyl chloride in CH_2Cl_2. The aqua complexes either used the crowns treated as above and subsequent addition of small amounts of water, or using crowns which were "dried" by pumping under vacuum at room temperature for a few hours (under these conditions ^{1}H NMR and IR spectra provide evidence for retention of some water). The anhydrous crowns were then stored in Schlenk flasks and manipulated in a dry box. The thioether crowns [12]aneS_4 and [15]aneS_5 were obtained from Aldrich and were dried under vacuum and handled in a dry box. [9]aneS_2O,[33, 34], [15]aneS_2O_3[33,34] and [18]aneS_3O_3[34,33] were synthesised by literature routes and dried similarly.

[$CrCl_3(thf)_3$] was synthesised by the literature route.[35] [$VCl_3(thf)_3$] was obtained from Aldrich. Once synthesised the freshly made complexes was characterised. A glove box (< 5ppm H_2O) was used for making up samples for analysis and for storage of the reagents and the products synthesised.

3.4.2 Chromium(III) Complexes

[$CrCl_3$(12-crown-4)]

[$CrCl_3(thf)_3$] (0.4 g, 1.1 mmol) in dry CH_2Cl_2 (5 mL) was combined with anhydrous 12-crown-4 (0.2 g, 1.1 mmol) in dry CH_2Cl_2 (5 mL). A precipitate formed; this was then filtered and dried under vacuum. The product was a pink solid (0.1 g, 27%). Anal: Calc. for $C_8H_{16}Cl_3CrO_4$.1/2 CH_2Cl_2: C, 27.1; H, 4.5; Found: C, 27.2; H, 4.9%. IR (Nujol)/cm^{-1}: 1299(s), 1261(m), 1228(m), 1145(s), 1096(m), 1063(s), 1026(vs), 992(m), 934(m), 908(s), 838(s), 803(m), 583 (w), 362(sh), 356(s), 341(sh). UV-vis (solid-$BaSO_4$): 13510, 19050 cm^{-1}.

[$CrCl_3$(15-crown-5)]

[$CrCl_3(thf)_3$] (0.2 g, 0.5 mmol) in dry CH_2Cl_2 (5 mL) was added to anhydrous15-crown-5 (0.1 g, 0.5 mmol) in dry CH_2Cl_2 (5 mL) producing a purple solution, hexane (5 mL) was added producing a precipitate. The solid was produced and then filtered and dried under vacuum. The product was a purple solid (0.15 g, 65%). Anal: Calc. for $C_{10}H_{22}Cl_3CrO_5.CH_2Cl_2$: C, 28.5%; H, 4.8%; Found: C, 27.5; H, 5.8%. IR (Nujol)/ cm^{-1}: 1305(m), 1261(m), 1149(m), 1110(w), 1067(m), 1022(m), 928(s), 915(sh), 846(m), 822(m), 796(m), 610(w), 589(w), 551(w), 530(w), 501(w), 465(w), 433(w), 377(sh), 357(s), 335(sh). UV-vis (solid-$BaSO_4$): 13195, 19230, 27930 cm^{-1}.

[$CrCl_3(H_2O)$(15-crown-5)]

[$CrCl_3(thf)_3$] (0.2 g, 0.54 mmol) in dry CH_2Cl_2 (5 mL) was added to anhydrous 15-crown-5 (0.1 g, 0.54 mmol) in dry CH_2Cl_2 (5 mL) producing a purple solution. Hexane (5 mL) was added producing a precipitate. The purple solid was then filtered and dried under vacuum. Initial spectroscopy showed the complex was dried. The solid was combined with CH_2Cl_2 (25 mL) containing *ca.* 1 mol. equiv. of H_2O. The solution was then left to stir overnight, then concentrated and hexane (5 mL) was added. A precipitate was seen this was filtered and dried under vacuum, producing a pink solid (0.19 g, 60%). Anal: Calc. for $C_{10}H_{22}Cl_3CrO_6$: C, 30.3; H, 5.6; Found: C, 29.5; H, 6.1%. IR (Nujol)/ cm^{-1}: 3300(br), 1630(m), 1303(m), 1249(m), 1140(s), 1120(s), 1110(s), 1073(vs), 1035(vs),

933(s), 913(m), 854(s), 823(w), 786(w), 365(sh), 343(m), 321(m). UV-vis (solid-$BaSO_4$): 13660, 19650, 20450, 29250 cm^{-1}.

[$CrCl_3$(18-crown-6)]

[$CrCl_3(thf)_3$] (0.14 g, 0.4 mmol) in dry CH_2Cl_2 (5 mL) was combined with anhydrous 18-crown-6 (0.2 g, 0.38 mmol) in dry CH_2Cl_2 (5 mL). The solution was left to stir for an hour and then dry hexane (6 mL) was added. A precipitate was then seen, which was filtered and dried under vacuum. The product was a pink solid (0.1 g, 53%). Anal: Calc. for $C_{12}H_{24}Cl_3CrO_6.1/2CH_2Cl_2$: C, 32.3; H, 5.4; Found: C, 32.5; H, 6.0%. IR (Nujol)/ cm^{-1}: 1306(m), 1261(m), 1120(s), 1066(s), 1021(m), 937(m), 922(m), 852(m), 822(m), 796(m), 588(w), 472(w), 441(w), 377(m), 351(s), 303(w). UV- vis (solid-$BaSO_4$): 13200(sh), 13500, 19380, 28900(sh) cm^{-1}.

[$CrCl_3(H_2O)$(18-crown-6)]

[$CrCl_3(thf)_3$] (0.14 g, 0.4 mmol) in dry CH_2Cl_2 (10 mL) was combined with 18-crown-6 (0.1 g, 0.38 mmol) in dry CH_2Cl_2 (10 mL). The solution was left to stir for an hour, addition of dry hexane (5 mL) a solid was produced, which was then filtered and dried under vacuum. The product produced was a pink solid (0.03 g, 19%). Anal: Calc. for $C_{12}H_{26}Cl_3CrO_7$: C, 32.7; H, 6.0; Found: C, 31.9; H, 7.0%. IR (Nujol)/ cm^{-1}: 3300(br), 1617(m), 1299(w), 1261(m), 1148(s), 1093(vs), 1060(s), 1046(w), 951(m), 865(s), 810(m), 356(m), 323(m). UV-vis (solid-$BaSO_4$): 13570, 19685, 29270(sh) cm^{-1}; (solution-CH_2Cl_2): (ε_{mol}/ $cm^{-1}dm^3mol^{-1}$) 28900(sh) cm^{-1}.

[{$CrCl_3$}$_2$(18-crown-6)]

[$CrCl_3(thf)_3$] (0.19 g, 0.5 mmol) in dry CH_2Cl_2 (5 mL) was combined with anhydrous 18-crown-6 (0.06 g, 0.23 mmol) in dry CH_2Cl_2 (5 mL). The solution was left to stir for an hour and then dry hexane (6 mL) was added. A precipitate was then seen, which was filtered and dried under vacuum. The product was a pink solid (0.1 g, 69%). Anal: Calc. for $C_{12}H_{24}Cl_6Cr_2O_6$: C, 24.8; H, 4.2; Found: C, 25.7; H, 5.9%. IR (Nujol)/ cm^{-1}: 1306(m), 1261(m), 1092(s), 1066(vs), 1021(vs), 937(m), 922(m), 852(m), 797(m), 367(m), 352(s). UV- vis (solid-$BaSO_4$): 13400, 13960(sh), 19450, 19190 cm^{-1}.

[$CrCl_3$([12]aneS_4)]

[$CrCl_3(thf)_3$] (0.05 g, 0.13 mmol) in dry CH_2Cl_2 (5 mL) was combined with dry [12]aneS_4 (0.03 g, 0.13 mmol) in dry CH_2Cl_2 (5 mL). The two solutions once combined created a blue/purple solution along with a small amount of precipitate. The solution was concentrated and the solid was filtered and dried under vacuum. The product was a blue solid (0.04 g, 76%). Anal: Calc. for $C_8H_{16}Cl_3CrS_4$: C, 24.1; H, 4.0; Found: C, 24.4; H, 4.6%. IR (Nujol)/ cm^{-1}: 1300(w), 1262(s), 1093(m), 1017(m), 951(m), 923(m), 861(m), 802(m), 744(s), 371(sh), 366(m), 329(w). UV- vis (solid-$BaSO_4$):14050, 19840, 29900 cm^{-1}.

[$CrCl_3$([15]aneS_5)]

[$CrCl_3(thf)_3$] (0.05 g, 0.13 mmol) in dry CH_2Cl_2 (5 mL) was combined with dry [15]aneS_5 (0.05 g, 0.13 mmol) in dry CH_2Cl_2 (5 mL). The solution was concentrated which produced a precipitate. The solid was filtered and dried under vacuum. The product was a purple solid (0.06 g, 88%). Anal: Calc. for $C_{10}H_{20}Cl_3CrS_5$: C, 26.2; H, 4.4; Found: **C**, 25.6; H, 4.9%. IR (Nujol)/ cm^{-1}: 1096(m), 1021(m), 792(m), 546(w), 340(w), 315(sh). UV- vis (solid-$BaSO_4$): 14290, 19380, 30490 cm^{-1}.

[$CrCl_3$([9]aneS_2O)]

[$CrCl_3(thf)_3$] (0.10 g, 0.27 mmol) in dry CH_2Cl_2 (5 mL) was combined with dry [9]aneS_2O (0.05 g, 0.30 mmol) in dry CH_2Cl_2 (5 mL). The solution was left to stir for an hour giving a precipitate, which was filtered and dried under vacuum. The product was a pink solid (0.05 g, 58%). Anal: Calc. for $C_6H_{12}Cl_3CrOS_2$.1/4thf: C, 22.3; H, 3.7; Found: C, 25.0; H, 4.0%. IR (Nujol)/ cm^{-1}: 1297(m), 1246(w), 1200(w), 1056(m), 1012(m), 989(m), 934(m), 929(sh), 912(m), 836(w), 772(w), 686(w), 358(s), 343(sh), 330(w). UV- vis (solid-$BaSO_4$): 14880, 19970 cm^{-1}.

[$CrCl_3$([15]aneS_2O_3)]

[$CrCl_3(thf)_3$] (0.2 g, 0.57 mmol) in dry CH_2Cl_2 (5 mL) was combined with dry [15]aneS_2O_3 (0.14 g, 0.54 mmol) in dry CH_2Cl_2 (5 mL). On concentration of the solution a small amount of precipitate was seen this was filtered and dried under vacuum. The

product was a purple solid (0.07 g, 32%). Anal: Calc. for $C_{10}H_{20}Cl_3CrO_3S_2$: C, 29.2; H, 4.9; Found: C, 28.9; H, 5.3%. IR (Nujol)/ cm^{-1}: 1301(w), 1260(s), 1098(m), 1075(w), 1011(m), 963(m), 916(m), 852(m), 803(m), 716(s), 497(w), 366(sh), 345(m), 300(w). UV-vis (solid-$BaSO_4$): 14450, 20000, 30860(sh) cm^{-1}.

[$CrCl_3$([18]aneS_3O_3)]

[$CrCl_3(thf)_3$] (0.2 g, 0.57 mmol) in dry CH_2Cl_2 (5 mL) was combined with dry [18]aneS_3O_3 (0.2 g, 0.64 mmol) in dry CH_2Cl_2 (5 mL). The solution was concentrated producing precipitate, Et_2O (5 mL) creating more precipitate, which was filtered and dried under vacuum. The product was a pink solid (0.16 g, 82%). Anal: Calc. for $C_{12}H_{24}Cl_3O_3S_3.1/2CH_2Cl_2$: C, 29.2; H, 4.9; Found: C, 28.9; H, 5.3%. IR (Nujol)/ cm^{-1}: 1300(w), 1260(s), 1167(w), 1093(m), 1019(m), 918(m), 859(m), 801(m), 563(w), 470(w), 355(sh), 345(m), 315(w). UV- vis (solid-$BaSO_4$): 14350, 19660, 30300 cm^{-1}.

3.4.3 Vanadium(III) Complexes

[VCl_3(12-crown-4)]

[$VCl_3(thf)_3$] (0.21 g, 0.56 mmol) in dry CH_2Cl_2 (5 mL) was combined with anhydrous 12-crown-4 (0.24 g, 1.36 mmol) in dry CH_2Cl_2 (5 mL). The solution was concentrated (*ca.* 5 mL) and a precipitate was formed, this was filtered and dried under vacuum. The product was a pink solid (0.14 g, 42 %). Anal: Calc. for $C_8H_{16}VCl_3O_4$: C, 28.8; H, 4.8; Found: C, 28.8; H, 5.6%. IR (Nujol) /cm^{-1}: 1299(s), 1262(w), 1232(m), 1145(s), 1066(vs), 1027(s), 995(w), 937(m), 909(s), 837(s), 803(m), 733(s), 579(w),483(m), 423(w), 364(sh), 339(s), 305(sh). UV-vis (solid-$BaSO_4$): 11870, 18900 cm^{-1}.

[VCl_3(15-crown-5)]

[$VCl_3(thf)_3$] (0.21 g, 0.56 mmol) in dry CH_2Cl_2 (5 mL) was combined with anhydrous 15-crown-5 (0.12 g, 0.56 mmol) in dry CH_2Cl_2 (5 mL). The solution was concentrated (*ca.* 5 mL) and a precipitate was formed, this was filtered and dried under vacuum. The product was a pink solid (0.14 g, 52%). Anal: Calc. for $C_{10}H_{20}VCl_3O_5.CH_2Cl_2$: C, 28.5; H, 5.2; Found C, 27.5; H, 6.1%. IR (Nujol)/ cm^{-1}: 1303(s), 1263(m), 1228(w), 1147(m), 1114(s),

1082(sh), 1067(s), 1020(sh), 1007(s), 933(m), 843(s), 824(s), 793(m), 606(m), 524(w), 477(w), 372(m), 340(s), 324(sh). UV-vis (solid-$BaSO_4$): 11500(sh), 12830, 19380 cm^{-1}.

[$VCl_3(H_2O)$(15-crown-5)]

[$VCl_3(thf)_3$] (0.17 g, 0.46 mmol) in dry CH_2Cl_2 (5 mL) was combined with 15-crown-5 (0.1 g, 0.46 mmol) in dry CH_2Cl_2 (5 mL). The solution was concentrated and a precipitate was formed, this was filtered and dried under vacuum. The product was a pink solid (0.12 g, 25%). Anal: Calc. for $C_{10}H_{22}Cl_3O_6V$: C, 27.5; H, 5.0; Found: C, 27.5; H, 6.1%. IR (Nujol)/ cm^{-1}: 3300(br), 1630(m), 1304(s), 1262(m), 1228(w), 1149(m), 1113(m), 1068(s), 1027(m), 1007(m), 933(m), 918(m), 846(s), 823(m), 793(s), 367(m), 342(s), 334(sh), 324(sh). UV-vis (solid-$BaSO_4$): 11300(sh), 12690, 19190 cm^{-1}; (solution-CH_2Cl_2): (ε_{mol}/ $cm^{-1}dm^3mol^{-1}$) 19570(293), 14900(516), 11590(696) cm^{-1}.

[VCl_3(18-crown-6)]

[$VCl_3(thf)_3$] (0.37 g, 1.0 mmol) in dry CH_2Cl_2 (20 mL) was combined with anhydrous 18-crown-6 (0.26 g, 1.0 mmol) in dry CH_2Cl_2 (10 mL). The solution was stirred for 1 hour and a pink precipitate was formed, this was concentrated (*ca.* 5 mL). The solid was filtered and dried under vacuum. The product was a pink solid (0.21 g, 50%). Anal: Calc. for $C_{12}H_{24}Cl_3O_6V.CH_2Cl_2$: C, 30.8; H, 5.2; Found: C, 31.2; H, 6.5%. IR (Nujol)/ cm^{-1}: 1350(w), 1297(m), 1261(m), 1240(w), 1100(sh), 1057(s), 1033(s), 928(s), 833(s), 799(s), 485(w), 432(w), 359(sh), 340(s) cm^{-1}. UV-vis (solid-$BaSO_4$): 12900, 18950 cm^{-1}.

[$VCl_3(H_2O)$(18-crown-6)]

[$VCl_3(thf)_3$] (0.17 g, 1.09 mmol) in dry CH_2Cl_2 (5 mL) was combined with 18-crown-6 (0.287 g, 1.09 mmol) in dry CH_2Cl_2 (5 mL). The solution was concentrated and a precipitate was formed, this was filtered and dried under vacuum. The product was a pink solid (0.2 g, 35%). Anal: Calc. for $C_{12}H_{26}Cl_3O_7V$:C, 32.8 ; H, 6.0 ; Found: C, 32.4; H, 6.3% . IR (Nujol)/ cm^{-1}: 3400(br), 1630(m), 1290(m), 1256(m), 1150(sh), 1093(br.,s), 1000(s), 952(s), 920(m), 837(m), 808(m), 389(w), 333(s), 310(sh) cm^{-1}. UV-vis (solid-$BaSO_4$): 119009(sh), 13400, 19800 cm^{-1}.

[{VCl_3}$_2$(18-crown-6)]

[$VCl_3(thf)_3$] (0.4 g, 1.09 mmol) in dry CH_2Cl_2 (5 mL) was combined with anhydrous 18-crown-6 (0.14 g, 0.55 mmol) in dry CH_2Cl_2 (5 mL). The solution was concentrated (*ca* 5 mL) and a precipitate was formed, this was filtered and dried under vacuum. The product was a pink solid (0.17 g, 54 %). Anal: Calc. for $C_{12}H_{24}Cl_3O_6V$: C, 24.9; H, 4.2; Found: C, 24.4; H, 4.4%. IR (Nujol)/ cm^{-1}: 1298(m), 1275(m), 1239(w), 1097(sh), 1056(s), 1031(s), 1005(sh), 981(sh), 930(s), 891(w), 833(s), 794(w), 731(s), 582(w), 536(w), 481(w), 431(w), 365(sh), 341(s), 311(sh). UV-vis (solid-$BaSO_4$): 12320, 19230 cm^{-1}.

[VCl_3([12]aneS_4)]

[$VCl_3(thf)_3$] (0.03 g, 0.08 mmol) in dry CH_2Cl_2 (5 mL) was combined with dry [[12]aneS_4 (0.02 g, 0.08 mmol) in dry CH_2Cl_2 (5 mL). The solution was concentrated and a precipitate was formed, this was filtered and dried under vacuum. The product was a pink solid (0.01 g, 30%). Anal: Calc. for $C_8H_{16}Cl_3S_4V$: C, 24.2; H, 4.1; Found: C, 25.1; H, 5.3%. IR (Nujol)/ cm^{-1}: 1345(w), 1260(s), 1090(s), 1041(m), 1015(s), 925(w), 841(m), 801(s), 677(w), 361(w), 346(m) cm^{-1}. UV-vis (solid-$BaSO_4$): 12690, 18250 cm^{-1}.

[VCl_3([9]aneS_2O)]

[$VCl_3(thf)_3$] (0.05 g, 0.13 mmol) in dry CH_2Cl_2 (5 mL) was combined with dry [9]aneS_2O (0.02 g, 0.12 mmol) in dry CH_2Cl_2 (5 mL). The solution was left to stir for an hour and then dry hexane (6 mL) was added. A precipitate was then seen, which was filtered and dried under vacuum. The product was a pink solid (0.02 g, 52%). Anal: Calc. for $C_6H_{12}Cl_3OS_2V$: C, 22.4; H, 3.8; Found: C, 22.4; H, 3.7%. IR (Nujol)/ cm^{-1}: 1260(m), 1182(w), 1096(sh), 1072(m), 1051(m), 1013(m), 988(m), 976(m), 935(m), 910(m), 834(w), 797(s), 687(w), 483(w), 392(w), 356(w), 339(w), 324(sh). UV-vis (solid-$BaSO_4$): 13440, 18880 cm^{-1}.

[VCl_3([15]aneS_2O_3)]

[$VCl_3(thf)_3$] (0.15 g, 0.4 mmol) in dry CH_2Cl_2 (5 mL) was combined with dry [15]aneS_2O_3 (0.1 g, 0.4 mmol) in dry CH_2Cl_2 (5 mL). The solution was concentrated (*ca.* 5 mL), the precipitate formed was filtered and dried under vacuum. The product was a pink solid

(0.1 g, 40%). Anal: Calc. for $C_{10}H_{20}Cl_3O_3S_2V.2CH_2Cl_2$: C, 24.8; H, 4.2; Found: C, 24.6; H, 4.9%. IR (Nujol)/ cm^{-1}: 1290(m), 1260(m), 1208(w), 1190(m), 1126(s), 1116(s), 1064(s), 1015(sh), 917(m), 905(m), 811(s), 796(sh), 485(w), 416(w), 360(s), 322(s). UV-vis (solid-$BaSO_4$): 12940, 13400(sh), 19850 cm^{-1}.

$[VCl_3([18]aneS_3O_3)]$

$[VCl_3(thf)_3]$ (0.23 g, 0.62 mmol) in dry CH_2Cl_2 (5 mL) was combined with dry $[18]aneS_3O_3$ (0.19 g, 0.62 mmol) in dry CH_2Cl_2 (5 mL). The solution was concentrated and Et_2O (5 mL) was added producing precipitate; this was filtered and dried under vacuum. The product was a pink solid (0.25 g, 87%). Anal: Calc. for $C_{12}H_{24}Cl_3O_3S_3V$: C, 30.7; H, 5.2; Found: C, 31.2; H, 5.7%. IR (Nujol)/ cm^{-1}: 1346(w), 1300(m), 1258(s), 1210(w), 1100(s), 1072(s), 1033(s), 919(m), 848(w), 805(s), 477(m), 355(sh), 343(s) cm^{-1}. UV-vis (solid-$BaSO_4$): 12800, 19690 cm^{-1}.

3.4.4 X-Ray Data

The X-ray data were obtained on a Nonius Kappa CCD diffractometer. The data were recorded at 120K using graphite monochromated M_o-K_α X-ray radiation (λ= 0.71073 Å). The structure and refinement used routine methods.[36,37]

3.5 References

[1] R. D. Rogers, C. B. Bauer, "*Comprehensive Supramolecular Chemistry*" (J. L. Atwood, J. E. D. Davies, D. D. MacNicol, F. Vögtle), 1, **(1996)**, 315.

[2] T. P. Hanusa, "*Comprehensive Coordination Chemistry II*", (J. A. McCleverty, T. J. Meyer), 3, **(2004)**, 1.

[3] S. A. Cotton, "*Comprehensive Coordination Chemistry II*", (J. A. McCleverty, T. J. Meyer), 3, **(2004)**, 93.

[4] M. D. Brown, W. Levason, D. C. Murray, M. C. Popham, G. Reid and M. Webster, *Dalton Trans.*, **(2003)**, 857.

[5] R. J. H. Clark, G. Natile, *Inorg. Chim. Acta,* 4, **(1970)**, 533.

[6] F. A. Cotton, S. A. Duraj, G. L. Powell and W. J. Roth, *Inorg. Chim. Acta,*113, **(1986)**, 81.

[7] S. G. Bott, U. Kynast, J. L. Atwood, *J. Inclusion Phenom.*, 4, **(1986)**, 241.

[8] U. Kynast, S.G. Bott, J. L Atwood, *J. Coord. Chem.*, 17, **(1988)**, 53.

[9] G. Frenzen, W. Massa, T. Ernst, K. Dehnicke, *Z. Naturforsch., Teil B*, 45, **(1990)**, 1393.

[10] T. Ernst, K. Dehnicke, H. Goesmann, D. Fenske, *Z. Naturforsch., Teil B*, 45, **(1990)**, 967.

[11] P. C. Junk, J. L Atwood, *J. Organomet. Chem.*, 565, **(1998)**, 179.

[12] M. Plate, G. Frenzen, K. Dehnicke, *Z. Naturforsch., Teil B*, 48, **(1993)**, 149.

[13] S. G. Bott, H. Prinz, A. Alvanipour, J. L. Atwood, *J. Coord. Chem.*, 16, **(1987)**, 303.

[14] W. Levason, M. C. Popham, G. Reid, M. Webster, *Dalton Trans.*, **(2003)**, 291.

[15] J. Hughes, G. R. Willey, *Inorg. Chim. Acta,* 11, **(1970)**, L25.

[16] S. J. A. Pope, N. R. Champness and G. Reid, *J. Chem. Soc., Dalton Trans.*, **(1997)**, 1639.

[17] S. C. Davies, M. C. Durrant, D. L. Hughes, C. Le Floc'h, S. J. A. Pope, G. Reid, R. L. Richards and J. R. Saunders, *J. Chem. Soc., Dalton Trans.*, **(1998)**, 2191.

[18] N. R. Champness, S. R. Jacob, G. Reid, C. S. Frampton, *Inorg. Chem.*, 34, **(1995)**, 396; M. C. Durrant, S. Davies, D.L. Hughes, C. Le Floc'h, R. L. Richards, J. R. Sanders, N. R. Champness, S. J. A. Pope, G. Reid, *Inorg. Chim. Acta*, 251, **(1996)**, 13; W. Levason, G. Reid, S. M. Smith, *Polyhedron*, 16, **(1997)**, 4253.

[19] D. S. McGuinness, P. Wasserscheid, D. H. Morgan, J. T. Dixon, *Organometallics*, 24, **(2005)**, 552.

[20] D. S. McGuinness, P. Wasserscheid, W. Keim, D. H. Morgan, J. T. Dixon, A. Bollman, H. Maumela, F. Hess, U. Englert, *J. Am. Chem. Soc.*, 125, **(2003)**, 5272.

[21] U. Kynast, S. G. Bott, J. L. Atwood, *J. Coord. Chem.*, 17, **(1988),** 53.

[22] X. Liu, J. E. Ellis, T. D. Miller, P. Ghalasi and J. S. Miller, *Inorg. Synth.*, 34, **(2004)**, 96.

[23] L. E. Manzer, J. Deaton, P. Sharp and R. R. Schrock, *Inorg. Synth.*, 21, **(1982)**, 135.

[24] G. R. Willey, M. T. Lakin and N. W. Alcock, *J. Chem. Soc., Chem. Commun.*, **(1991),** 1414.

[25] J. P. Collman, E. T. Kittleman, *Inorg. Synth.*, 8, **(1966),** 141.

[26] H. J. Kuppers and K. Wieghardt, *Polyhedron,* 8, **(1989)**, 1770.

[27] G. J. Grant, K. E. Rogers, W. N. Setzer and D. G. VanDerveer, *Inorg. Chim. Acta,* 234, **(1995),** 35.

[28] T. S. Cameron, A. Decken, E. G. Ilyin, G. B. Mikiforov and J. Passmore, *Eur. J. Inorg. Chem.*, **(2004)**, 3865.

[29] A. J. Blake, R.O. Gould, C. Radek, M. Schröder, *J. Chem. Soc., Dalton Trans.*, **(1995)**, 4045.

[30] D. A. Fletcher, R. F. McMeeking, D. Parkin, *J. Chem. Inf. Comput. Sci.*, 36, **(1996)**, 746.

[31] I. J. Bruno, J. C. Cole, P. R. Edgington, M. Kessler, C. F. Macrae, P. McCabe, J. Pearson, R. Taylor, *Acta Crystallogr., Sect. B,* 58, **(2002)**, 389.

[32] B. R. Elvidge, S. Arndt, P. M. Zeimentz, T. P. Spaniol, J. Okuda, *Inorg. Chem.*, 44, **(2005)**, 6777.

[33] J. S. Bradshaw, J. Y. Hui, B. L. Haymore, J. J. Christensen and R. M. Izatt, *J. Heterocyclic Chem.*,10 **(1973),** 1.

[34] C. J. Pedersen, *J. Am. Chem. Soc.*, 89, **(1967),** 7017.

[35] H. Herwig, H. Zeiss, *J. Organomet. Chem.*, 23, **(1958)**, 1404.

[36] SHELXS-97, program for crystal structure, solution, G. M. Sheldrick, University of Göttingen. Germany, 1997.

[37] SHELXS-97, program for crystal structure, refinement, G. M. Sheldrick, University of Göttingen. Germany, 1997.